

Status of X-ray astronomy and first eROSITA highlights

Andrea Merloni (MPE)



The solar corona



The solar corona in X-rays

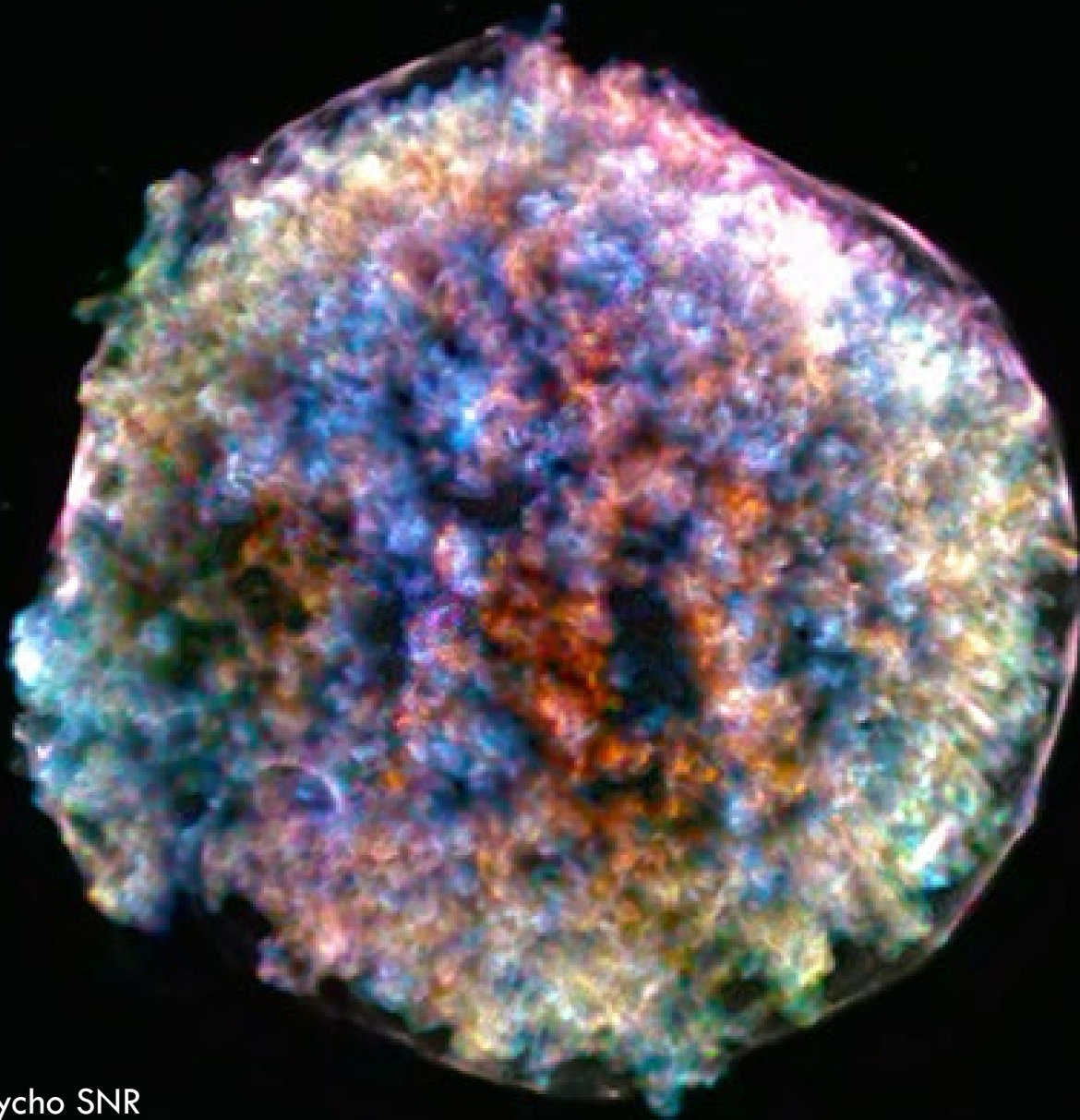
NASA, SDO, NuSTAR



Credit: NASA NuSTAR SDO

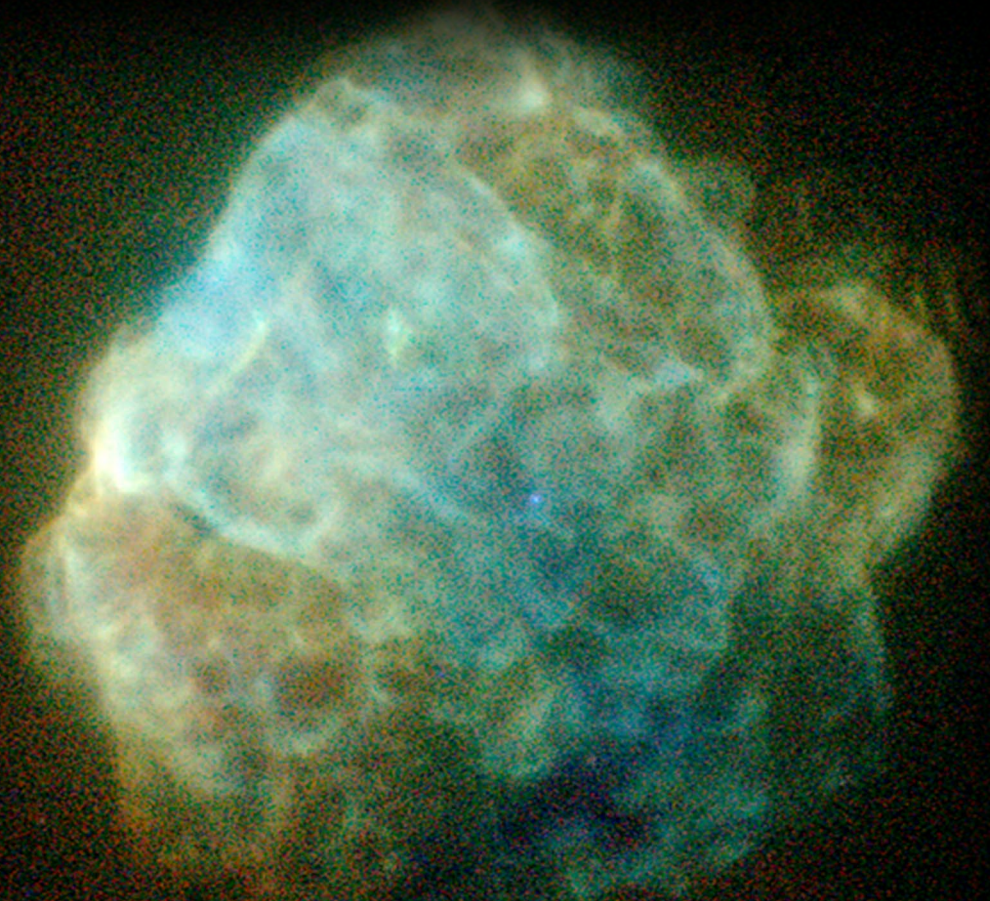
Merloni, CTAO, 15/4/2024

Dying Stars in X-rays



Tycho SNR

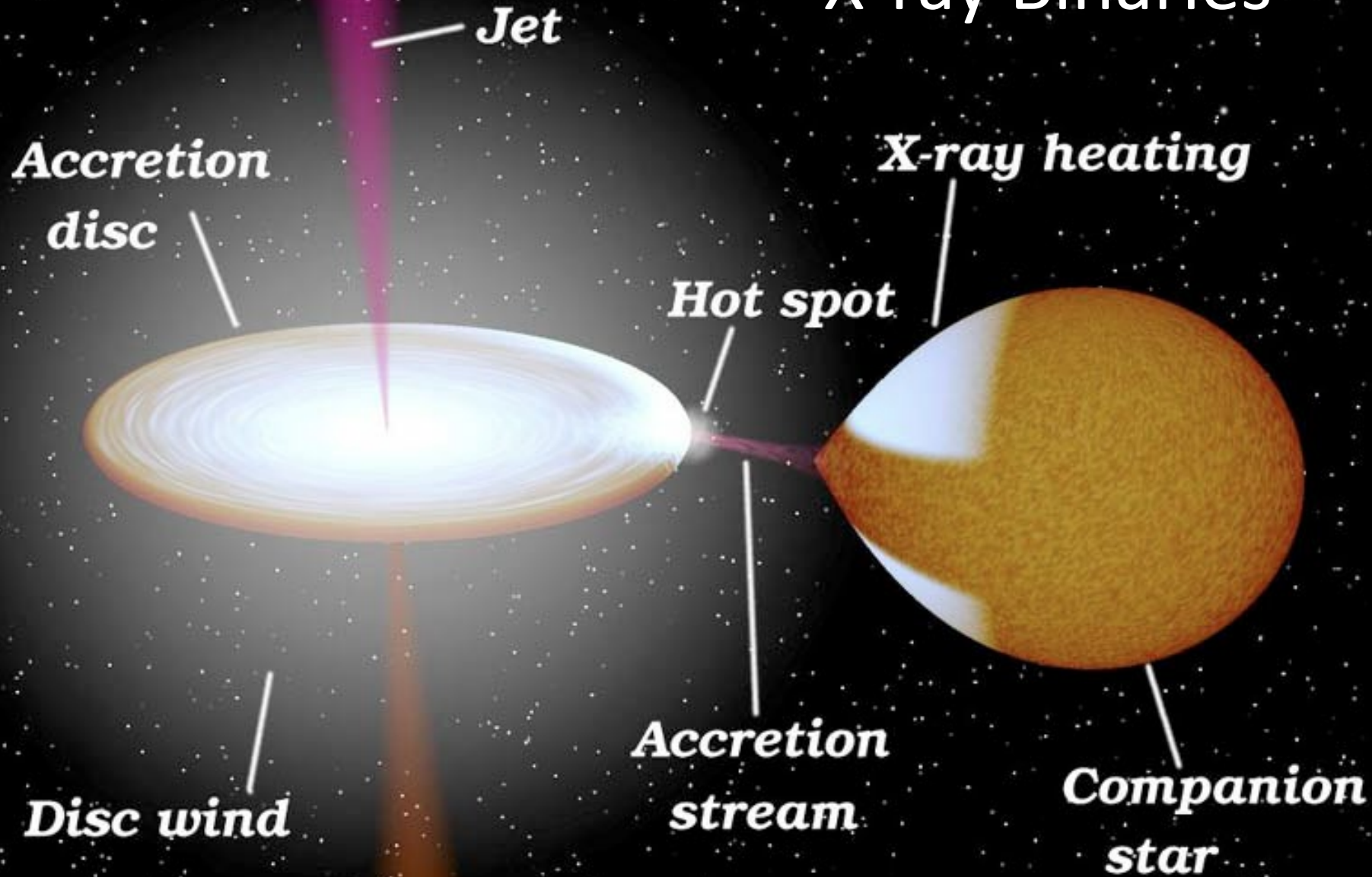
Credit: NASA/CXC/RIKEN & GSFC/T. Sato et al



Puppis A SNR

Credit: SRG/eROSITA MPE Predehl

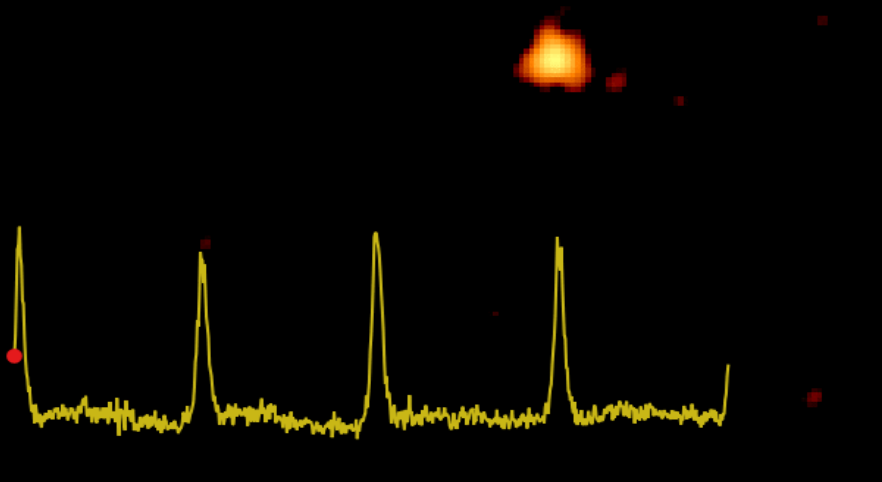
X-ray Binaries



Accreting black holes

Chandra Deep Field South: The deepest X-ray image of the sky ever taken (Xue et al. 2011)

Quasi Periodic Eruptions (QPE)



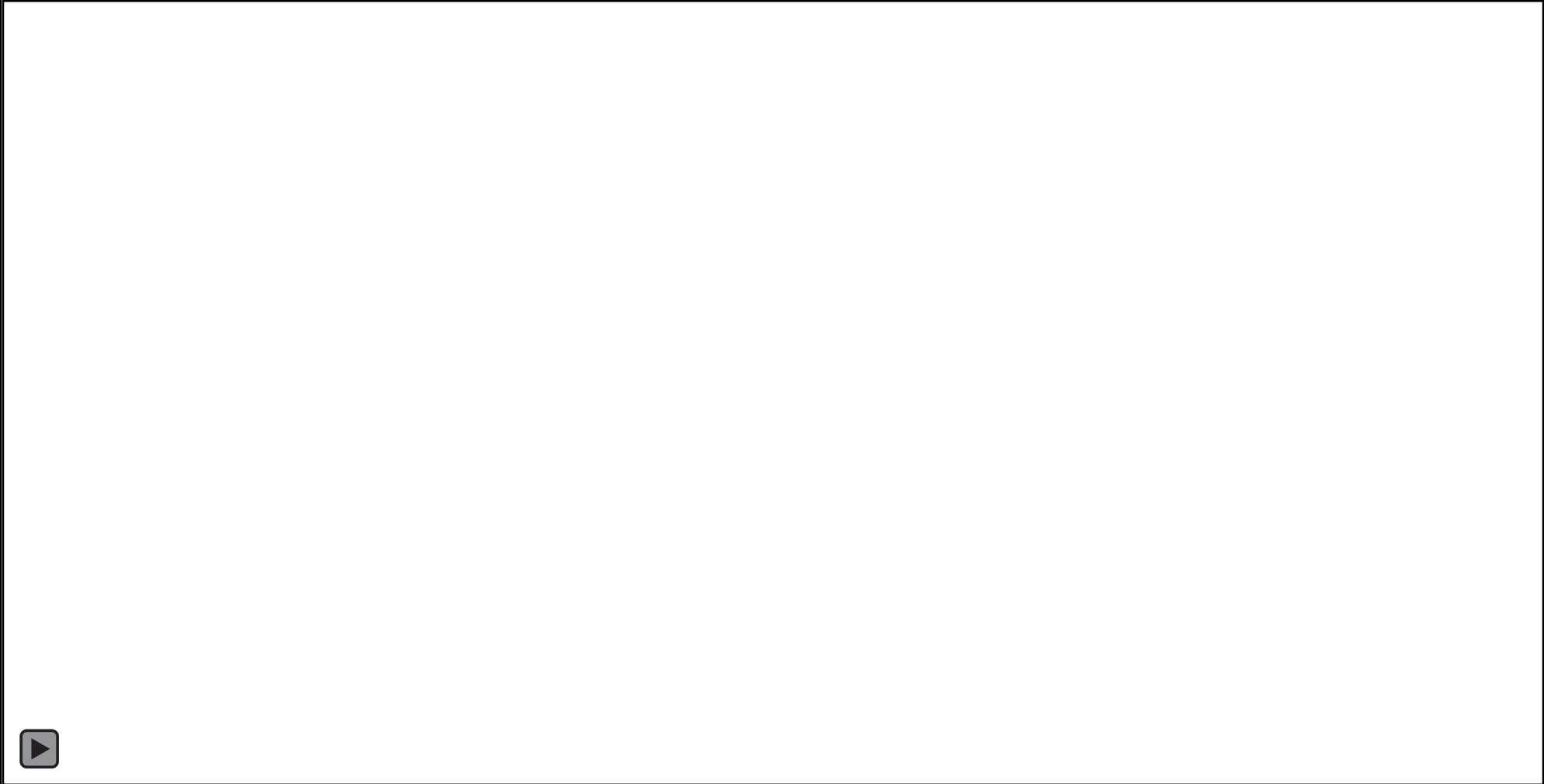
Credit: ESA XMM-Newton, G. Miniutti

Every dot is a (supermassive) black hole!

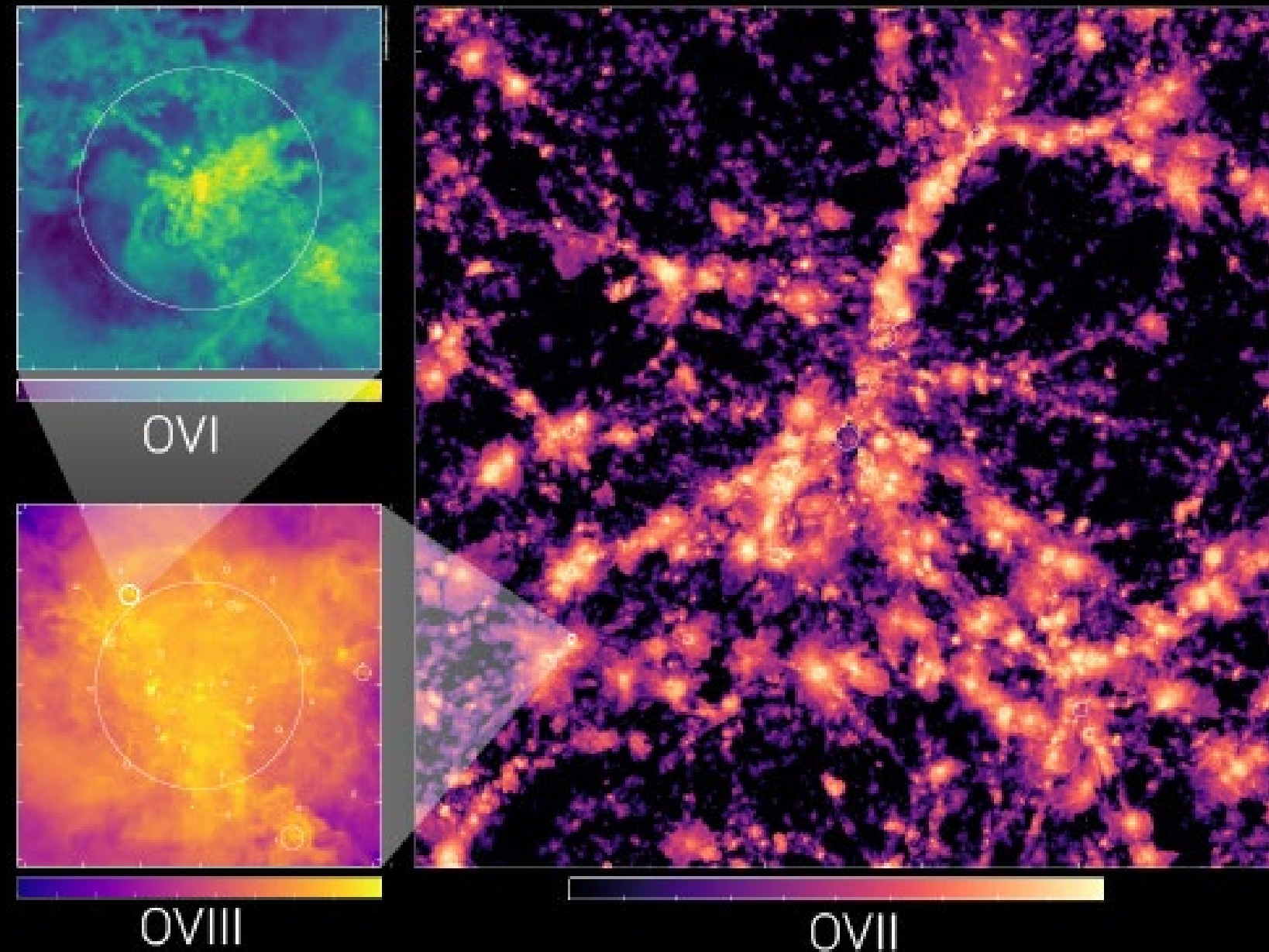
Merloni, CTAO, 15/4/2024

Accreting black holes

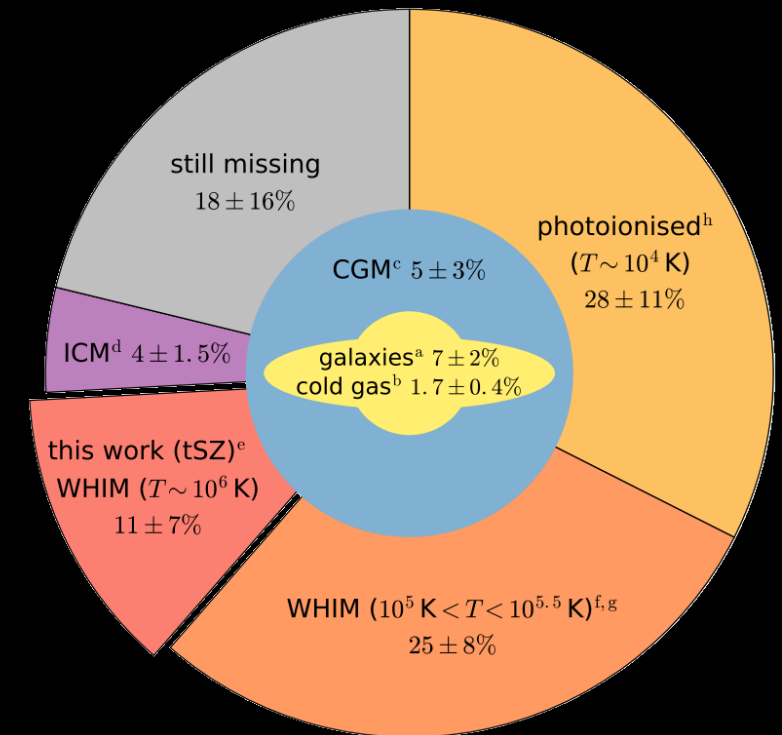
Probes of GR



WHIM, Filaments, the hot CGM and the “missing baryons”



Credit: D. Nelson, Illustris TNG



Credit: de Graaf et al. 2020

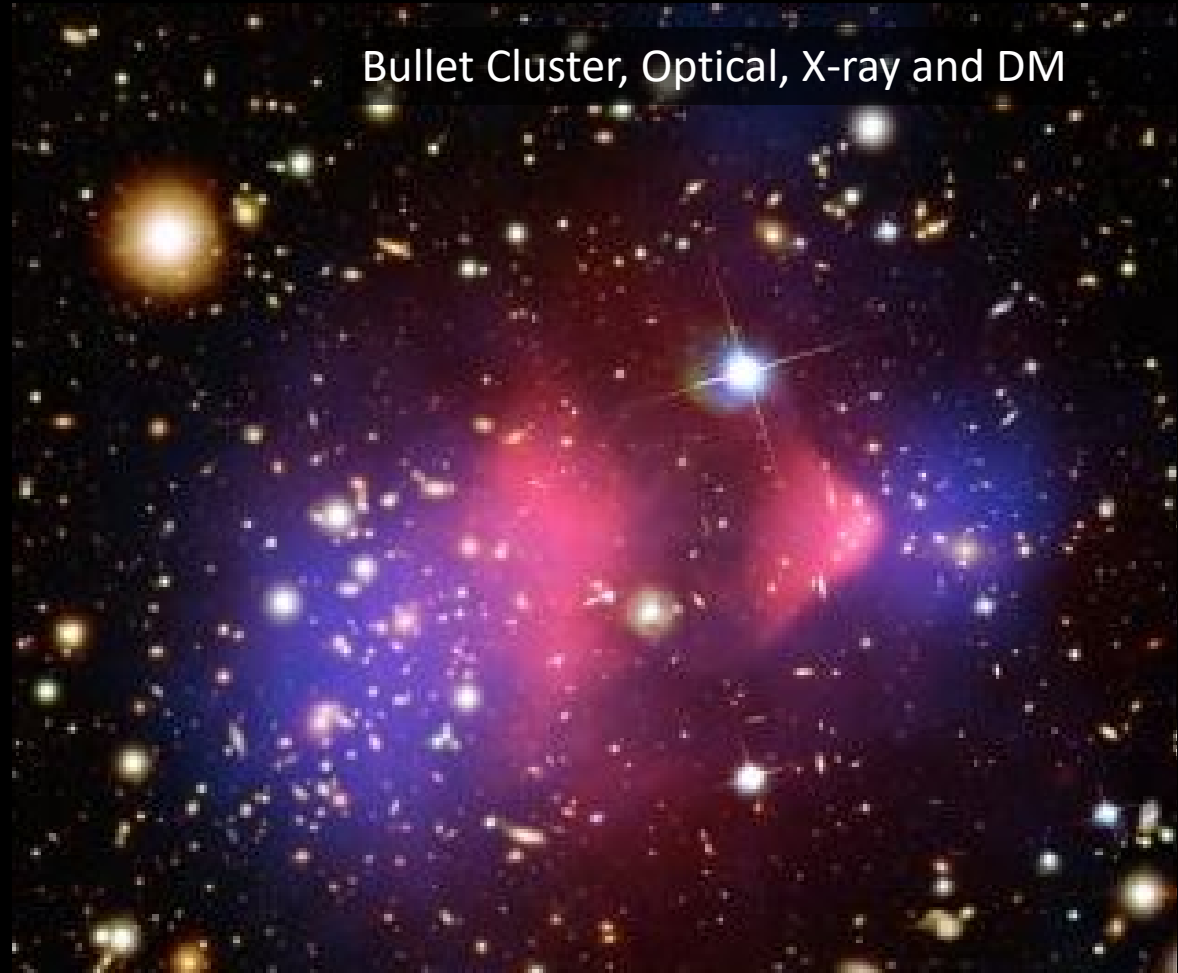
Clusters of Galaxies

Perseus Cluster, edge enhanced X-ray emission



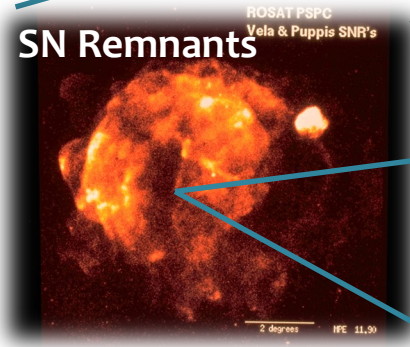
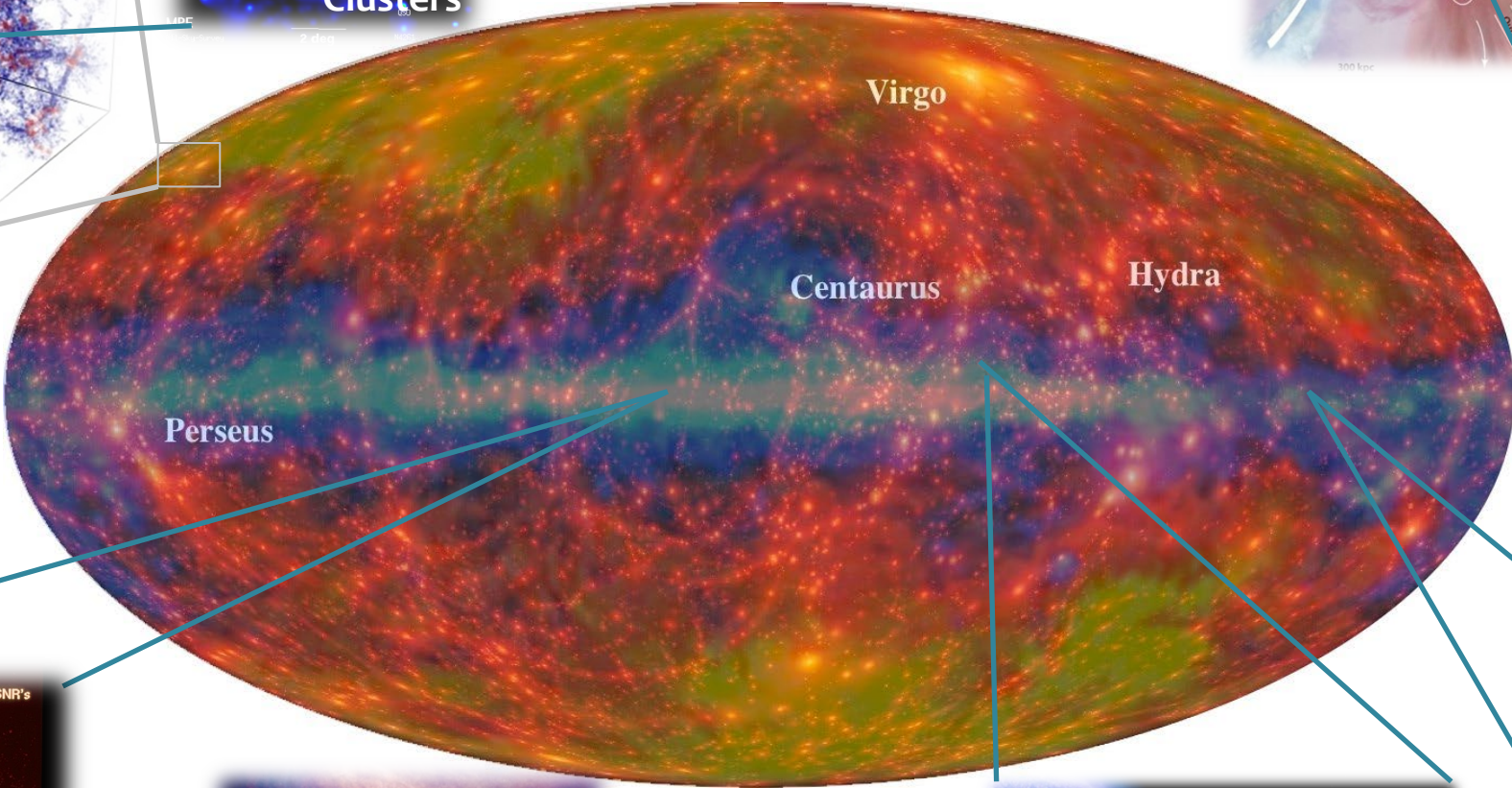
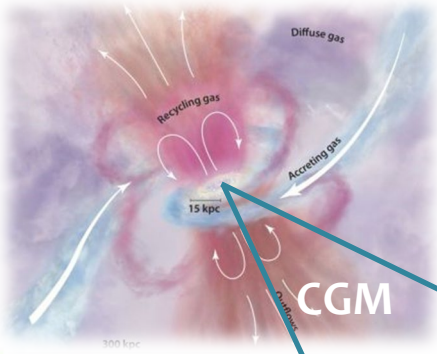
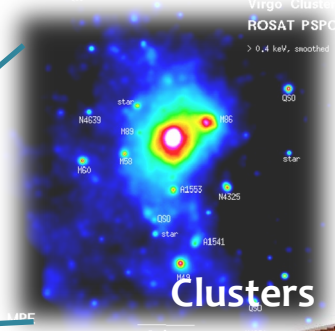
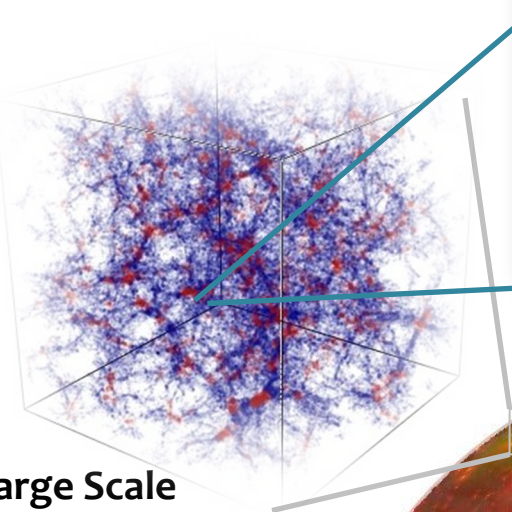
Credit: NASA, Chandra, J. Sanders

Bullet Cluster, Optical, X-ray and DM

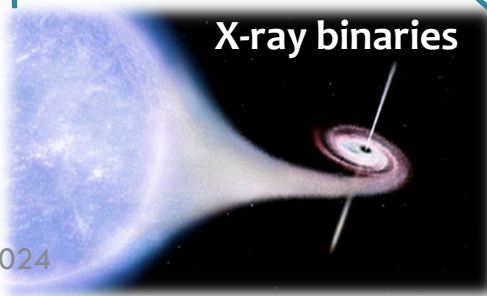


Credit: X-ray: NASA/CXC/CfA/M.Markevitch,
Optical and lensing map: NASA/STScI,
Magellan/U.Arizona/D.Clowe, Lensing map: ESO WFI

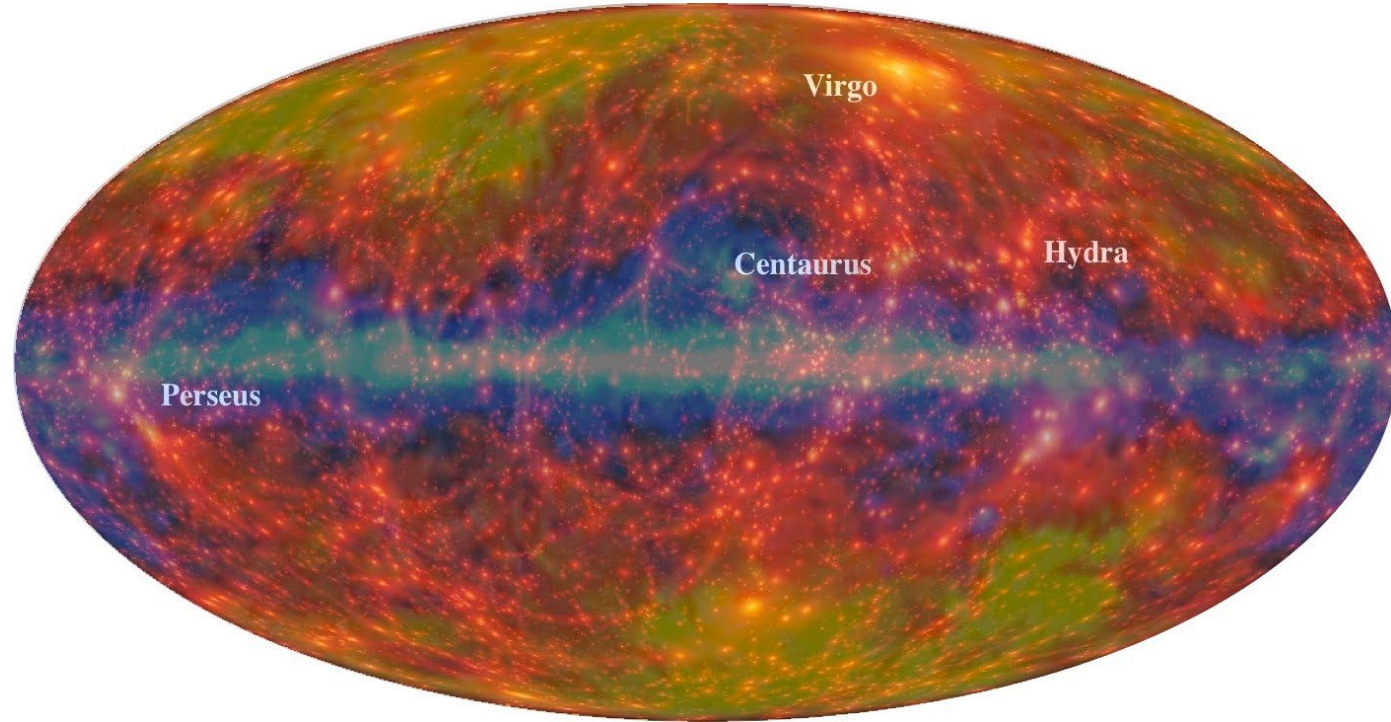
The X-ray Sky



SN Remnants



The X-ray Sky Observatories



Chandra [1999]



XMM-Newton [1999]



SWIFT [2004]



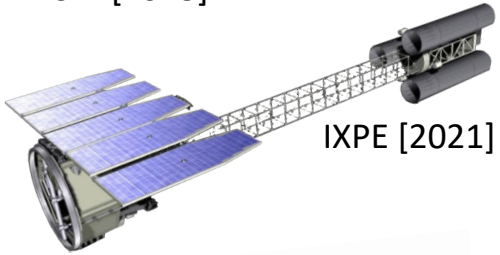
Einstein Probe [2024]



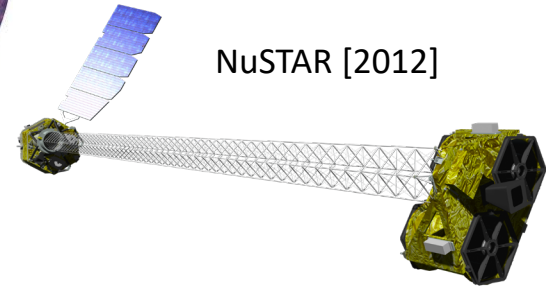
XRISM [2023]



IXPE [2021]



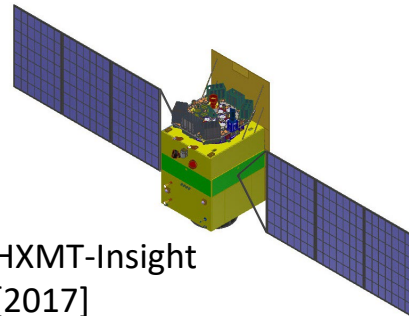
NuSTAR [2012]



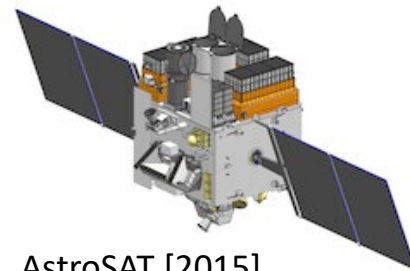
NICER [2017]



HXMT-Insight [2017]



AstroSAT [2015]



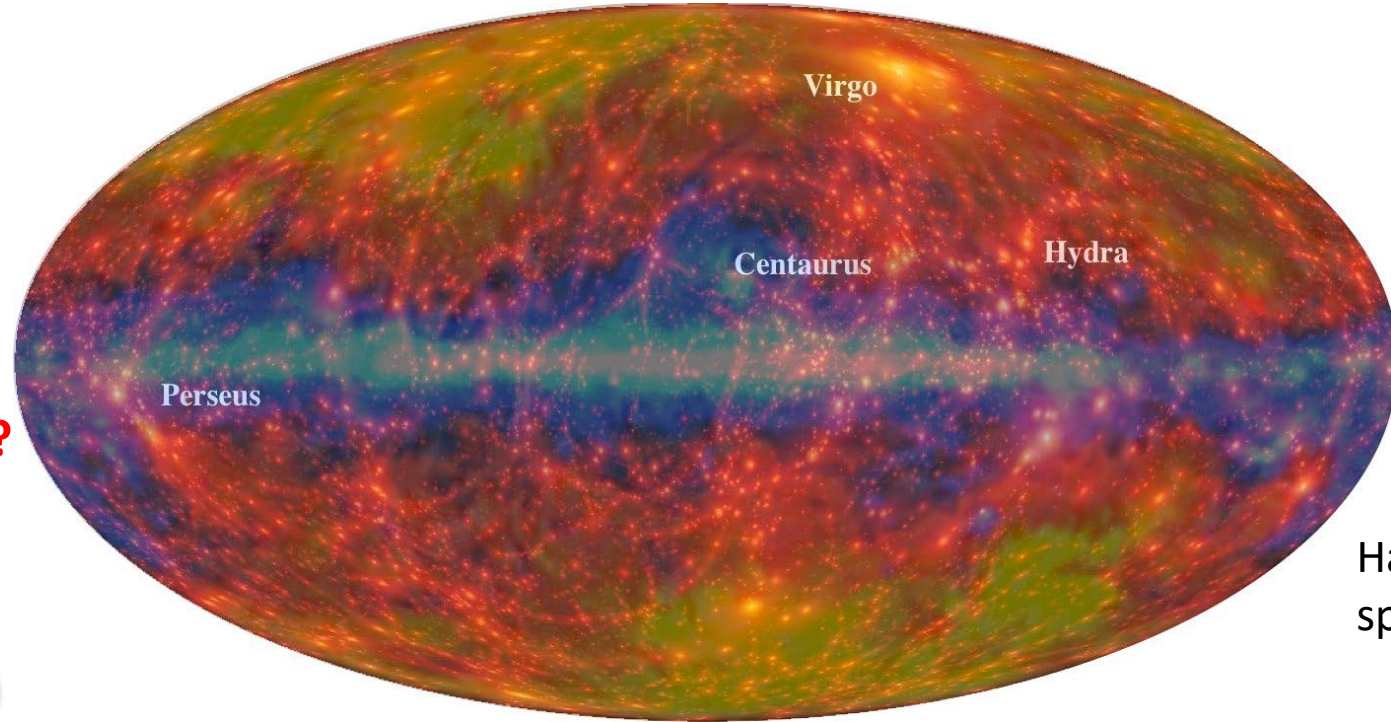
MAXI [2009]



SRG eROSITA
ART-XC [2019]



The X-ray Sky Observatories



Chandra [1999]

Sub-arcsec resolution imaging,
Soft and Hard X-ray gratings
spectroscopy

XMM-Newton [1999]

High-throughput CCD
spectroscopy, soft X-ray gratings
spectroscopy

Sensitive Soft X-ray ~all-sky
imaging and fast follow-up
of transients

Einstein Probe [2024]

Wide FoV imaging and high-
resolution calorimeter
spectroscopy

Guainazzi's talk?

XRISM [2023]

IXPE [2021]

Zane's talk

Imaging Polarimetry

NICER [2017]

High-throughput
(non-imaging)
timing and
spectroscopy of
bright sources

Hard X-ray imaging and
timing

HXMT-Insight
[2017]

All-sky monitor,
high-throughput
timing, multi-
wavelength

AstroSAT [2015]

MAXI [2009]

All-sky monitor,
high-cadence
observations of
bright sources

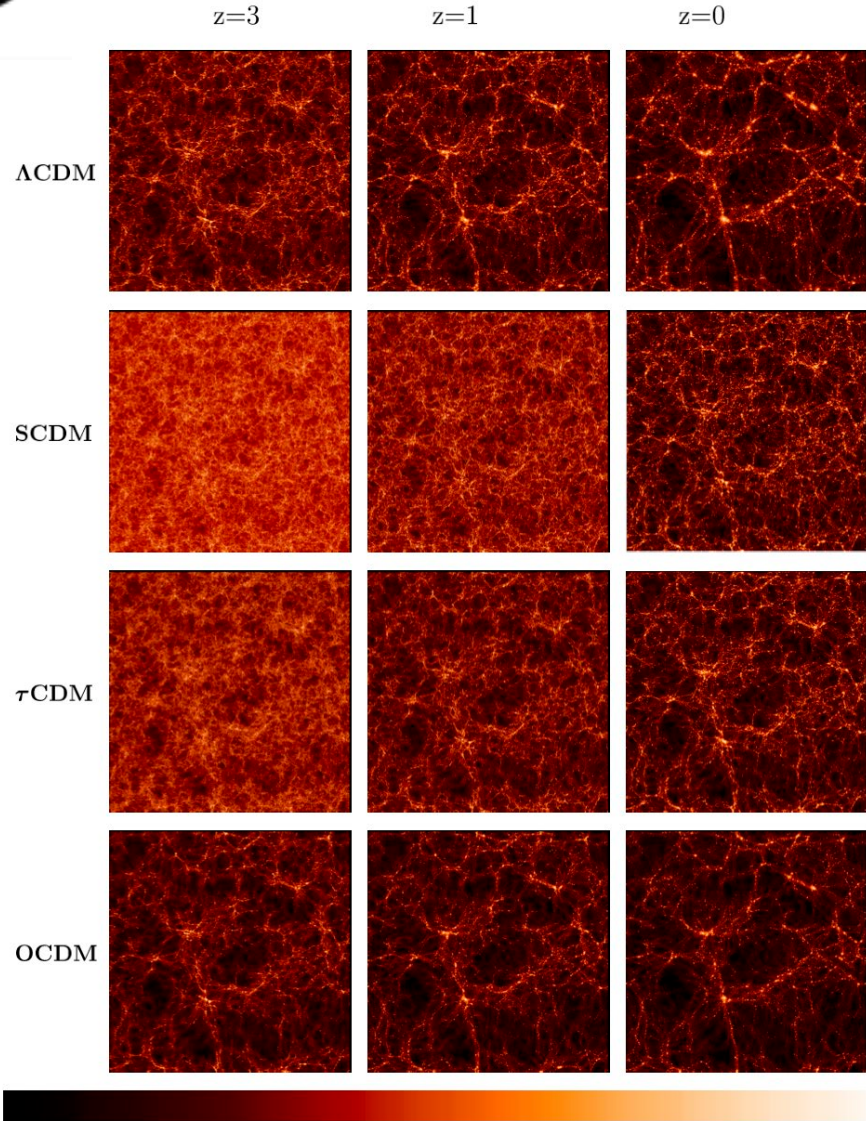
NuSTAR [2012]
Hard X-ray imaging and CCD
spectroscopy

SWIFT [2004]
Fast response, ToO,
flexible scheduling, CCD
imaging and
spectroscopy

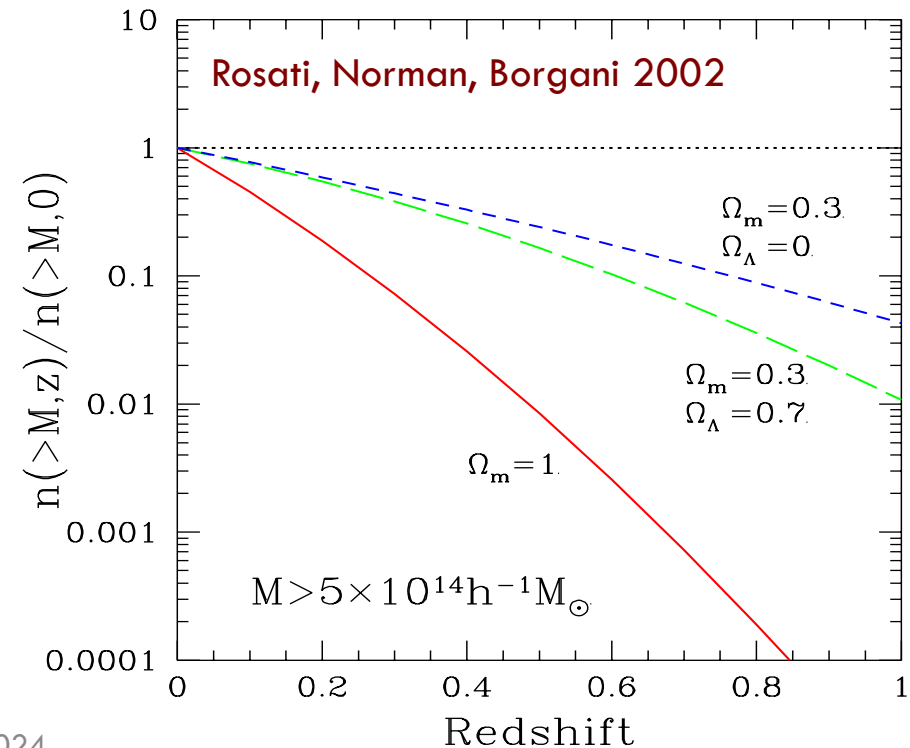
This talk

SRG eROSITA
ART-XC [2019]

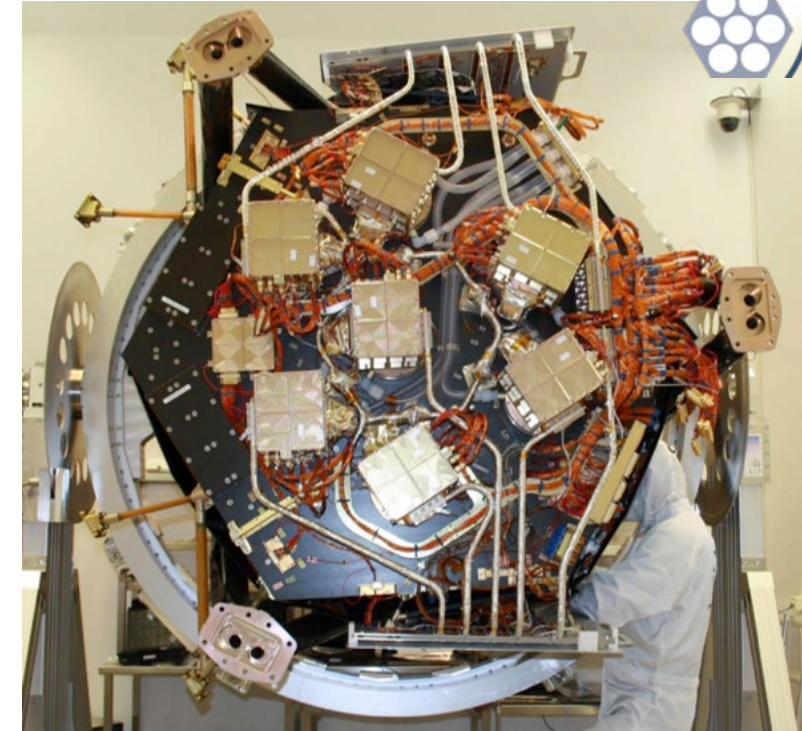
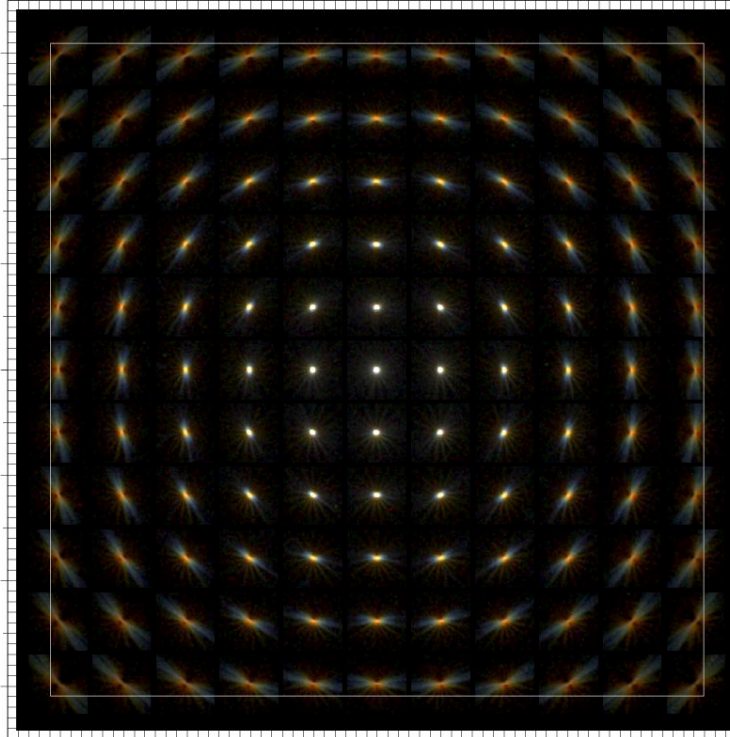
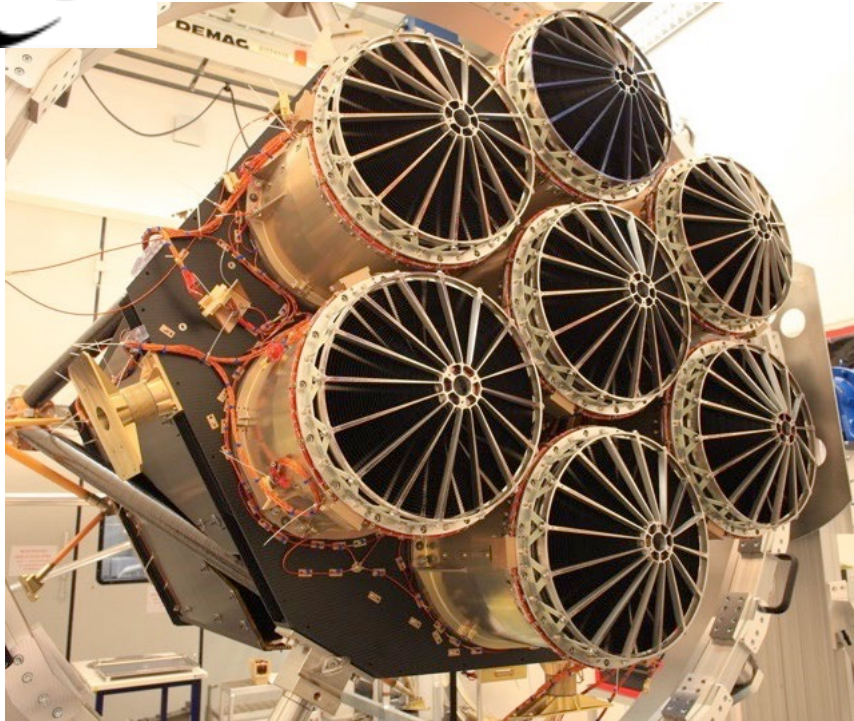
Why eROSITA? Clusters Cosmology



- Clusters are *exponentially sensitive* tracers of **growth of structures**
- A signature of clusters is the hot ($\sim 10^7$ K), extended X-ray ICM
- eROSITA (PSF, sensitivity) was designed to be able to detect $> 10^5$ clusters (Pillepich+ 2018)



The Virgo Collaboration; Jenkins et al. 1998



- Large Effective area ($\sim 1300 \text{ cm}^2$ @1keV, \sim XMM-Newton)
- Large Field of view: 1 degree (diameter)
- Half-Energy width (HEW) $\sim 18''$ (on-axis, point.); $\sim 30''$ (FoV avg., survey)
 - Positional accuracy: $\sim 4.5''$ (1σ)
- X-ray baffle: 92% stray light reduction
- pnCCD with framestore: $384 \times 384 \times 7 \sim 10^6$ pixels ($9.4''$), no chip gaps, no 'out of time' events,
- **Spectral resolution** at all measured energies within specs ($\sim 80 \text{ eV}$ @1.5keV)



SRG/eROSITA 0.4-3.0 keV

Abell 3391/3395

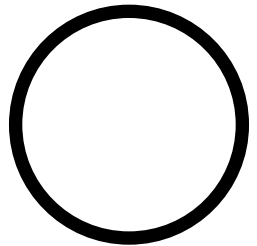


Moon diameter
30 arcmin



Gr
- 5
- 1

XMM-Newton
Field of view ~ 30 arcmin



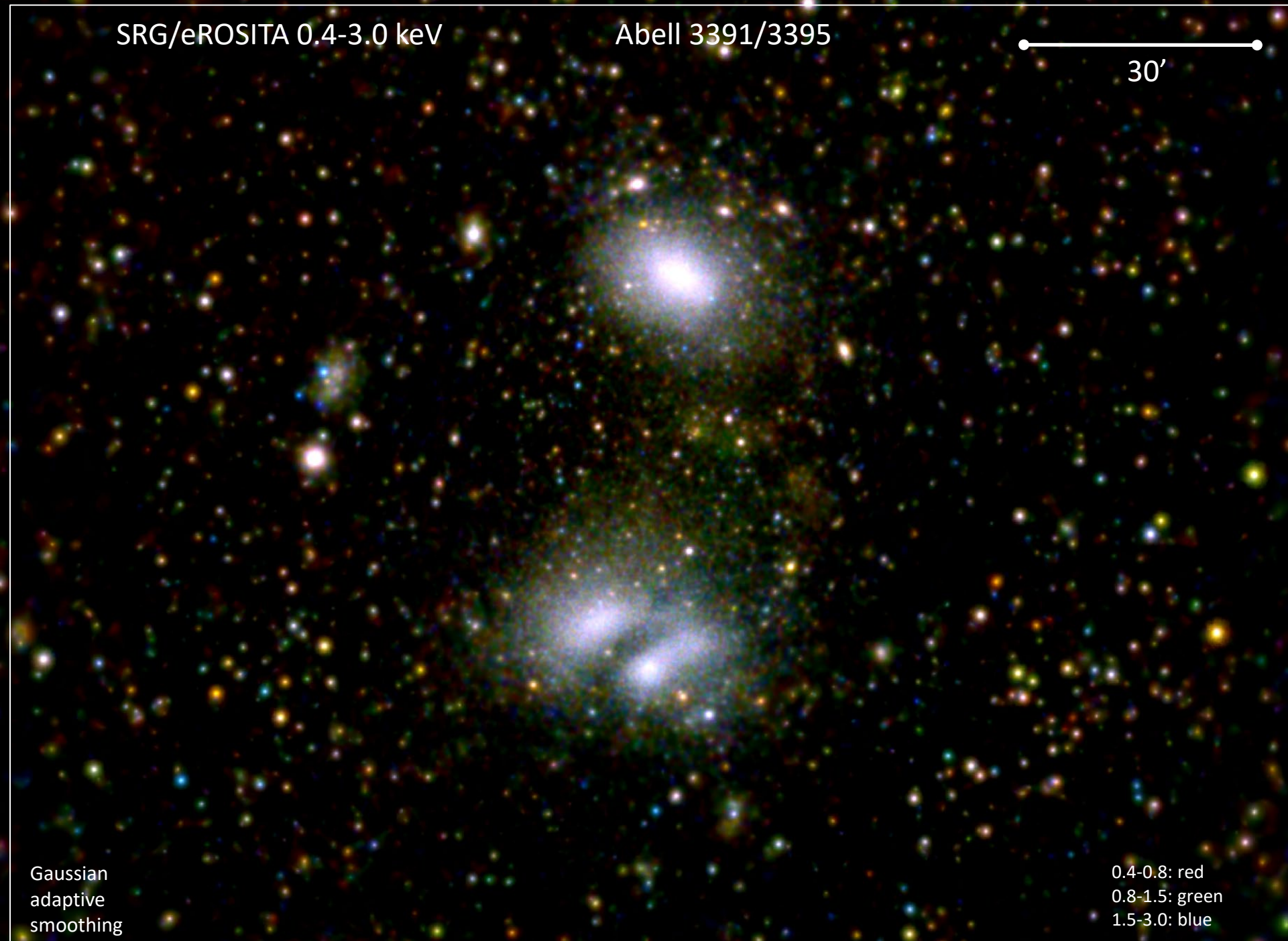
Chandra
Field of view ~ 17 arcmin



3
c

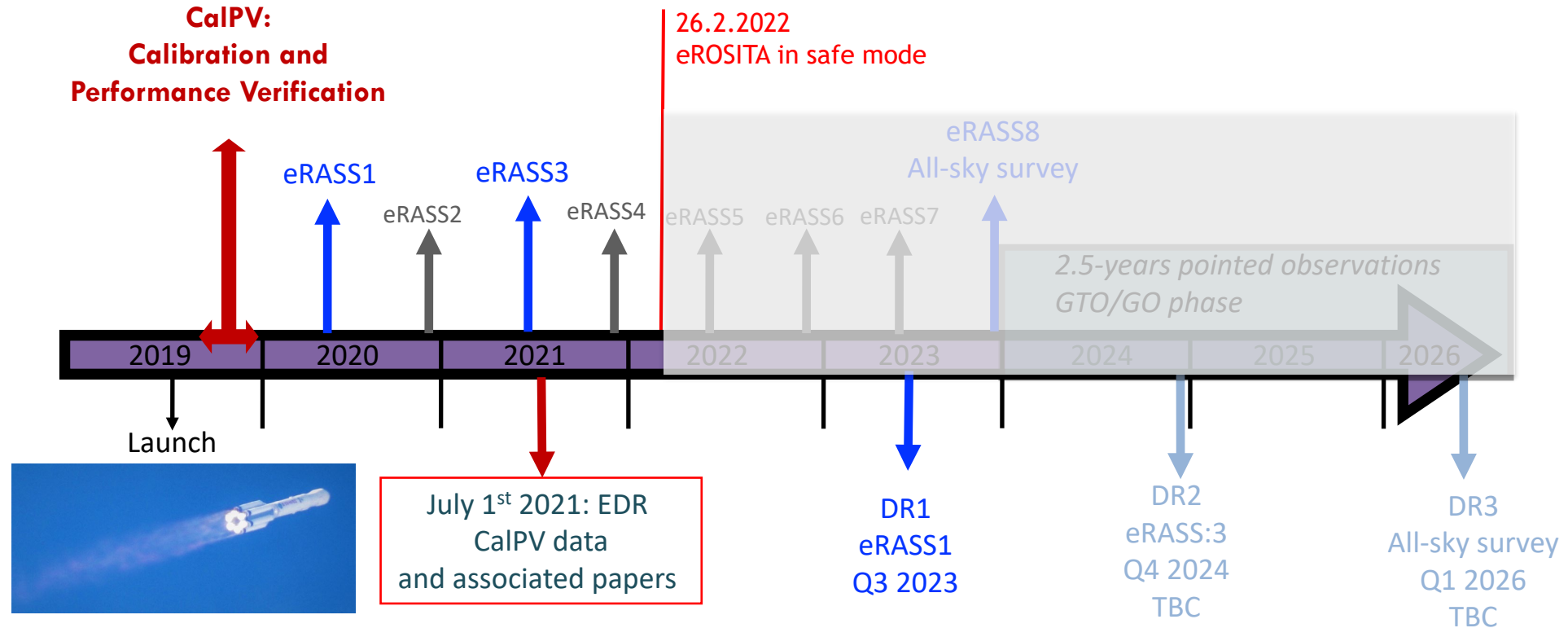
Gaussian
adaptive
smoothing

0.4-0.8: red
0.8-1.5: green
1.5-3.0: blue



Programmatics

eRASS = eROSITA All-Sky Survey



- Early Data Release (EDR) in 2021: several fields, including eFEDS mini-survey
- DR1 on 31.1.2024
- DR2 (eRASS:4.x) TBD (about two years from now)



The All-Sky Surveys by Numbers



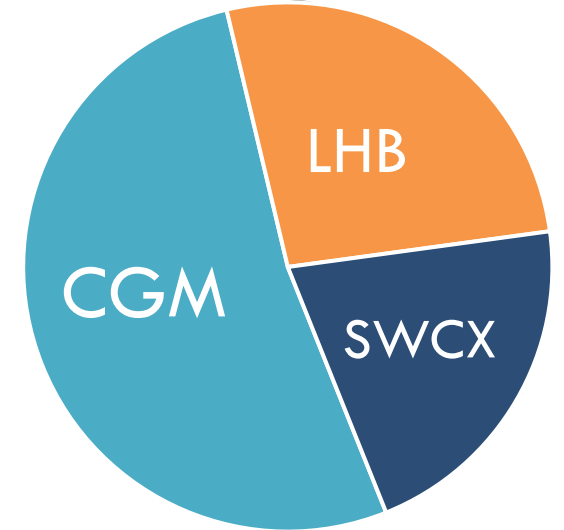
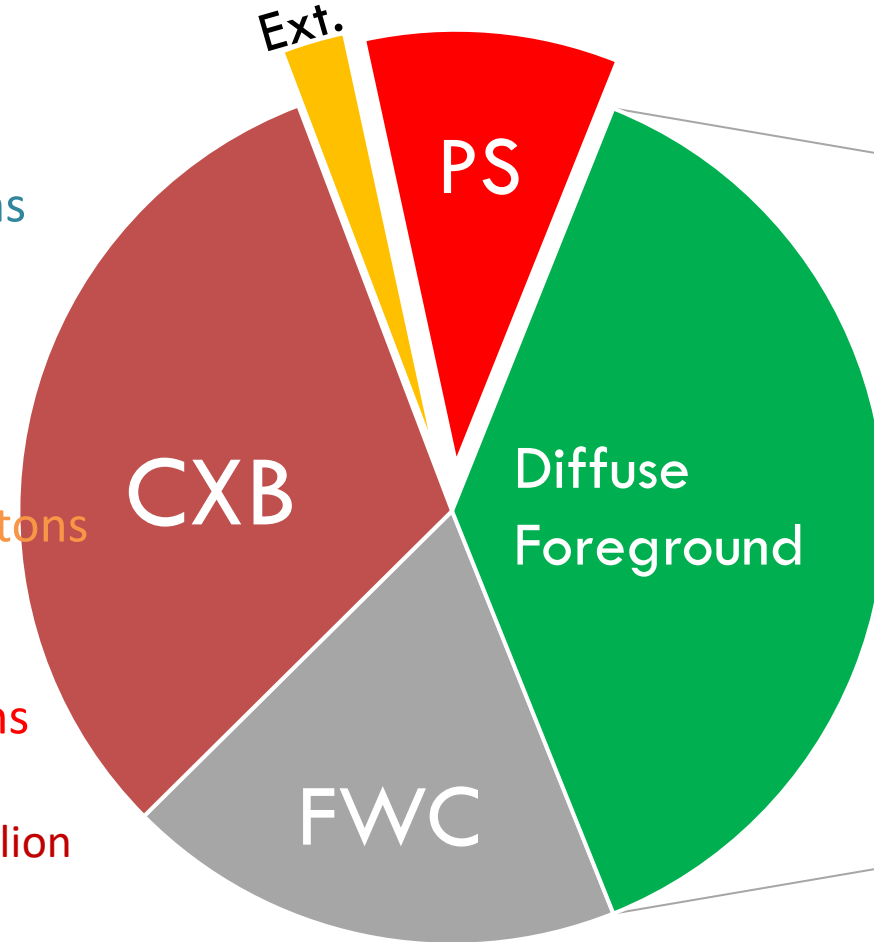
- Completed 4 all-sky survey (12/2019 – 12/2021)
- Uniform exposure, avg. ~ 800 s; up to 120ks at the Ecliptic Poles (confusion limited)
- Very few background flares, flexible mission planning: no gaps in exposure
- **~ 1.6 Billion** 0.2-5keV calibrated photons (~ 350 Gb telemetry)
- Typical (point-source) sensitivity:
 - Single pass (eRASS1,2,3,4)
 - $\sim 5 \times 10^{-14}$ erg/s/cm² [0.2-2.3 keV]; **4-5x deeper than RASS**
 - $\sim 7 \times 10^{-13}$ erg/s/cm² [2.3-5 keV]
 - Cumulative (eRASS:4)
 - $\sim 2 \times 10^{-14}$ erg/s/cm² [0.2-2.3 keV]
 - $\sim 2 \times 10^{-13}$ erg/s/cm² [2.3-5 keV]
- eRASS1 (half-sky): 0.9M point sources \sim doubles the number of known X-ray sources!
- eRASS:4 (half-sky): 2.8M point sources; 87k extended; ~ 45 k confirmed clusters



The eRASS1 (soft) photon Pie

~340 Million calibrated events

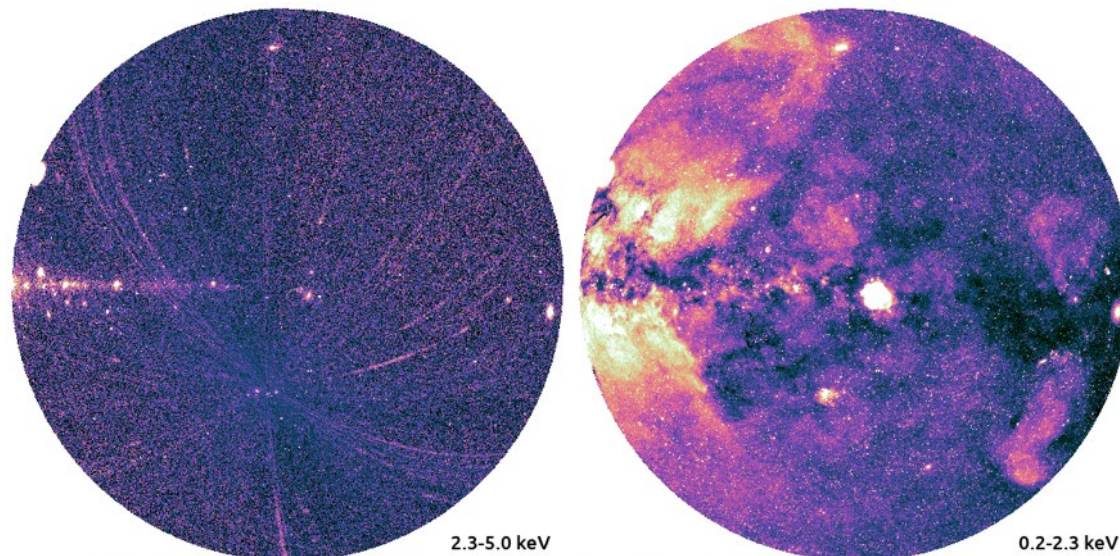
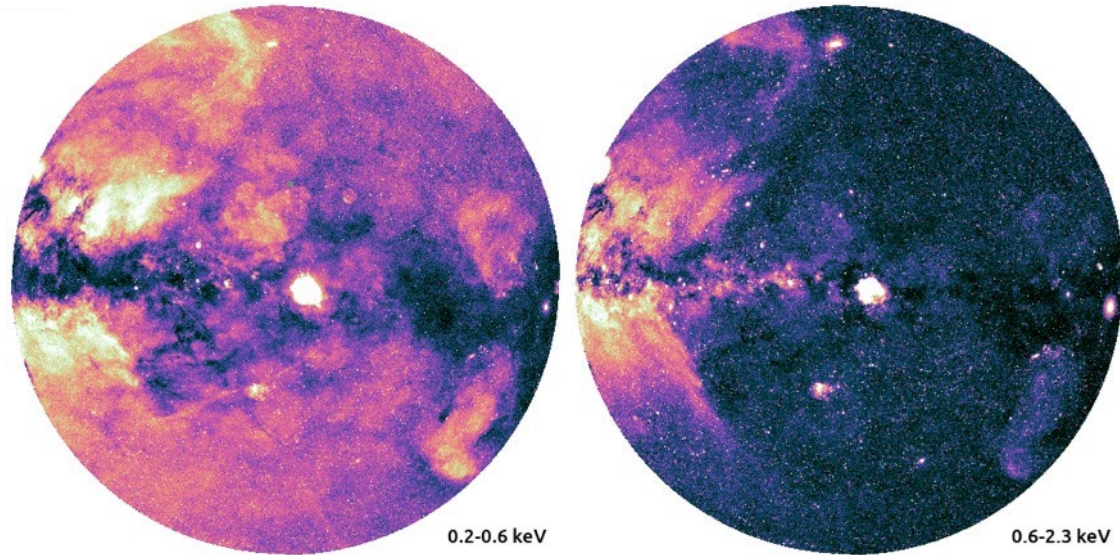
- 107 Million CXB photons
- 67 Million MW Hot CGM photons (58M halo + 9M 'Corona'; Ponti+'23)
- 63 Million Instrumental BKG photons (FWC)
- 34 Million Local Hot Bubble photons
- 27 Million Solar Wind Charge Exchange photons
- 32 Million Point Sources' photons
 - 24 Million AGN photons; 8 Million Stars photons
- 8 Million Extended Sources' photons



0.2-2.0 keV

Merloni et al. (2024)

erosita.mpe.mpg.de/dr1/

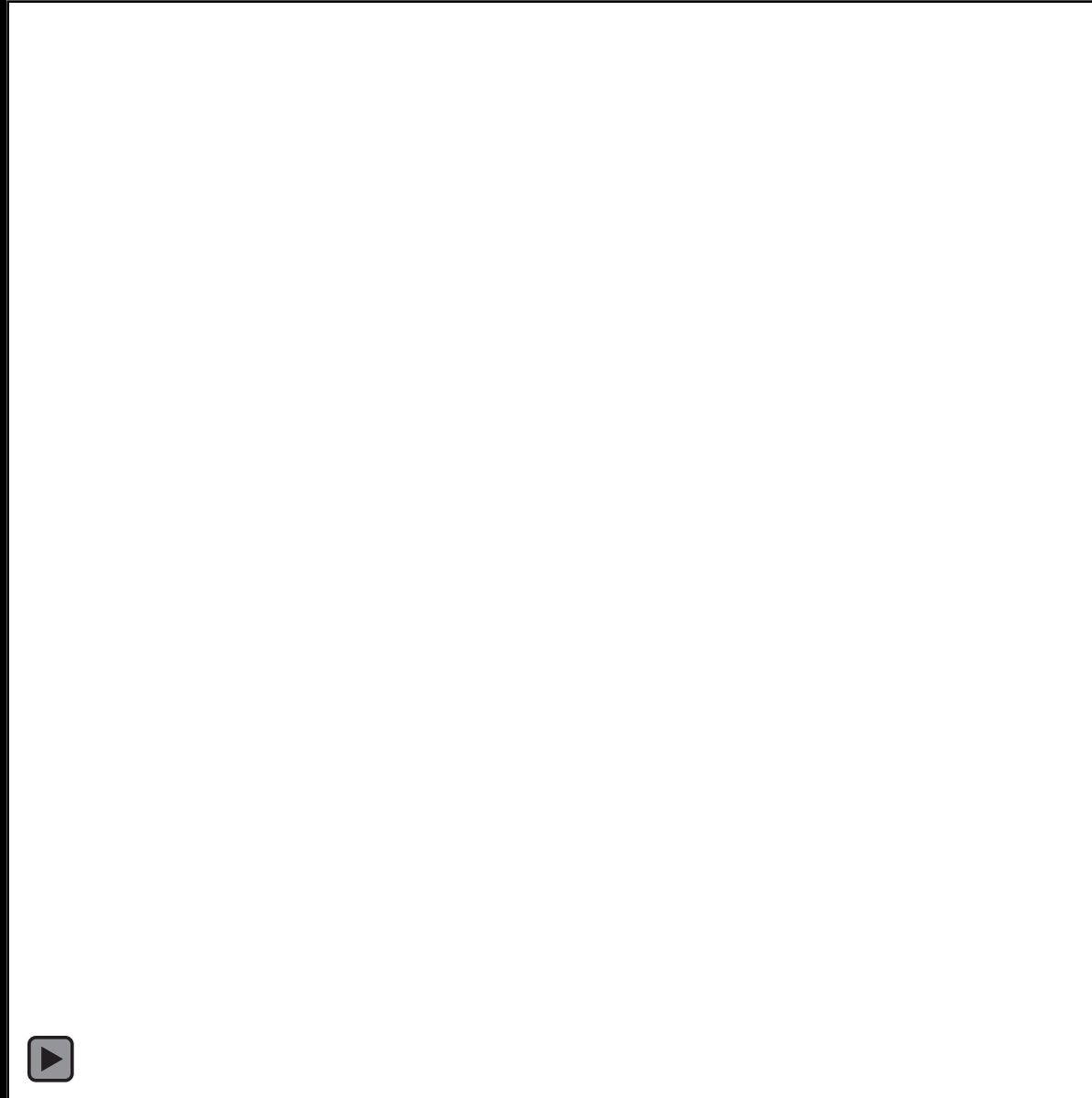


- Software
- Calibration DB
- Attitude files
- Exposure maps
- Events
- Count rate maps
- Source catalogues
- X-ray Spectra
- Light-curves

Merloni et al. (2024)

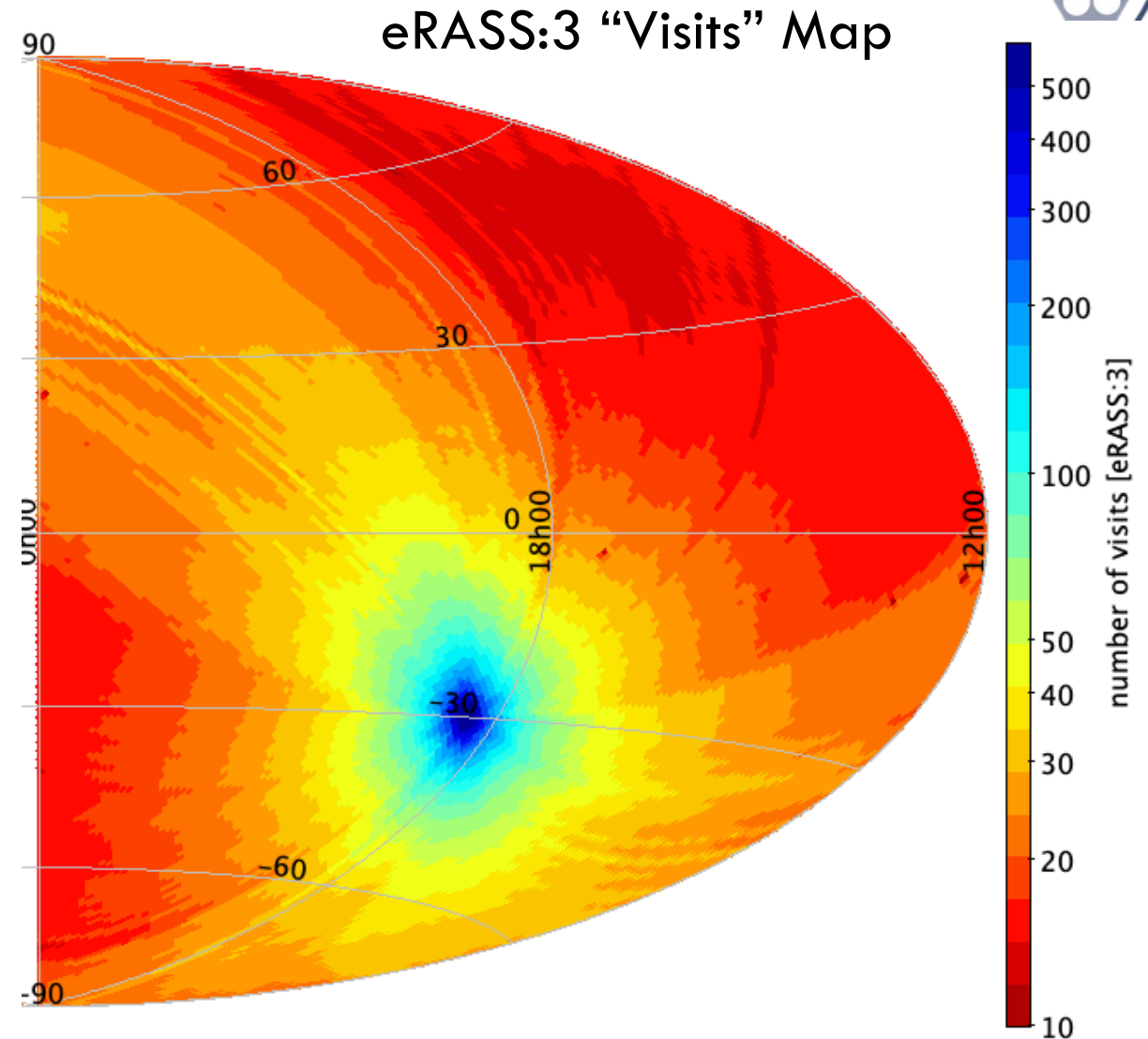
AO, 15/4/2024

eRASS1 in time domain



eRASS1 cts rate image
Movie courtesy
of J. Sanders (MPE)

- **50 msec [Readout]:** Time resolution of each CCD (frame readout cycle)
- **40 sec [Visit]:** Scan speed + 1 deg. FoV (avg effective exposure)
- **4 hours [eRoday]:** Rotation period of SRG (Interval between scans/visits)
- **1 day [Visibility]:** avg. visibility length (~6 visits)
- **6 months [eRASS]:** one complete all-sky survey (revisit period for most of the sky)
- **2 years: 4** all-sky surveys



- 50 msec [CCD (fram
- 40 sec [Vi
- effective
- 4 hours (Interval
- 1 day [V visits)
- 6 month survey (
- 2 years:

Article

X-ray detection of a nova in the fireball phase

<https://doi.org/10.1038/s41586-022-04635-y>

Received: 11 January 2022

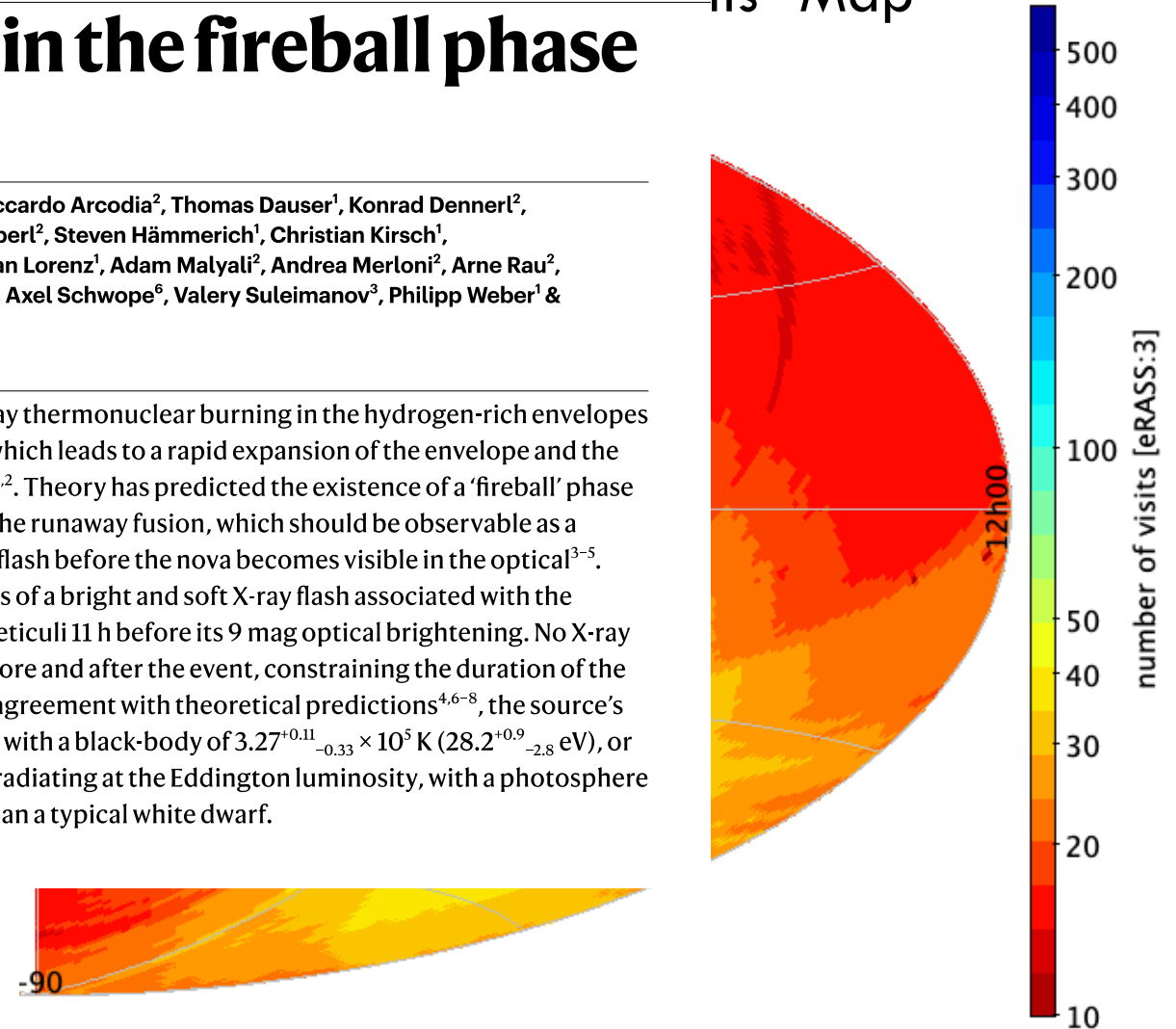
Accepted: 14 March 2022

Ole König¹✉, Jörn Wilms¹✉, Riccardo Arcodia², Thomas Dauser¹, Konrad Dennerl², Victor Doroshenko³, Frank Haberl², Steven Hämmerich¹, Christian Kirsch¹, Ingo Kreykenbohm¹, Maximilian Lorenz¹, Adam Malyali², Andrea Merloni², Arne Rau², Thomas Rauch³, Gloria Sala^{4,5}, Axel Schwobe⁶, Valery Suleimanov³, Philipp Weber¹ & Klaus Werner³

Novae are caused by runaway thermonuclear burning in the hydrogen-rich envelopes of accreting white dwarfs, which leads to a rapid expansion of the envelope and the ejection of most of its mass^{1,2}. Theory has predicted the existence of a ‘fireball’ phase following directly on from the runaway fusion, which should be observable as a short, bright and soft X-ray flash before the nova becomes visible in the optical^{3–5}. Here we report observations of a bright and soft X-ray flash associated with the classical Galactic nova YZ Reticuli 11 h before its 9 mag optical brightening. No X-ray source was detected 4 h before and after the event, constraining the duration of the flash to shorter than 8 h. In agreement with theoretical predictions^{4,6–8}, the source’s spectral shape is consistent with a black-body of $3.27^{+0.11}_{-0.33} \times 10^5$ K ($28.2^{+0.9}_{-2.8}$ eV), or a white dwarf atmosphere, radiating at the Eddington luminosity, with a photosphere that is only slightly larger than a typical white dwarf.



its” Map



- **50 msec [Readout]:** Tin CCD (frame readout cycle)
- **40 sec [Visit]:** Scan speed (effective exposure)
- **4 hours [eRoday]:** Rotation period (Interval between scans, 12h00)
- **1 day [Visibility]:** avg. number of visits
- **6 months [eRASS]:** one survey (revisit period for each source)
- **2 years: 4 all-sky surveys**

Article

X-ray quasi-periodic eruptions from two previously quiescent galaxies

<https://doi.org/10.1038/s41586-021-03394-6>

Received: 23 November 2020

Accepted: 25 February 2021

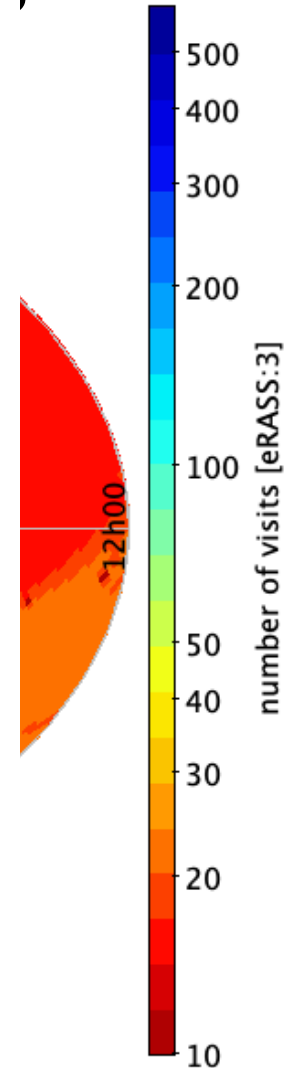
Published online: 28 April 2021

Open access

 Check for updates

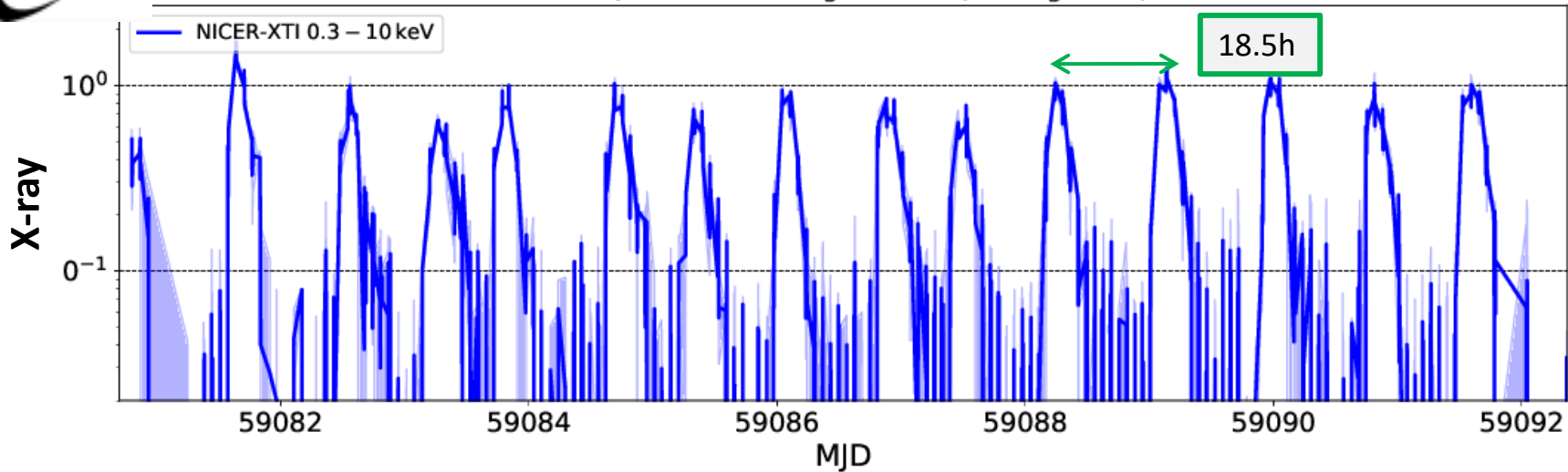
R. Arcodia^{1,2,3}, A. Merloni¹, K. Nandra¹, J. Buchner¹, M. Salvato¹, D. Pasham², R. Remillard², J. Comparat¹, G. Lamer³, G. Ponti^{1,4}, A. Malyali¹, J. Wolf¹, Z. Arzoumanian⁵, D. Bogensberger¹, D. A. H. Buckley⁶, K. Gendreau⁵, M. Gromadzki⁷, E. Kara², M. Krumpel³, C. Markwardt⁵, M. E. Ramos-Ceja¹, A. Rau¹, M. Schramm⁸ & A. Schwobe³

Quasi-periodic eruptions (QPEs) are very-high-amplitude bursts of X-ray radiation recurring every few hours and originating near the central supermassive black holes of galactic nuclei^{1,2}. It is currently unknown what triggers these events, how long they last and how they are connected to the physical properties of the inner accretion flows. Previously, only two such sources were known, found either serendipitously or in archival data^{1,2}, with emission lines in their optical spectra classifying their nuclei as hosting an actively accreting supermassive black hole^{3,4}. Here we report observations of QPEs in two further galaxies, obtained with a blind and systematic search of half of the X-ray sky. The optical spectra of these galaxies show no signature of black hole activity, indicating that a pre-existing accretion flow that is typical of active galactic nuclei is not required to trigger these events. Indeed, the periods, amplitudes and profiles of the QPEs reported here are inconsistent with current models that invoke radiation-pressure-driven instabilities in the accretion disk⁵⁻⁹. Instead, QPEs might be driven by an orbiting compact object. Furthermore, their observed properties require the mass of the secondary object to be much smaller than that of the main body¹⁰, and future X-ray observations may constrain possible changes in their period owing to orbital evolution. This model could make QPEs a viable candidate for the electromagnetic counterparts of so-called extreme-mass-ratio inspirals¹¹⁻¹³, with considerable implications for multi-messenger astrophysics and cosmology^{14,15}.



Quasi Periodic Eruptions (QPEs)

eRO-QPE1 - NICER light curve (19 Aug 2020)



QPE1

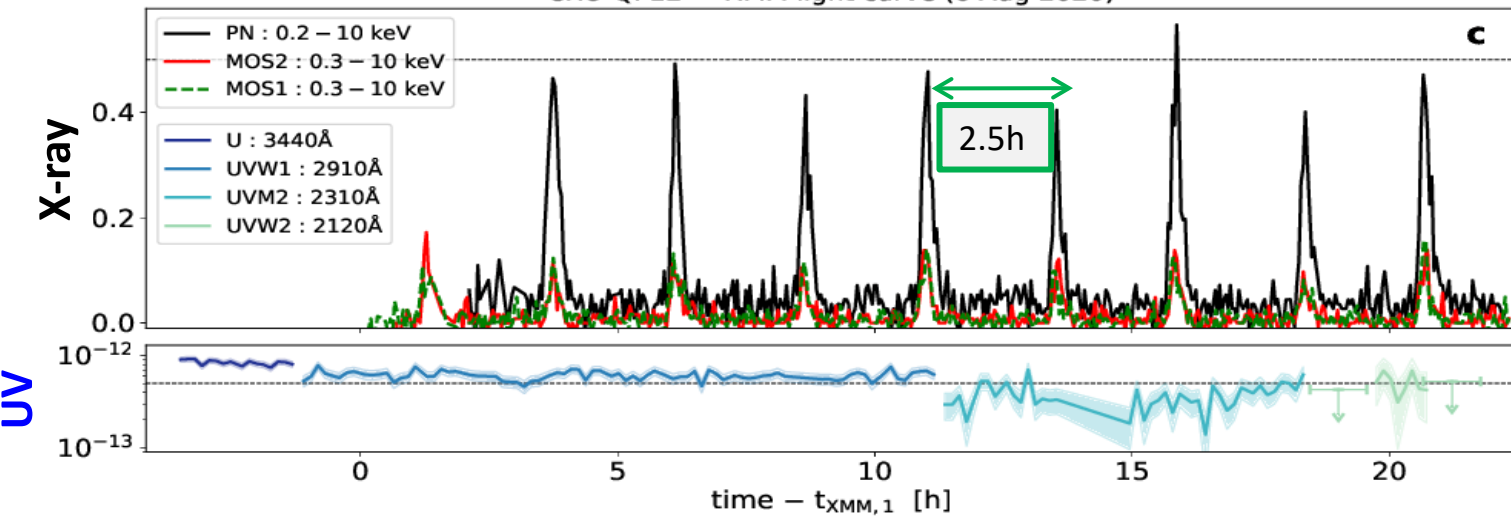
followed-up with XMM+NICER

$$Lx_{0.5-2keV}^{peak} \approx 1e43 \text{ erg s}^{-1}$$

11 days!

Arcodia+21

eRO-QPE2 - XMM light curve (6 Aug 2020)



QPE2

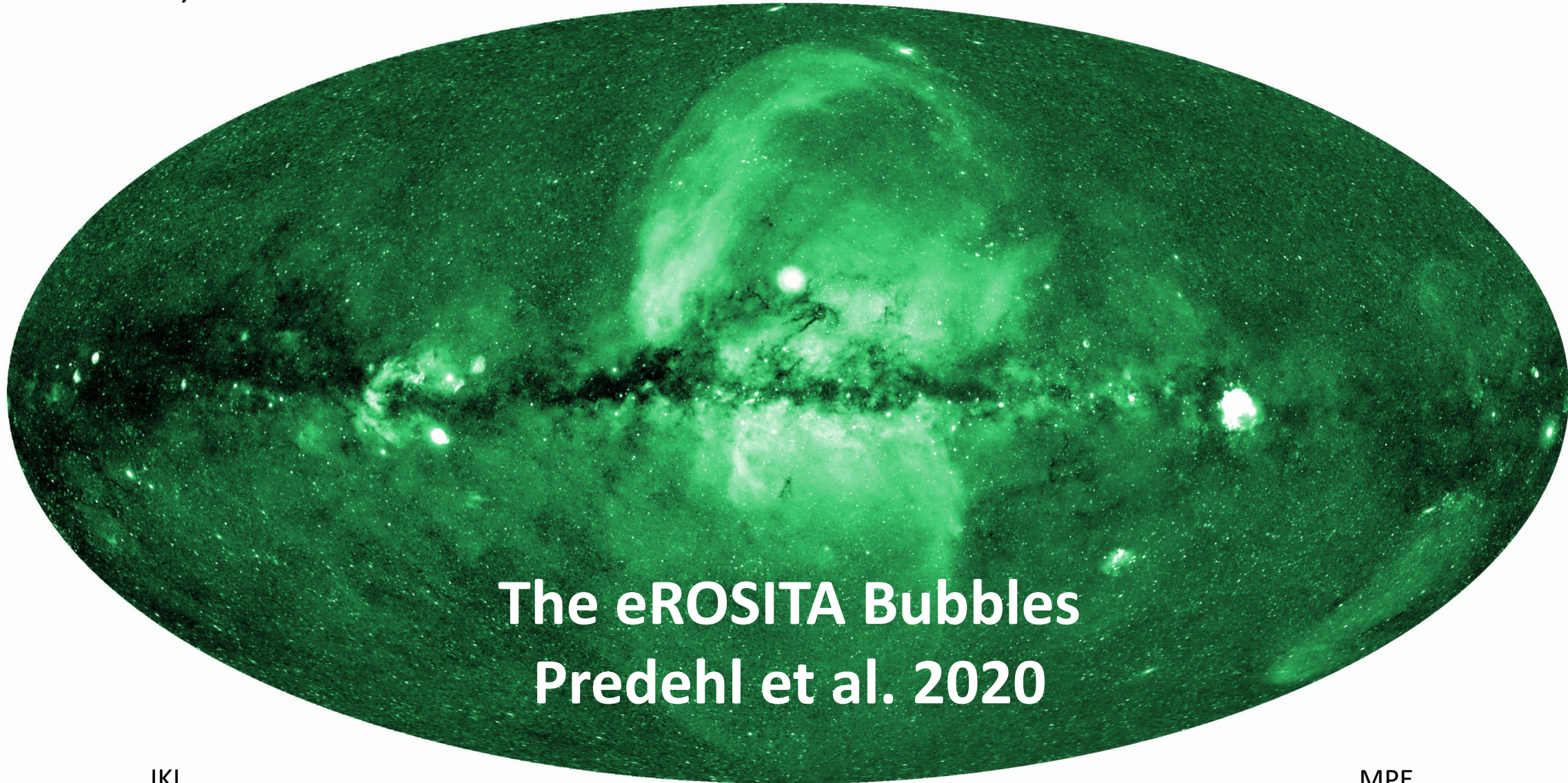
followed-up with XMM-Newton

$$Lx_{0.5-2keV}^{peak} \approx 1e42 \text{ erg s}^{-1}$$

1 day!

Arcodia et al. 2021, Nature

Arcodia+21



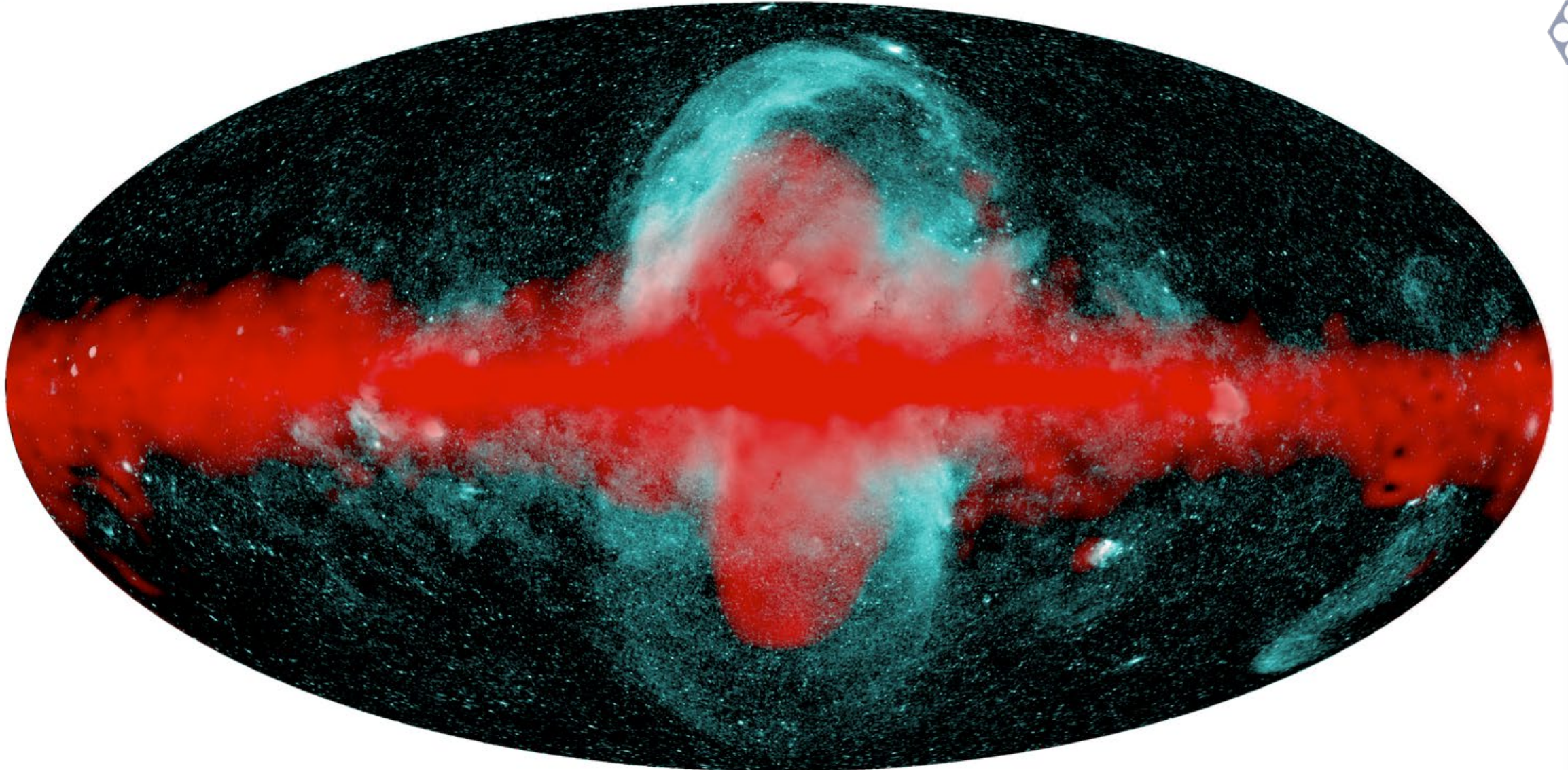
The eROSITA Bubbles Predehl et al. 2020

IKI

MPE

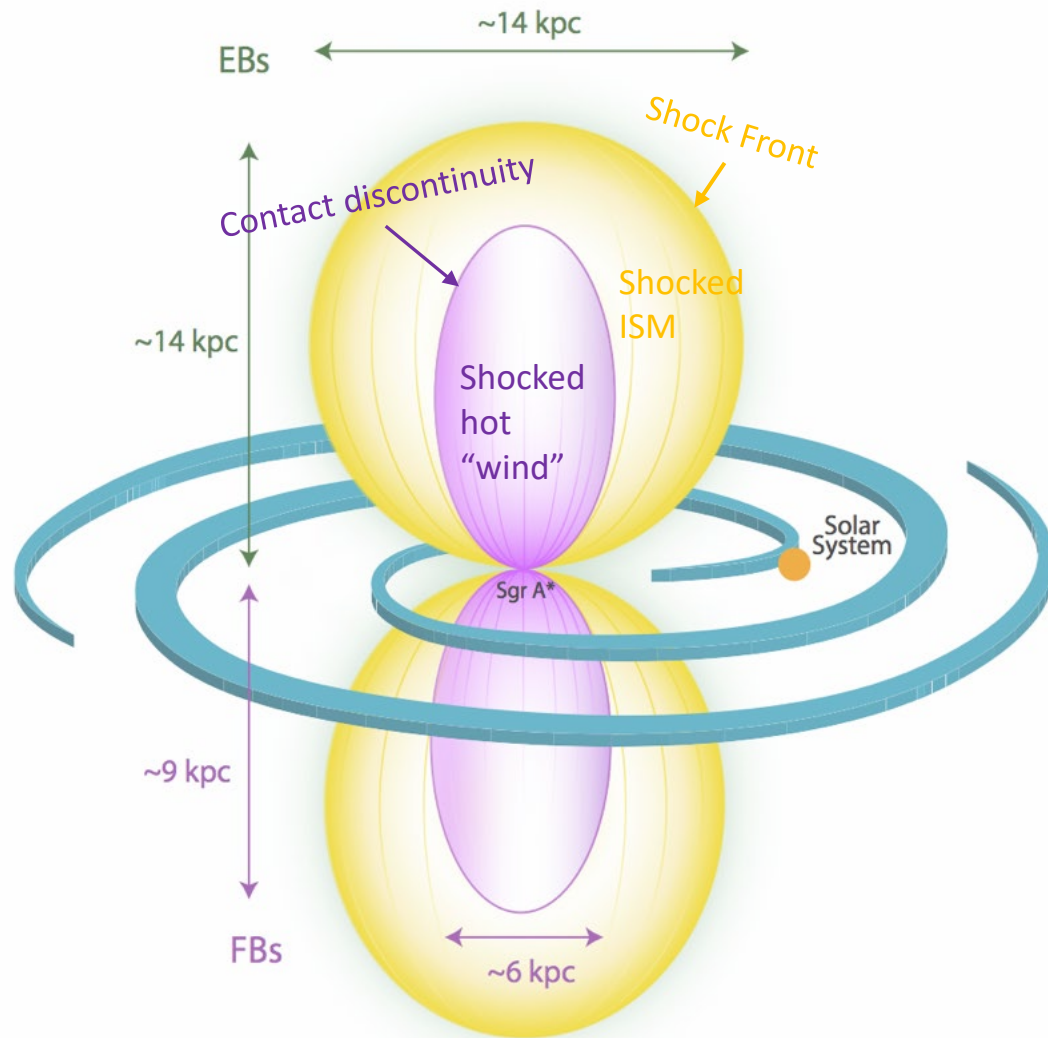
Credit: Sanders, Brunner (MPE); Churazov, Gilfanov (IKI)

Fermi ($>1\text{GeV}$) vs. eRASS1, 0.6-1 keV



Credit: Khabibullin, Selig (MPA)

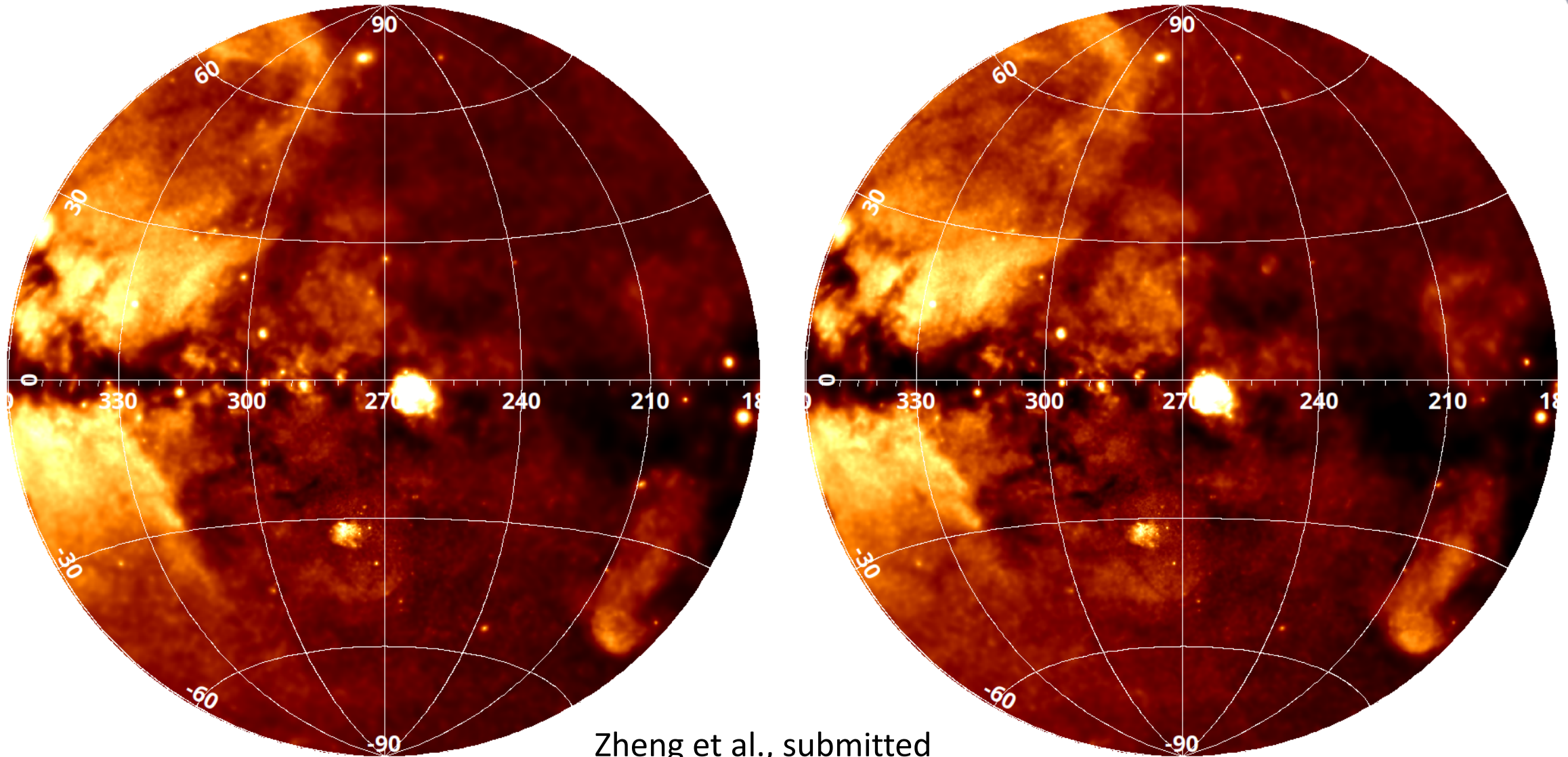
The eROSITA Bubbles



- $L_{X,tot} \sim 10^{39}$ erg/s
- Energetics:
 - Assume $kT=0.3$ keV and abundances of 0.2 Solar
 - Shock with $M \sim 1.5$ (from T jump)
- $E_{tot} \sim 10^{56}$ erg (~ 10 x Fermi bubbles!)
 - Age ~ 20 Myr
 - Energy release rate of $\sim 1-3 \times 10^{41}$ erg/s
- Gas Cooling time $\sim 2 \times 10^8$ years (\gg age of bubbles)

Predehl, Sunyaev et al. Nature (2020)

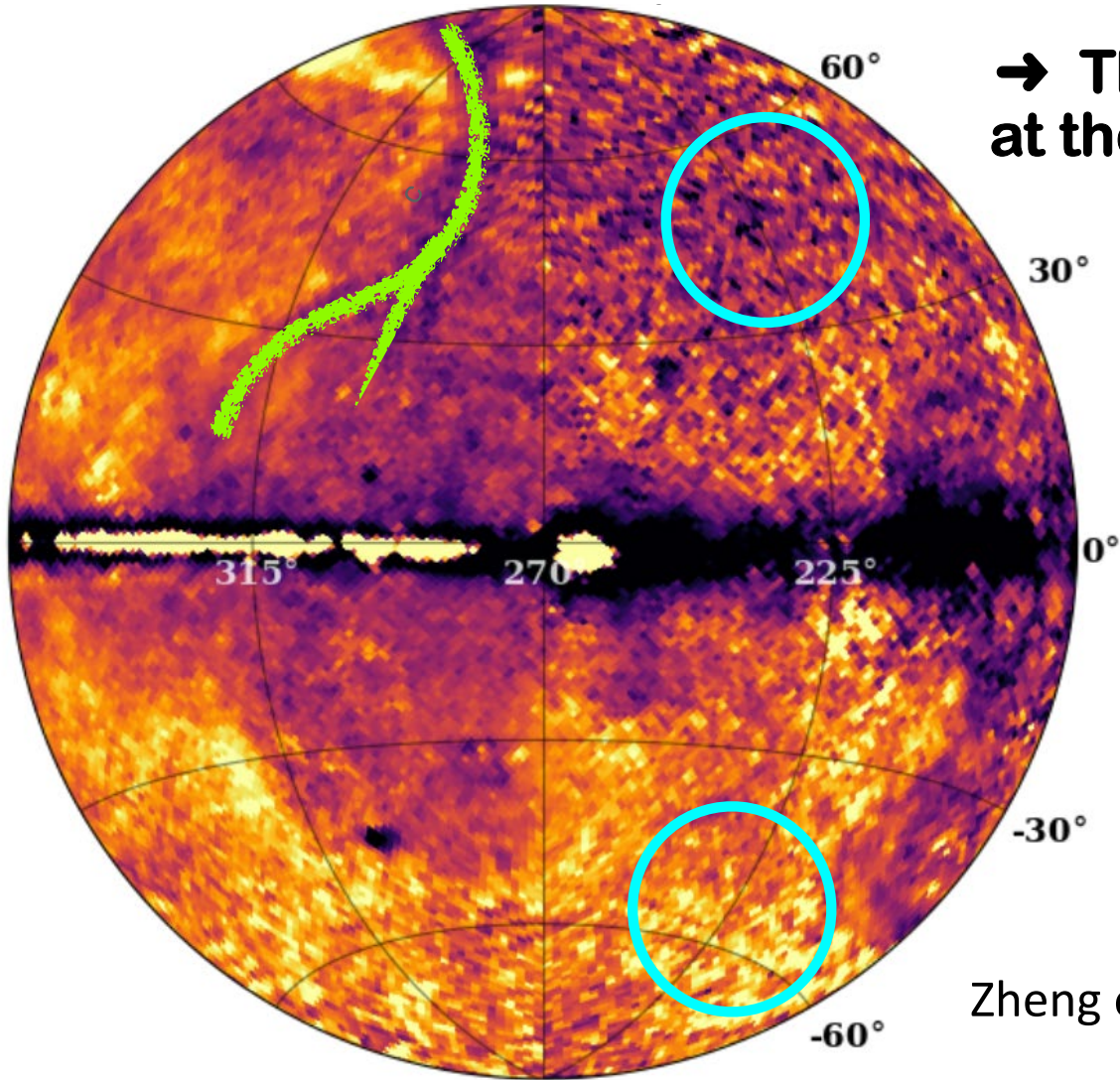
Narrow band maps: OVII and OVIII



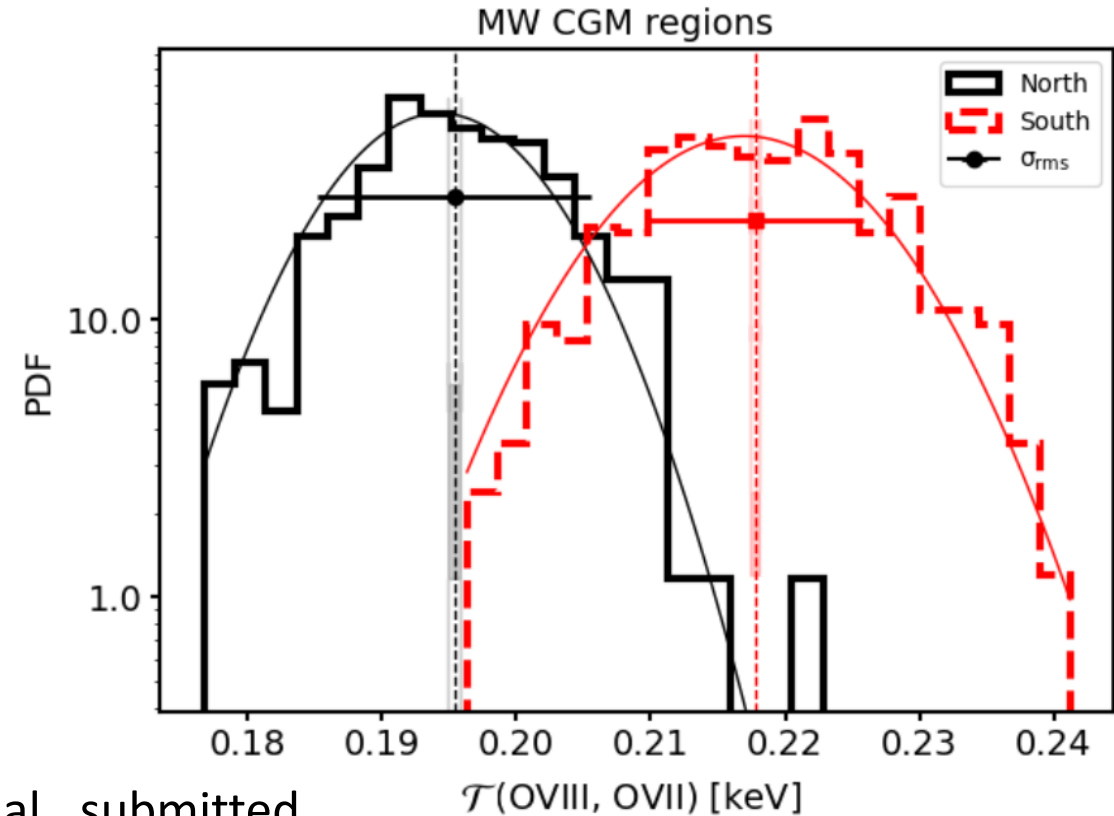
Zheng et al., submitted



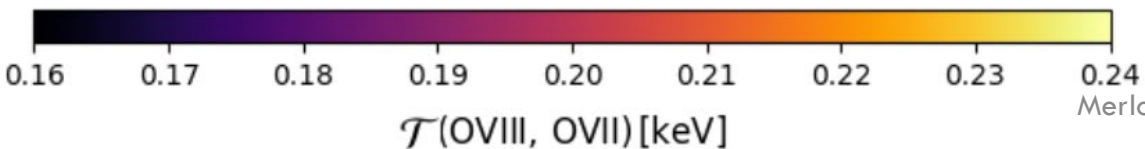
Pseudo-temperature map from OVIII/OVII



→ Thick (~10°) shell of (colder?) plasma at the interface with the Galactic outflow



Zheng et al., submitted

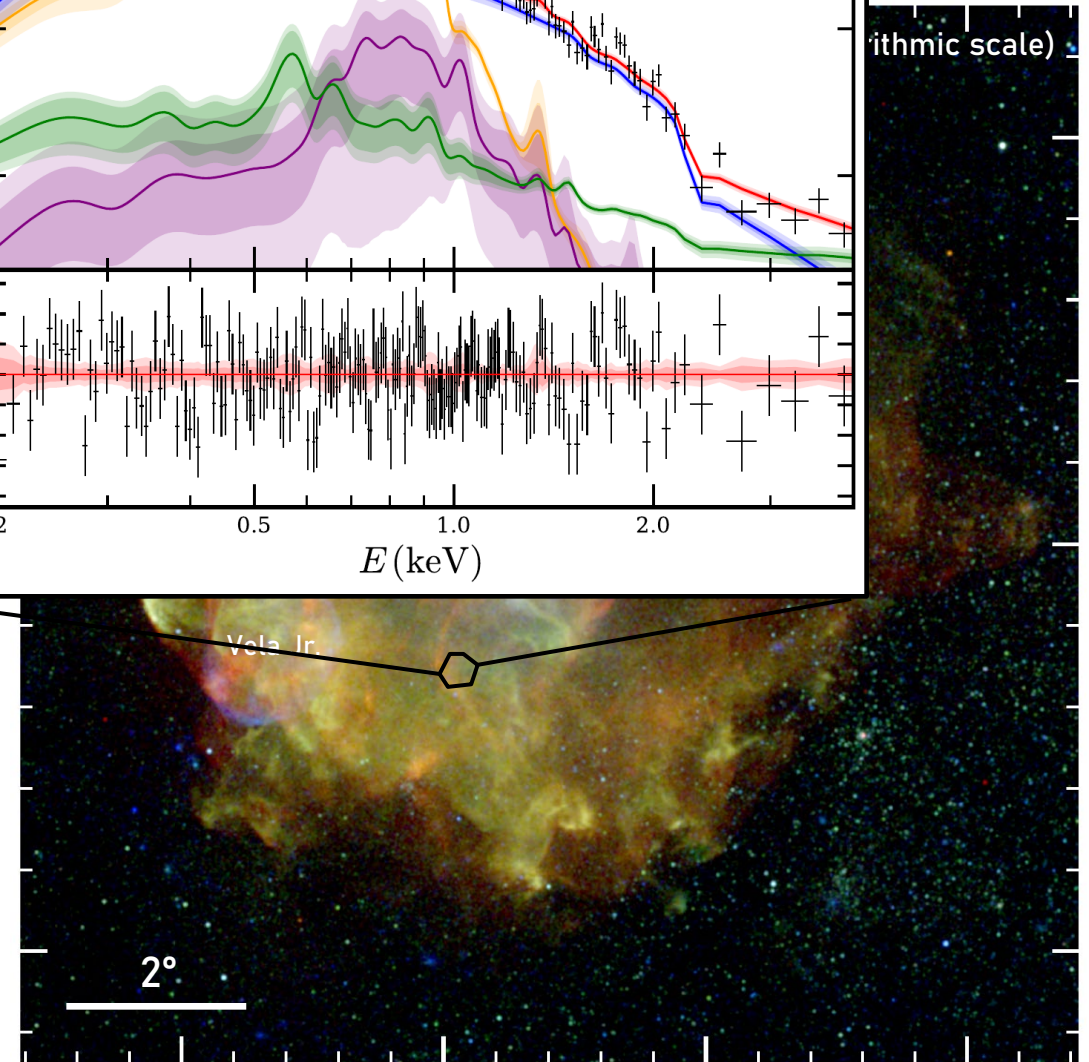
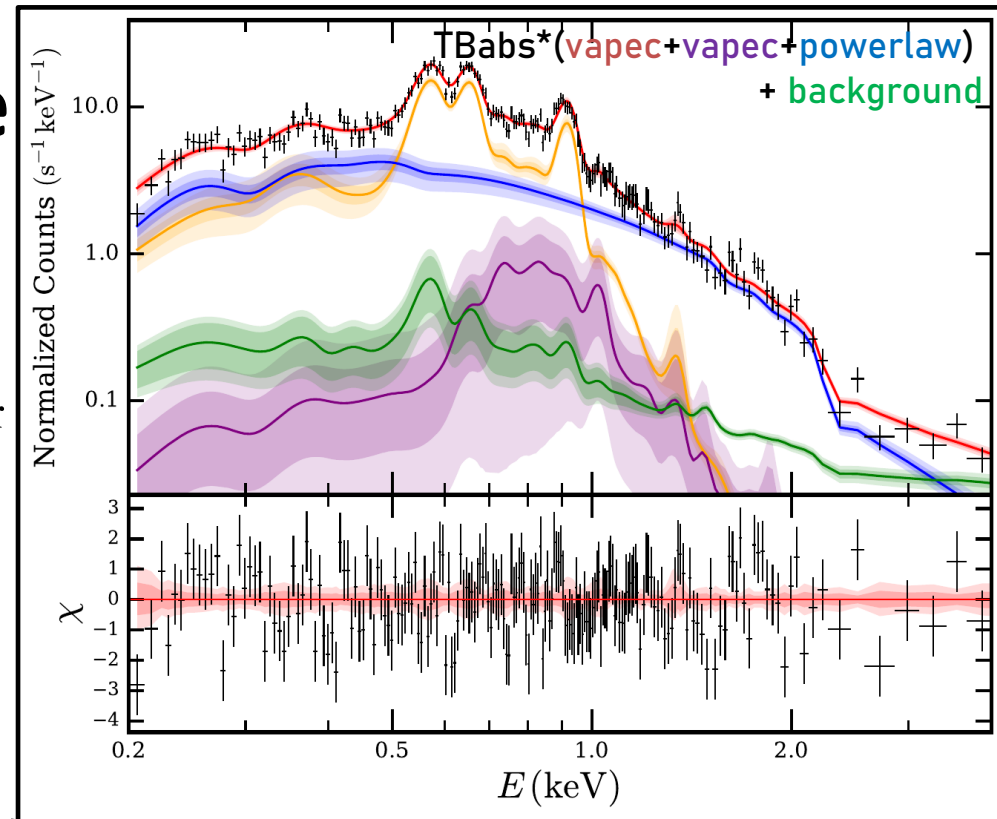


→ $\Delta kT_{\text{CGM}} < 4\%$ on small (2°-20°) scales

The Vela Supe

- Very extended X-ray-bright core-collapse SNR
 - Central energetic pulsar PSR B0833-45 & pulsar wind nebula (Vela X)
 - Nearby (~ 290 pc; *Dodson+03*)
 - Age $\sim 11 - 30$ kyr (*Manchester+05, Espinoza+17*)

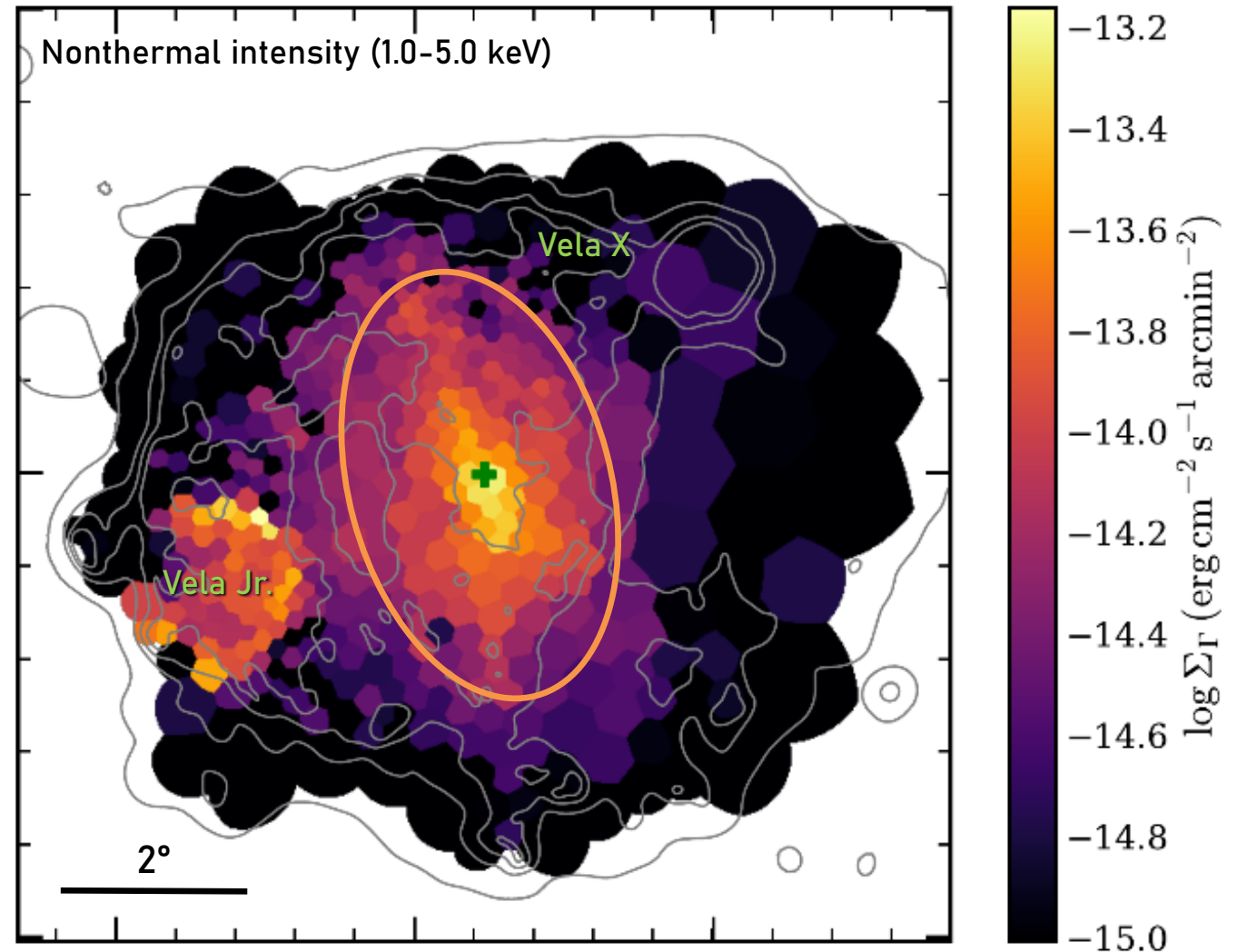
- eRASS:4 data provide opportunity to study
 - Foreground absorption (➤ Local ISM properties)
 - Ejecta distribution & composition (➤ SN nucleosynthesis)
 - Synchrotron emission from PWN (➤ Cosmic ray acceleration)



Mayer, Becker et al. (2023)

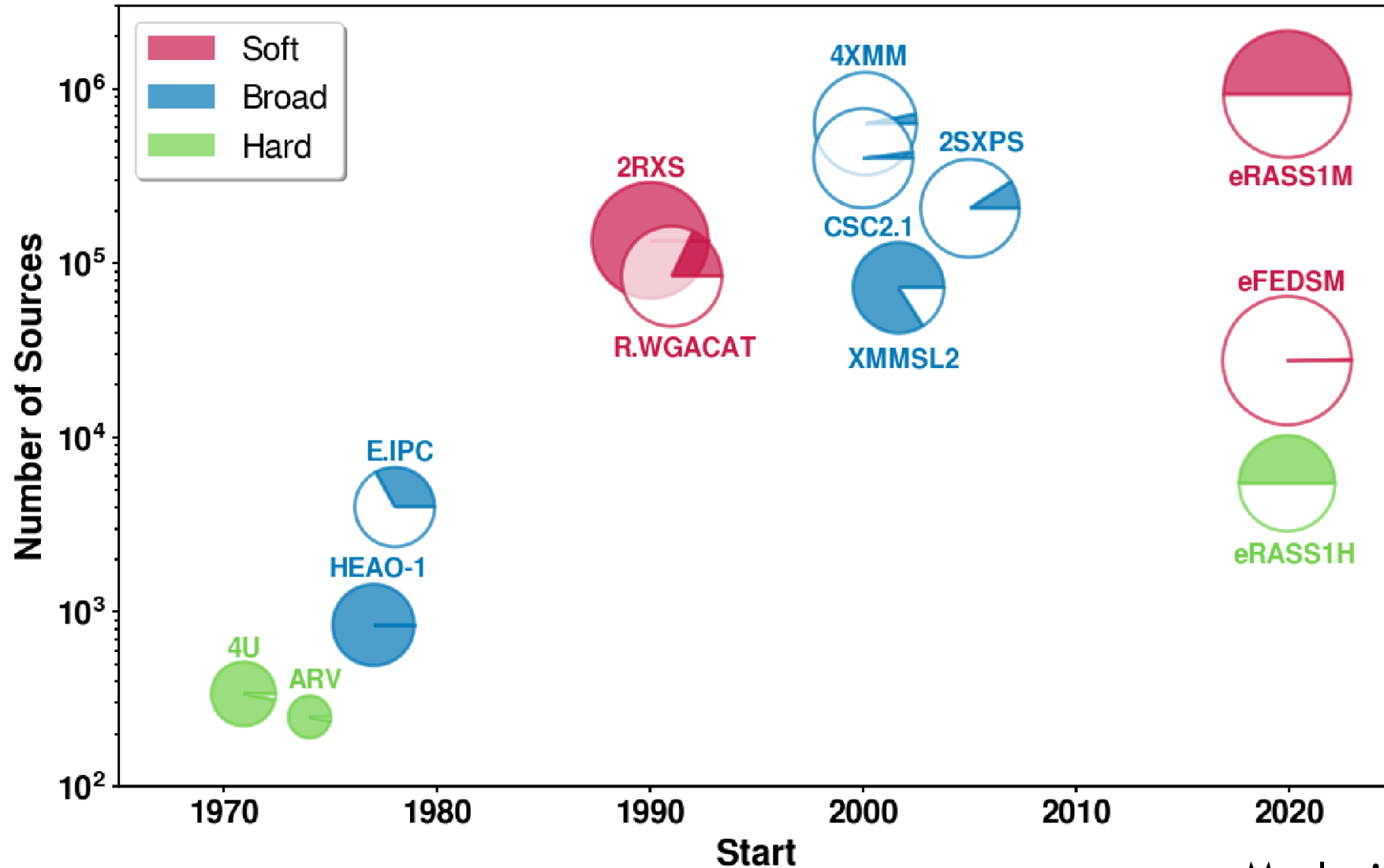
Vela SNR: Non-thermal Emission

- Vela X, prior to eROSITA:
 - Synchrotron emission in „Cocoon“ visible with ROSAT & XMM (*e.g.* *Slane+2018*)
- With eROSITA, observe much larger size of pulsar’s diffuse X-ray nebula, with a radial extent of $2^\circ - 3^\circ$



Mayer, Becker et al. (2023)

eRASS1 and X-ray catalogues



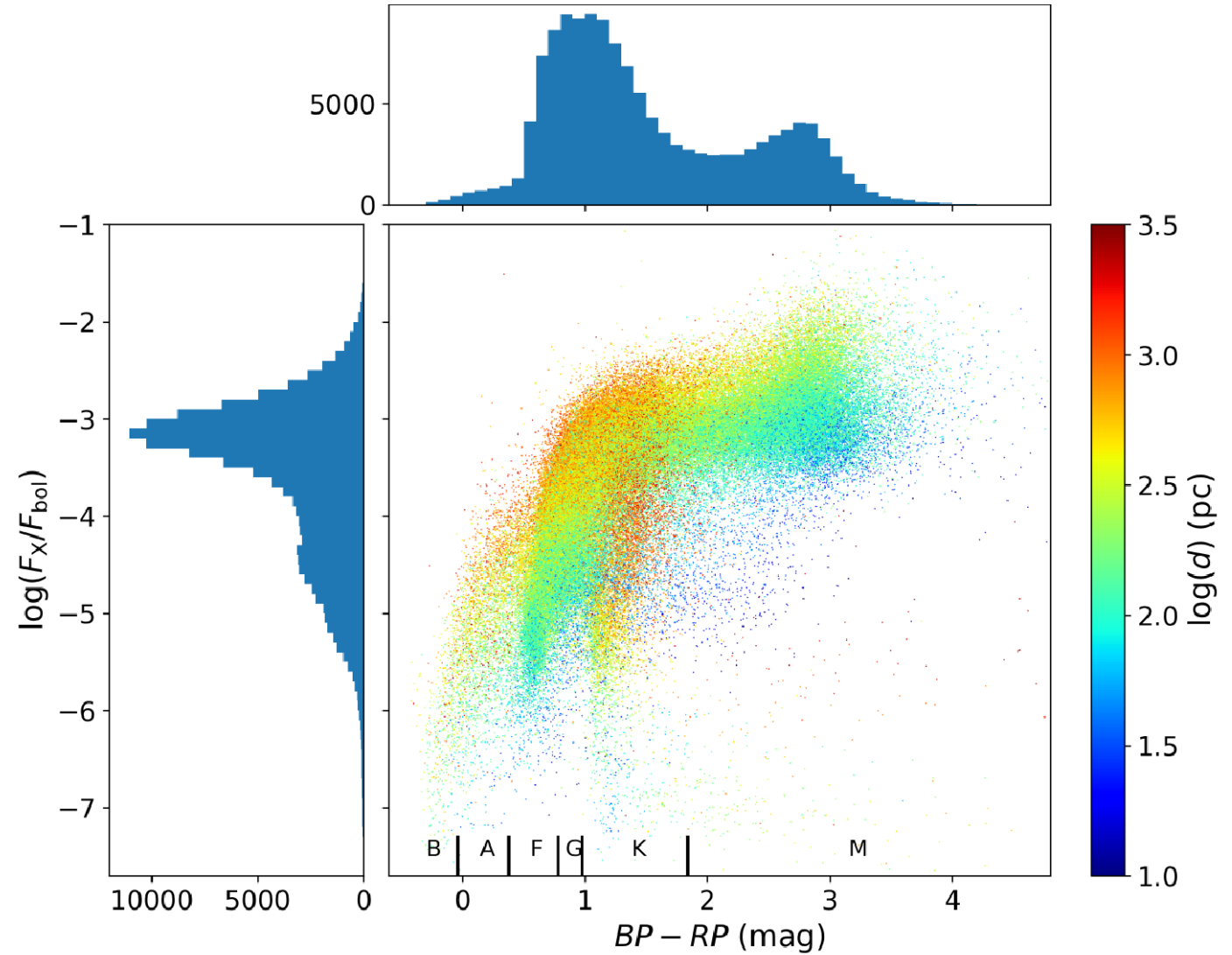
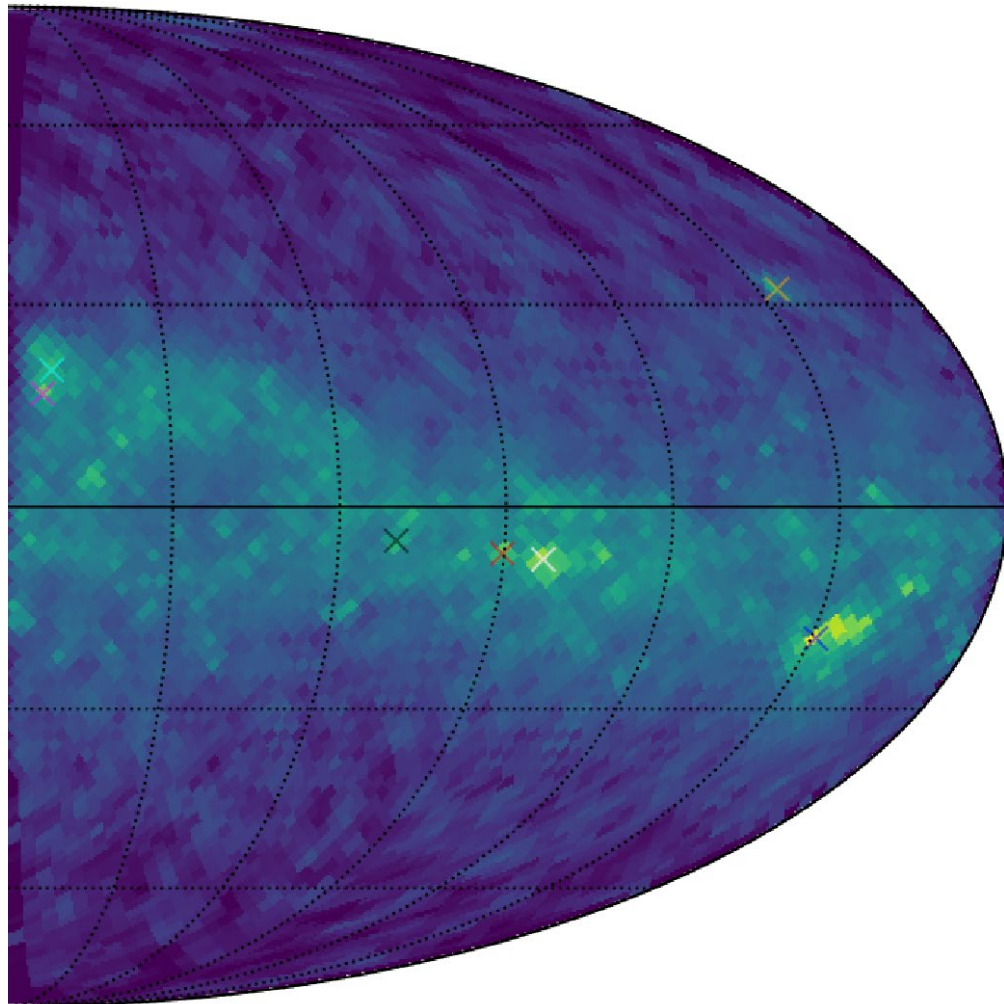
Merloni et al. (2024)

The SRG/eROSITA all-sky survey: Identifying ~130k coronal-emitting stars

Freund et al. (2024)



- ✕ rho Oph Cloud
- ✕ Orion Nebula
- ✕ gam Vel Cluster
- ✕ omi Vel Cluster
- ✕ IC2602
- ✕ Praesepe
- ✕ Upper Sco



Searching for X-ray counterparts of unassociated Fermi-LAT sources and rotation-powered pulsars with SRG/eROSITA



Mayer and Becker, (2024)

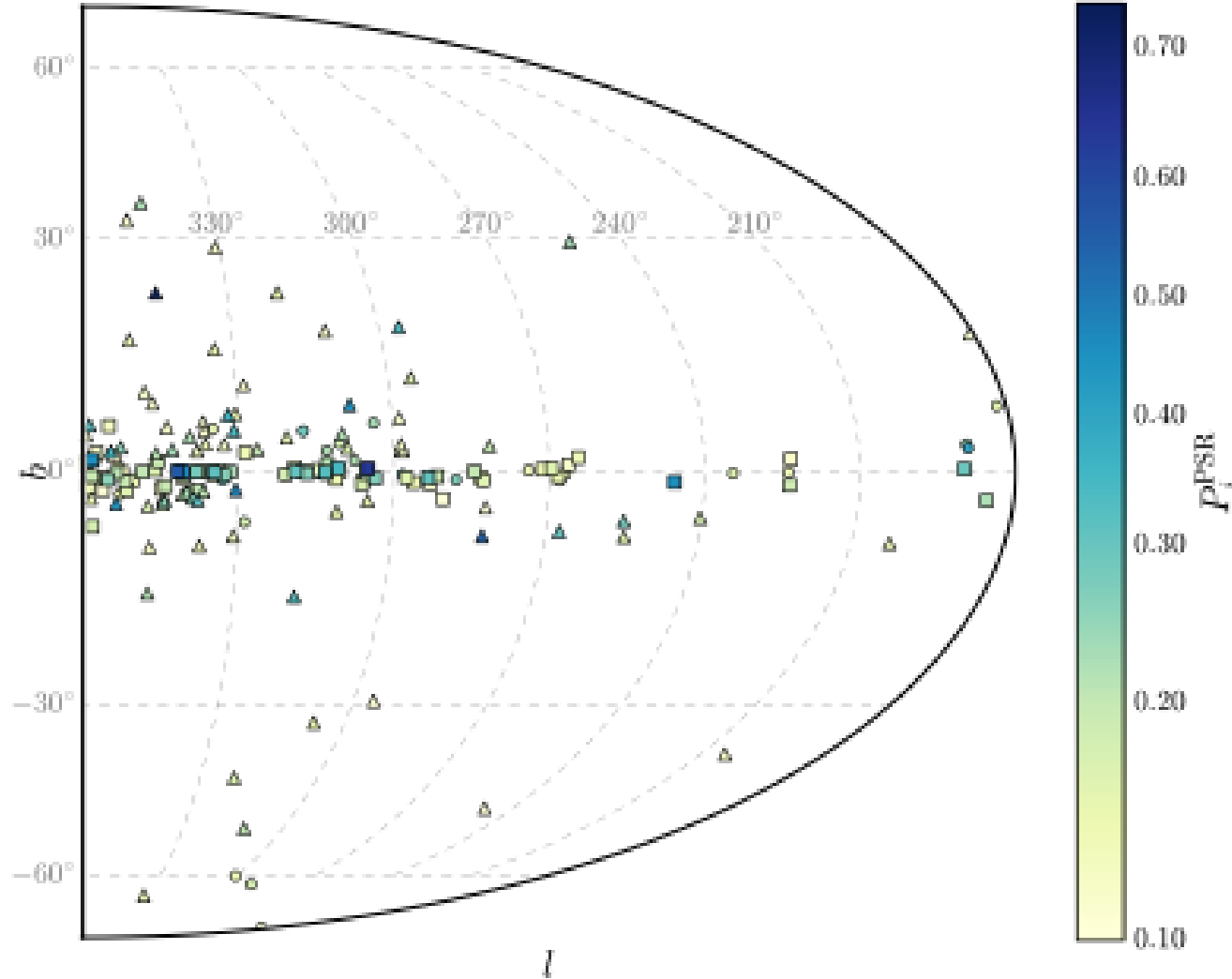
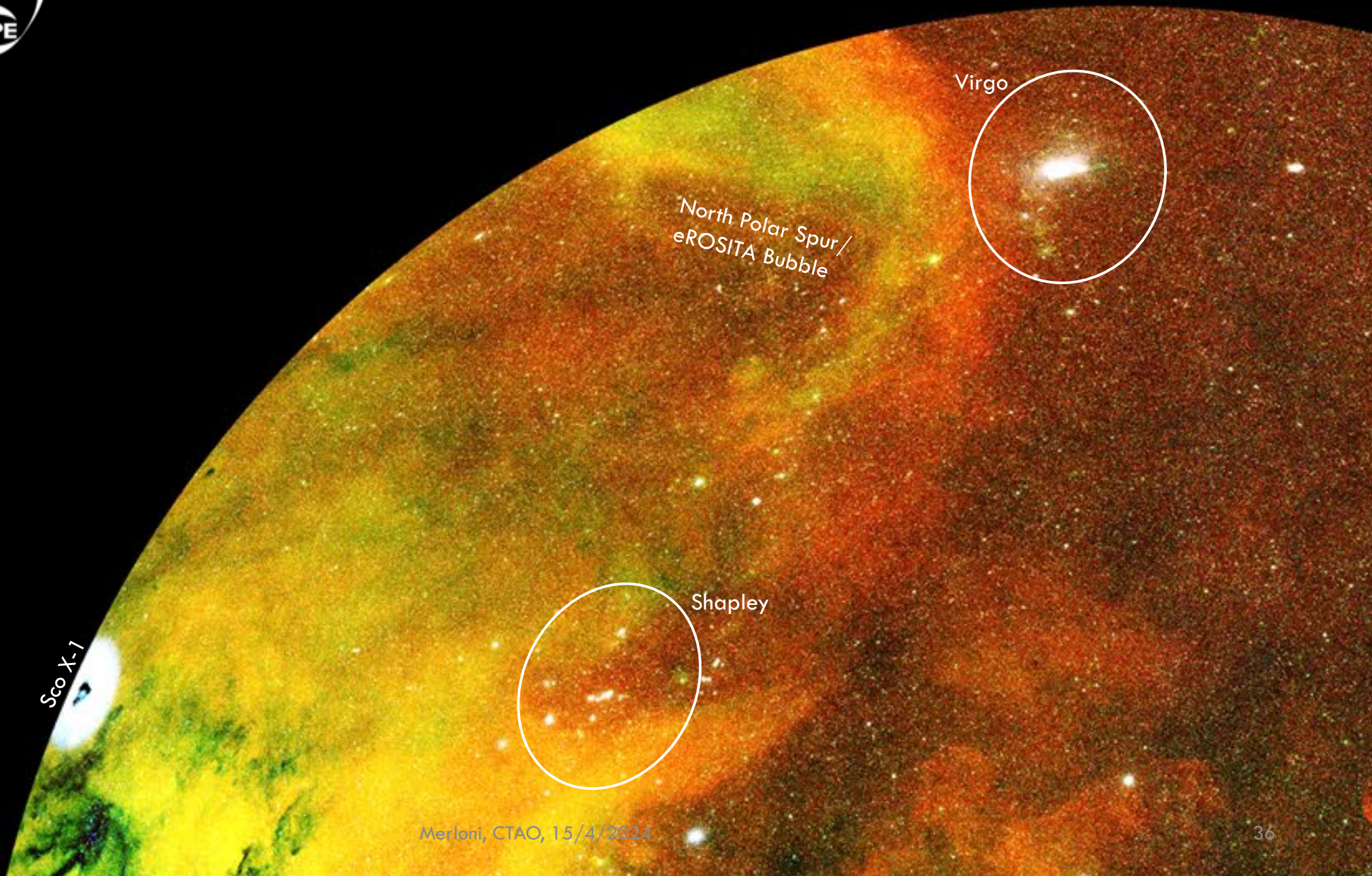


Table 4: List of top 50 candidate pulsar-type matches to 4FGL sources.

#	α_x deg	δ_x deg	σ_x arcsec	\mathcal{L}_{det}	\mathcal{L}_{ext}	Source_Name_4FGL	P_γ^{PSR}	P_i^{PSR}	P_i^{NG}	P_i^{MSP}	P_i^{AGN}	Comment
1	236.06418	-25.92528	3.0	19.8	0.0	4FGL J1544.2-2554	0.997	0.753	0.000	0.753	0.001	
2	197.23184	-62.41172	1.6	180.0	0.0	4FGL J1309.1-6223	0.997	0.637	0.630	0.007	0.003	
3	253.31237	-43.82513	4.2	5.2	0.0	4FGL J1653.2-4349	0.989	0.563	0.562	0.000	0.000	(a)
4	143.50470	-62.56495	2.5	38	0.0	4FGL J0933.8-6232	1.000	0.540	0.032	0.509	0.000	(a)
5	244.20254	-53.69458	2.3	48	0.0	4FGL J1616.6-5341	1.000	0.480	0.176	0.303	0.000	(b)
6	252.34131	-44.73401	1.8	112	0.0	4FGL J1649.3-4441	0.990	0.477	0.460	0.017	0.009	(b)
7	118.04167	-29.50531	1.6	217	0.0	4FGL J0752.0-2931	0.999	0.452	0.436	0.016	0.003	(c)
8	263.86181	-29.75370	7.7	18.0	6.1	4FGL J1735.4-2944	0.913	0.451	0.427	0.024	0.291	
9	201.34839	-54.23968	3.8	10.3	0.0	4FGL J1325.3-5413	0.968	0.448	0.018	0.430	0.005	(d)
10	266.41332	-36.42802	3.0	37	0.0	4FGL J1745.6-3626	0.751	0.448	0.023	0.425	0.267	
11	236.33279	-45.90416	2.2	77	0.0	4FGL J1545.2-4553	0.911	0.361	0.024	0.337	0.131	
12	260.52566	-32.08855	4.2	5.4	0.0	4FGL J1722.1-3205	0.971	0.349	0.033	0.316	0.003	
13	209.23867	-61.38800	1.8	130	0.0	4FGL J1357.3-6123	0.952	0.348	0.337	0.011	0.037	(b, e)
14	236.81672	-48.00443	3.5	16.1	0.0	4FGL J1547.4-4802	0.944	0.348	0.035	0.313	0.018	
15	183.49466	-44.25681	4.0	10.8	0.0	4FGL J1213.9-4416	0.945	0.335	0.002	0.332	0.007	
16	214.66390	-61.19200	5.2	10.3	0.0	4FGL J1418.7-6110	0.917	0.326	0.318	0.007	0.005	
17	260.15801	-26.87634	2.5	33	0.0	4FGL J1720.6-2653c	0.400	0.324	0.031	0.293	0.539	
18	245.57301	-72.05278	4.1	13.2	0.0	4FGL J1622.2-7202	0.997	0.323	0.000	0.323	0.001	
19	253.57303	-49.11719	3.3	12.6	0.0	4FGL J1654.2-4907c	0.287	0.319	0.046	0.273	0.306	
20	246.53852	-49.29462	2.6	28.3	0.0	4FGL J1626.0-4917c	0.483	0.311	0.293	0.018	0.248	
21	225.02645	-58.77219	5.1	7.5	0.0	4FGL J1500.1-5846	0.509	0.306	0.301	0.005	0.068	
22	171.97380	-62.02326	1.5	163	0.0	4FGL J1127.9-6158	0.998	0.303	0.291	0.012	0.001	(f)
23	126.56484	-50.90072	4.2	8.9	0.0	4FGL J0826.1-5053	0.986	0.301	0.002	0.298	0.001	
24	92.18263	20.59542	4.0	39	0.0	4FGL J0608.8+2034c	0.969	0.299	0.286	0.013	0.018	
25	249.93840	-46.68515	4.9	10.2	0.0	4FGL J1639.8-4642c	0.957	0.280	0.279	0.001	0.001	(e)
26	118.73457	-39.88257	4.4	7.4	0.0	4FGL J0754.9-3953	1.000	0.279	0.003	0.276	0.000	
27	252.85143	-44.36273	1.1	1220	0.0	4FGL J1650.9-4420c	0.915	0.279	0.270	0.009	0.258	(b, e)
28	254.16530	-48.22062	2.6	39	0.0	4FGL J1656.9-4814	0.722	0.270	0.077	0.194	0.110	
29	194.20780	-63.66546	4.2	6.8	0.0	4FGL J1257.0-6339	0.959	0.265	0.155	0.111	0.001	
30	221.32135	-60.00743	3.1	18.7	0.0	4FGL J1445.1-5958c	0.816	0.259	0.254	0.005	0.027	
31	244.81362	-50.78953	3.2	22.0	0.0	4FGL J1619.3-5047	0.982	0.258	0.253	0.005	0.002	
32	259.37013	-44.03974	2.4	62	0.0	4FGL J1717.6-4404	0.760	0.253	0.095	0.158	0.238	
33	258.72454	-33.38508	3.6	10.9	0.0	4FGL J1714.9-3324	0.999	0.252	0.046	0.206	0.000	
34	264.39070	-33.54471	2.5	22.3	0.0	4FGL J1737.3-3332	0.942	0.250	0.212	0.038	0.007	(b)
35	198.12297	-62.57599	2.4	41	0.0	4FGL J1312.6-6231c	0.987	0.245	0.200	0.045	0.004	(g)
36	246.65399	-48.96485	3.5	18.8	0.0	4FGL J1626.5-4858c	0.882	0.237	0.231	0.006	0.013	(b)
37	252.33402	-45.23386	4.2	15.8	0.0	4FGL J1649.2-4513c	0.964	0.232	0.221	0.011	0.002	
38	148.43061	-15.16169	5.3	5.2	0.0	4FGL J0953.6-1509	1.000	0.229	0.000	0.228	0.000	
39	251.25342	-41.38724	2.7	27.5	0.0	4FGL J1645.1-4123c	0.947	0.228	0.022	0.206	0.031	
40	254.48273	-46.92163	1.9	96	0.0	4FGL J1657.7-4656c	0.527	0.226	0.102	0.123	0.433	(b)
41	243.00184	-51.42570	3.7	17.5	0.0	4FGL J1611.9-5125c	0.957	0.224	0.222	0.002	0.001	(b)
42	86.16917	22.63266	2.8	44	0.0	4FGL J0544.4+2238	0.688	0.222	0.180	0.042	0.103	
43	228.44197	-15.34978	4.9	9.2	0.0	4FGL J1513.7-1519	0.989	0.219	0.002	0.217	0.004	
44	246.72777	-42.87342	2.9	25.0	0.0	4FGL J1626.6-4251	0.908	0.217	0.025	0.192	0.016	(b)
45	205.67808	-57.48130	4.0	17.2	0.0	4FGL J1342.6-5730	0.473	0.216	0.064	0.152	0.281	
46	275.72745	-47.31907	5.3	5.2	0.0	4FGL J1822.9-4718	0.961	0.212	0.000	0.212	0.008	
47	213.09350	-60.30956	2.4	37	0.0	4FGL J1412.2-6018	0.427	0.212	0.191	0.021	0.625	
48	254.33750	-39.28219	3.9	13.1	0.0	4FGL J1657.4-3917c	0.630	0.211	0.083	0.128	0.059	
49	198.15828	-62.95837	3.1	18.7	0.0	4FGL J1312.3-6257	0.606	0.209	0.201	0.008	0.025	
50	262.51595	-34.32575	3.1	22.1	0.0	4FGL J1730.1-3422	0.930	0.208	0.193	0.014	0.002	



Virgo

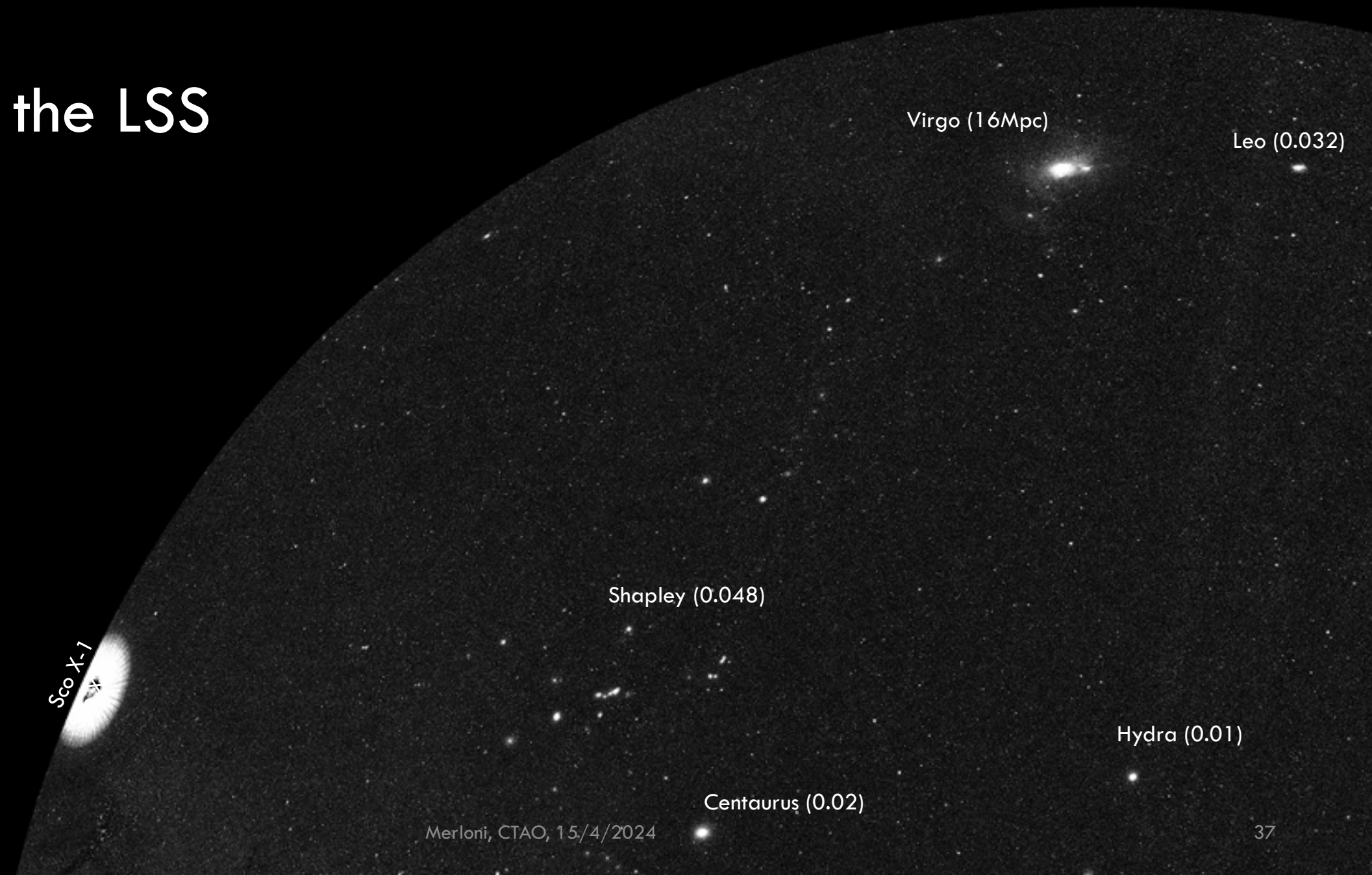
North Polar Spur/
eROSITA Bubble

Shapley

Sco X-1

1.04-2.3 keV

Imaging the LSS



Virgo (16Mpc)

Leo (0.032)

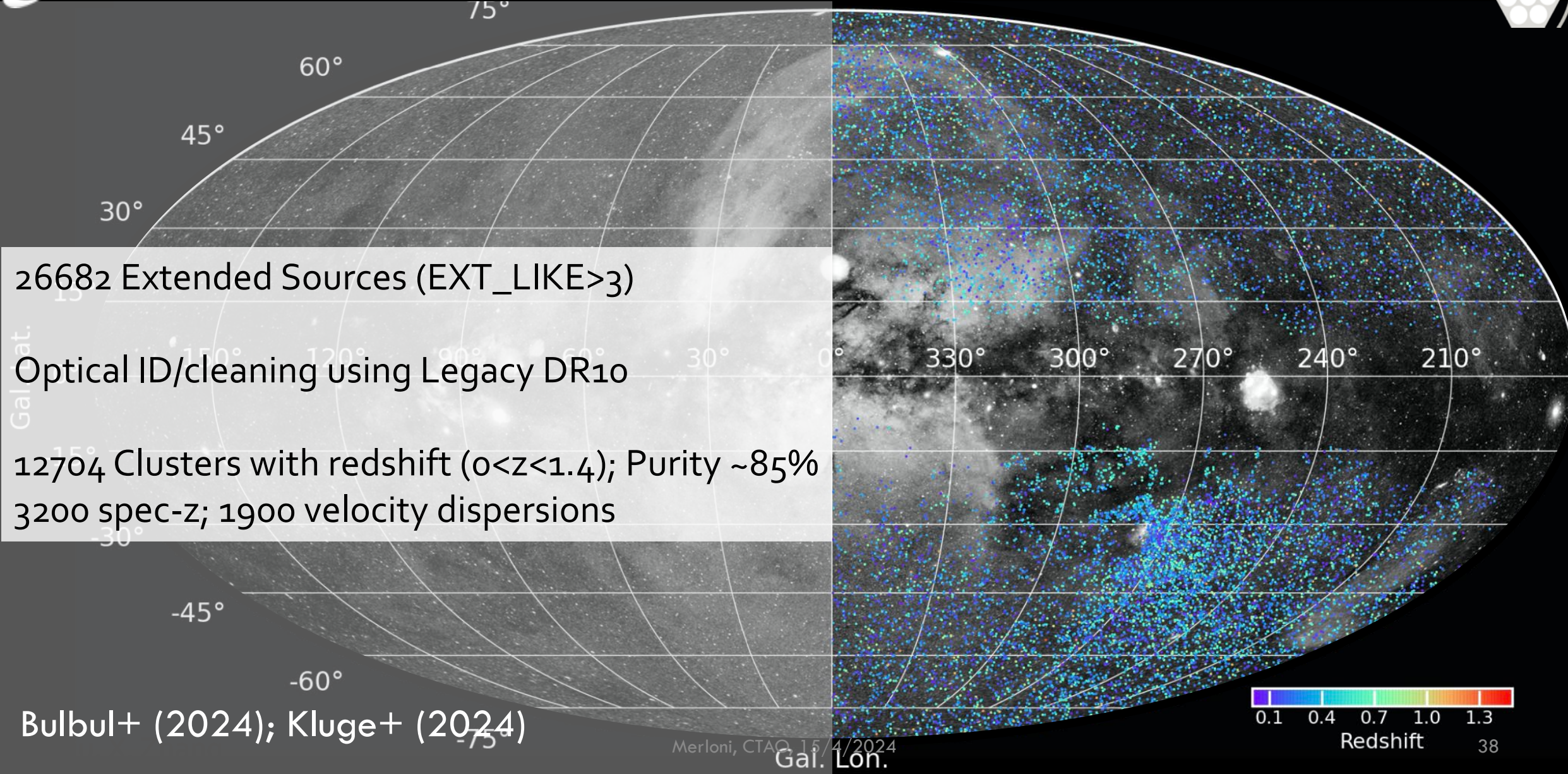
Shapley (0.048)

Hydra (0.01)

Centaurus (0.02)

Sco X-1

Clusters and Groups in eRASS1



26682 Extended Sources (EXT_LIKE>3)

Optical ID/cleaning using Legacy DR10

12704 Clusters with redshift ($0 < z < 1.4$); Purity ~85%

3200 spec-z; 1900 velocity dispersions

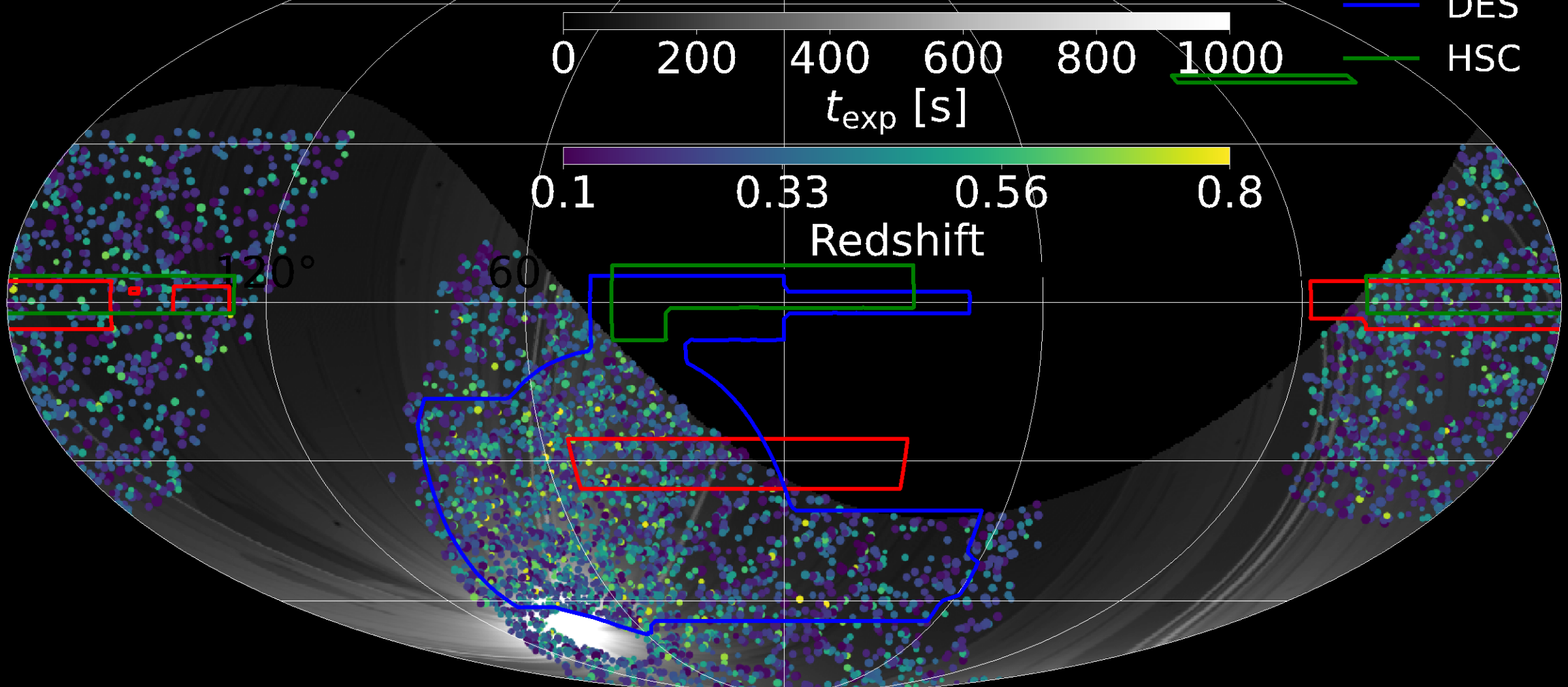
Bulbul+ (2024); Kluge+ (2024)

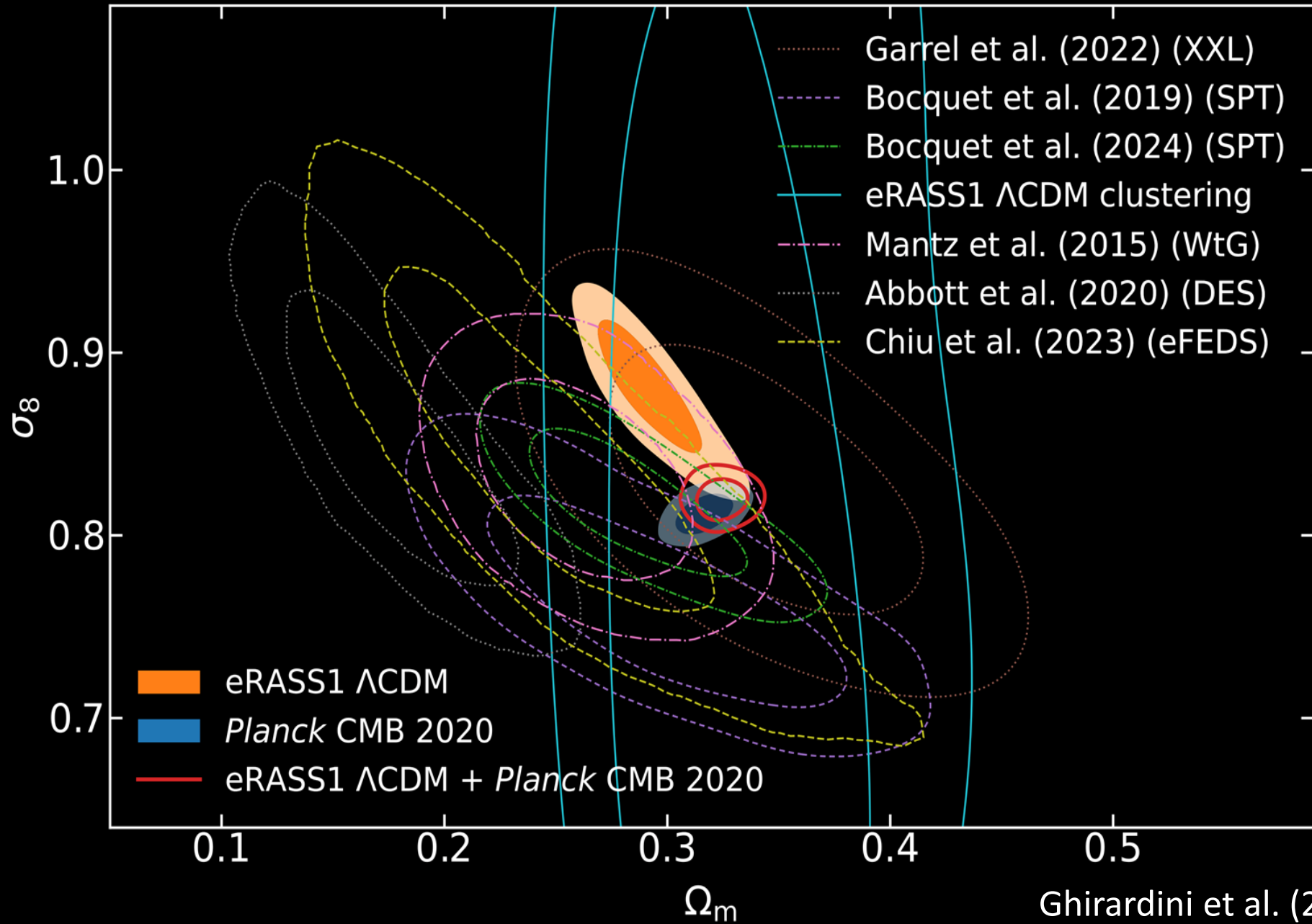


Clusters Cosmology sample

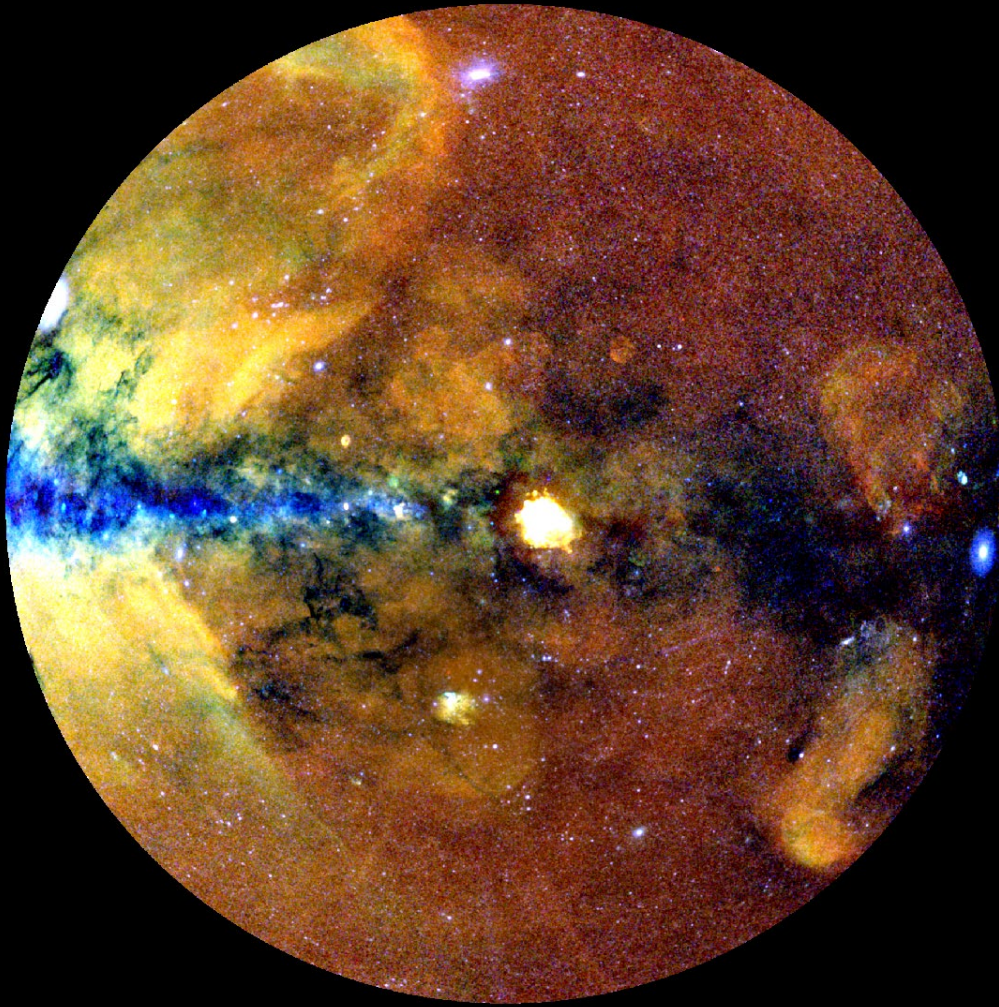
5263 Extended Sources (EXT_LIKE>6) in LS10 area with redshift ($0.1 < z < 0.8$); Purity $\sim 95\%$

— KiDS
— DES
— HSC

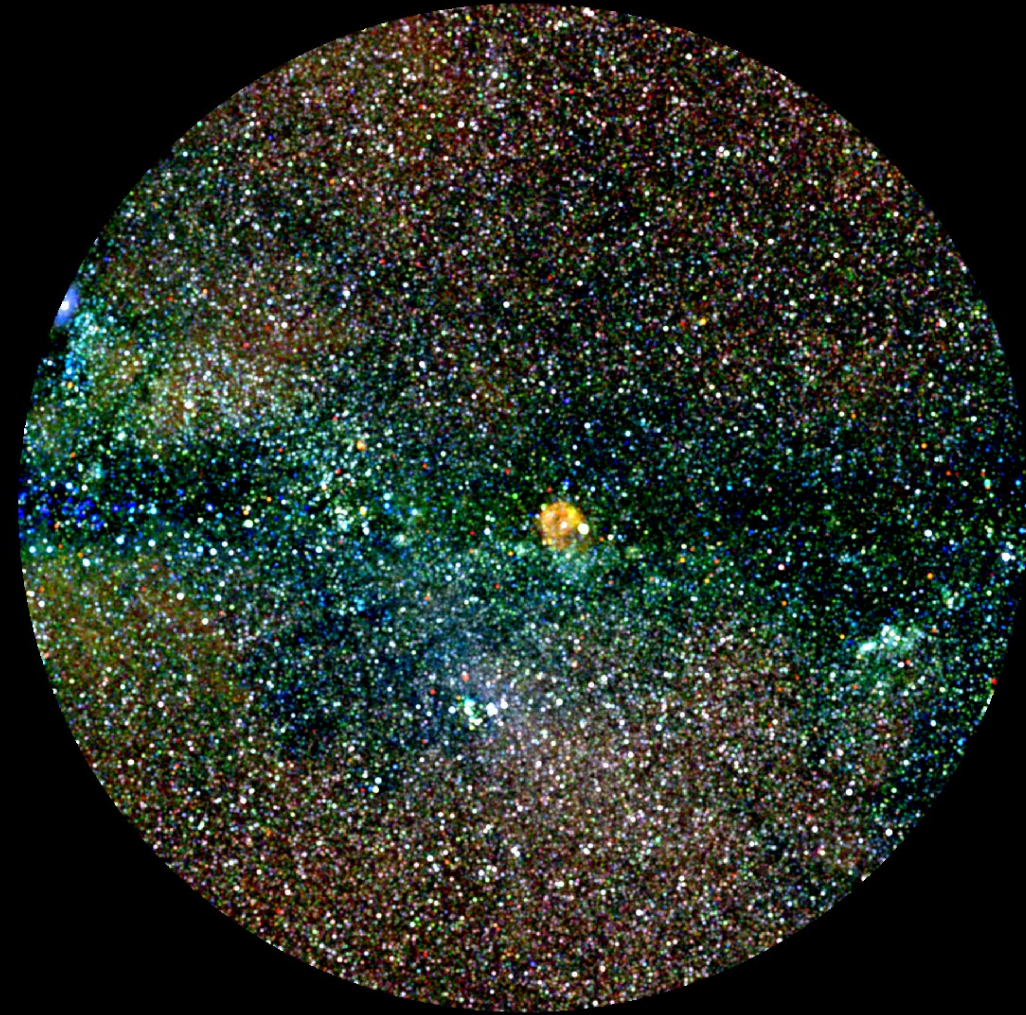




Ghirardini et al. (2024)



eRASS1 Point sources subtracted map



eRASS1 Point sources map

Credit: J. Sanders, MPE

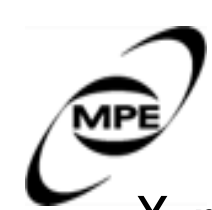
First results from the SRG/eROSITA All-sky Survey From Stars to Cosmology

RESEARCH CAMPUS,
GARCHING, GERMANY
September 15-20, 2024

For information and registration see:

<https://events.mpe.mpg.de/event/>

Abstract Submission Deadline: May 15, 2024



Conclusions



X-ray astronomy is a key contributor to our exploration of the Universe, as it reveals both fundamental and exotic phenomena

The field has reached a high level of maturity and is well diversified

eROSITA on SRG is the most powerful wide-field X-ray telescope to date. It has been in operation since Q3 2019, for more than 2 years, having completed 4.4 all-sky surveys

Thanks to its large Grasp, stable background and observing cadence eROSITA opens up new parameter space for X-ray astronomy

eRASS1 marks the coming of age of clusters cosmology as a Stage IV experiment

Numerous science highlights from DR1!

eRASS1 is now fully public! <https://erosita.mpe.mpg.de/dr1/>



www.mpe.mpg.de/eROSITA

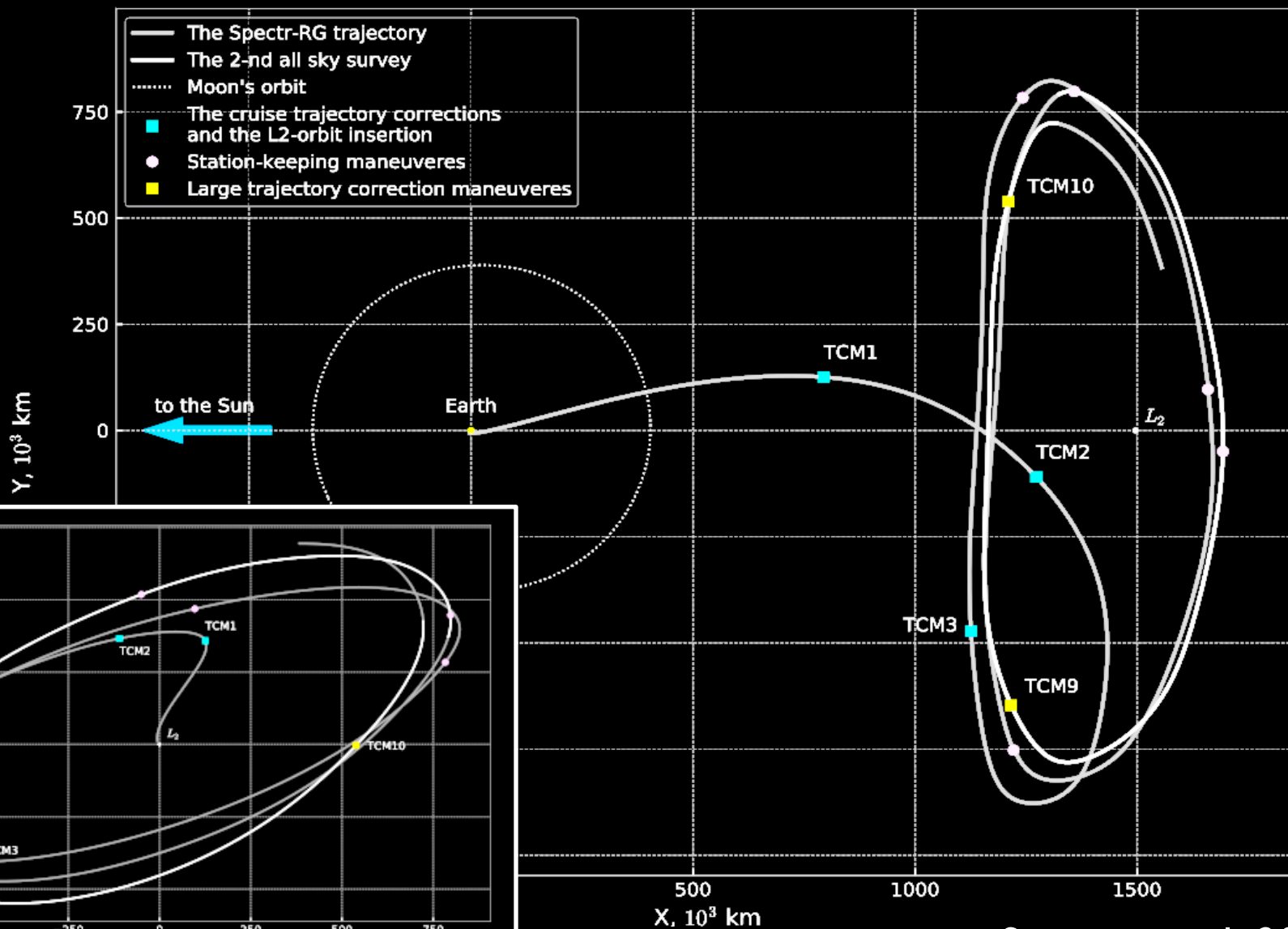
Thank you



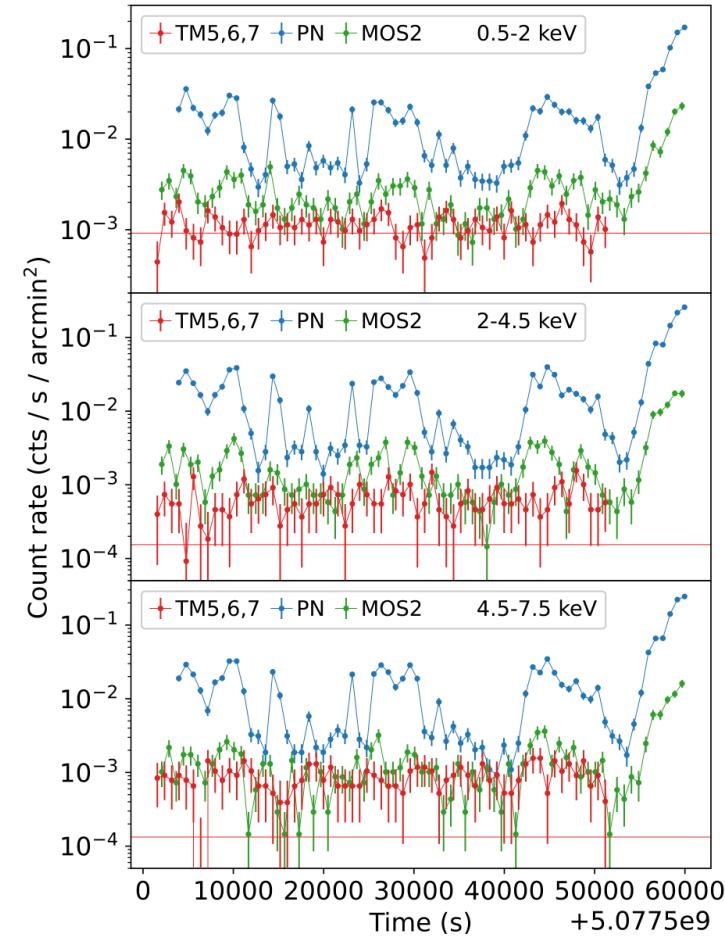
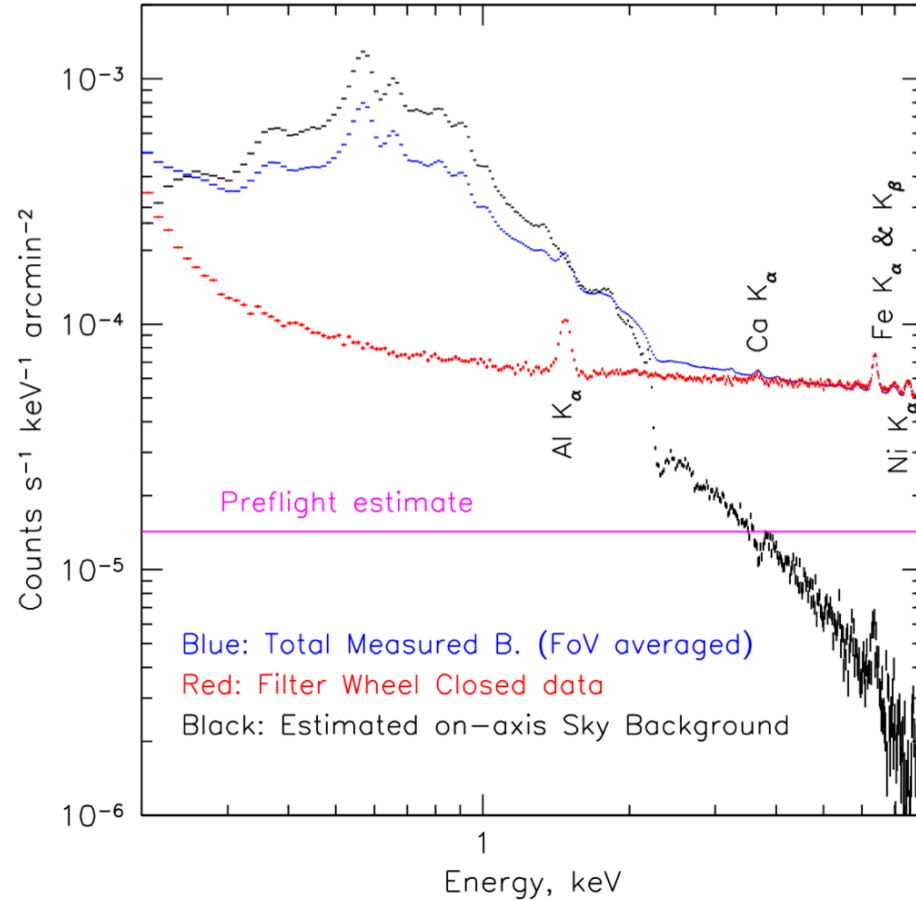
Extra Slides



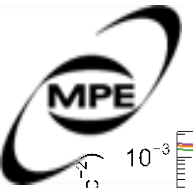
A large Halo L2 orbit



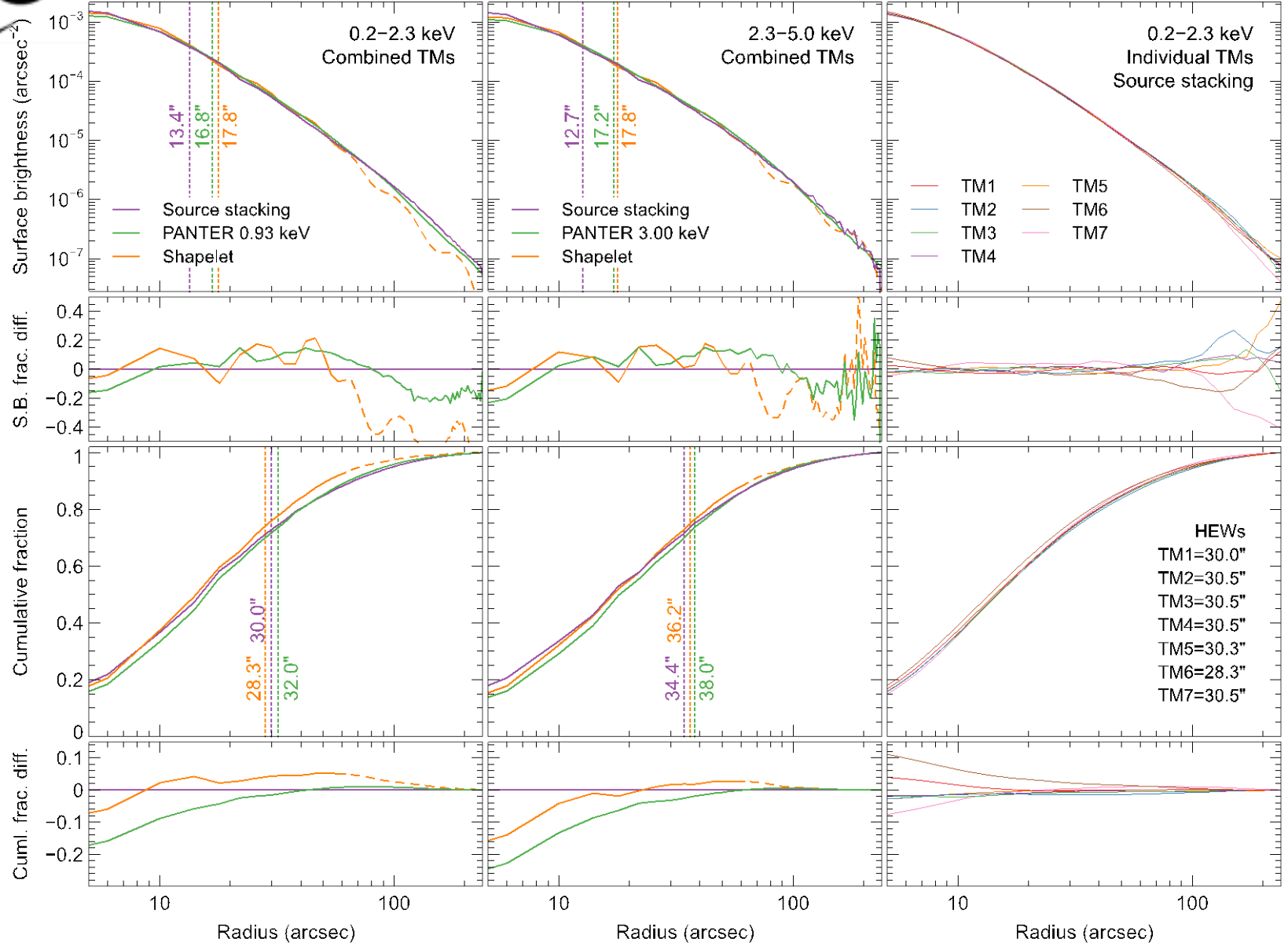
Sunyayev et al. 2021



- 1) Background much less variable than in the XMM and Chandra data
- 2) A factor of ~ 3 higher particle bkgnd than predicted in the White Book
- 3) Less fluorescence lines than EPICpn due to graded shields
- 4) But: iron line (+others) likely from impurities in the graded shield itself



Calibration: PSF

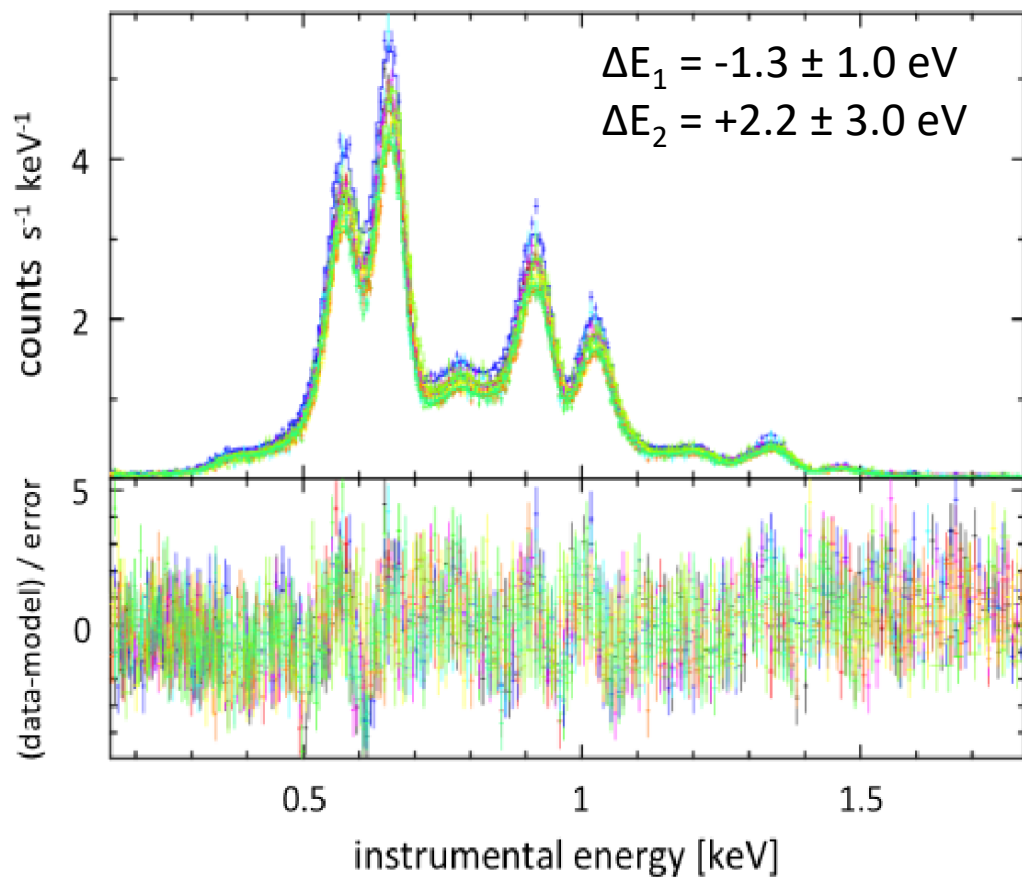


Survey HEW ~30" [0.2-2.3 keV]

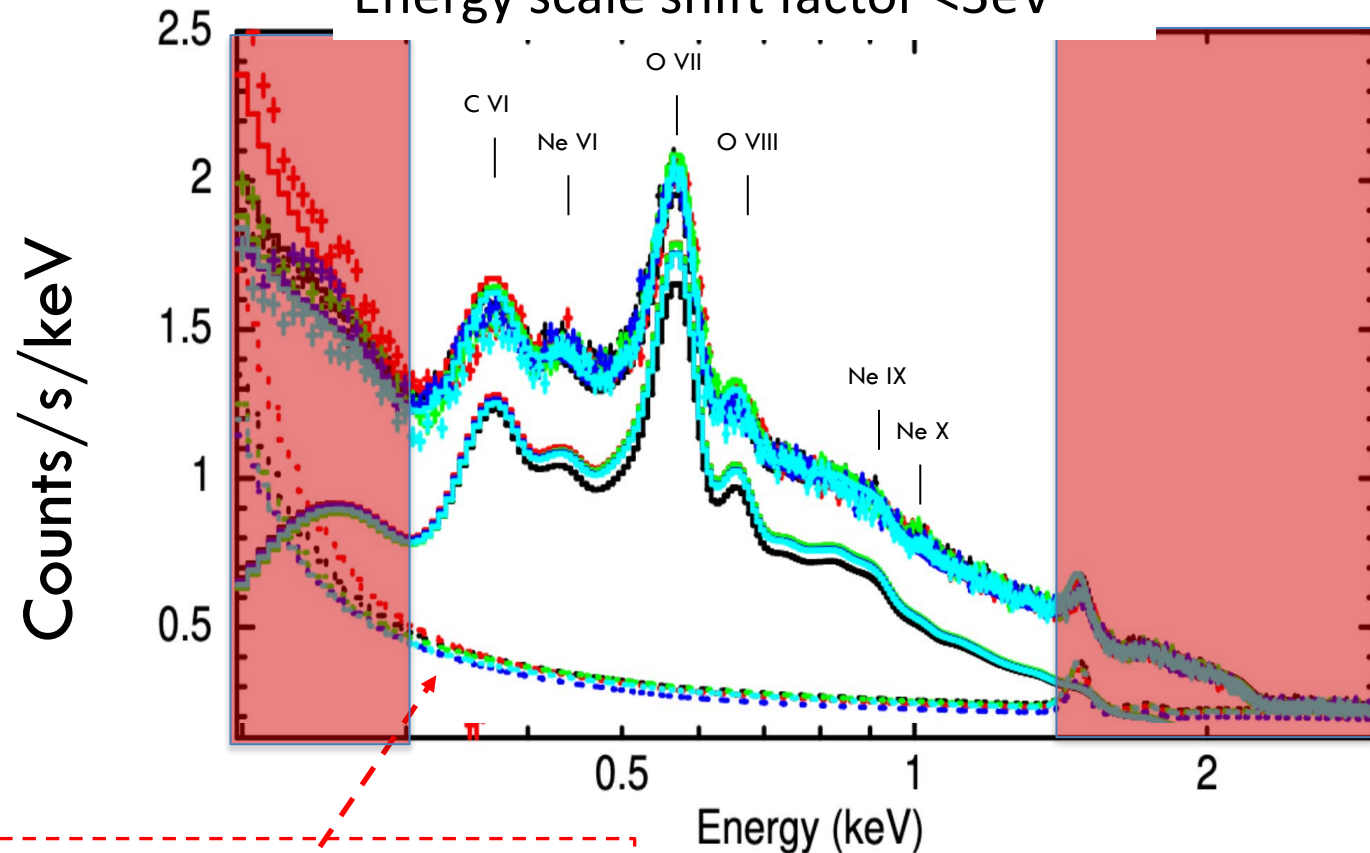
Merloni et al. 2024

Calibration: Energy scale

eROSITA spectrum of SNR 1E 0102-7219



eROSITA spectrum of eFEDS
 Energy scale shift factor <math>< 3\text{eV}</math>



Instrumental background
 (particles + detector noise)

G. Ponti, X. Zheng et al. (2022)

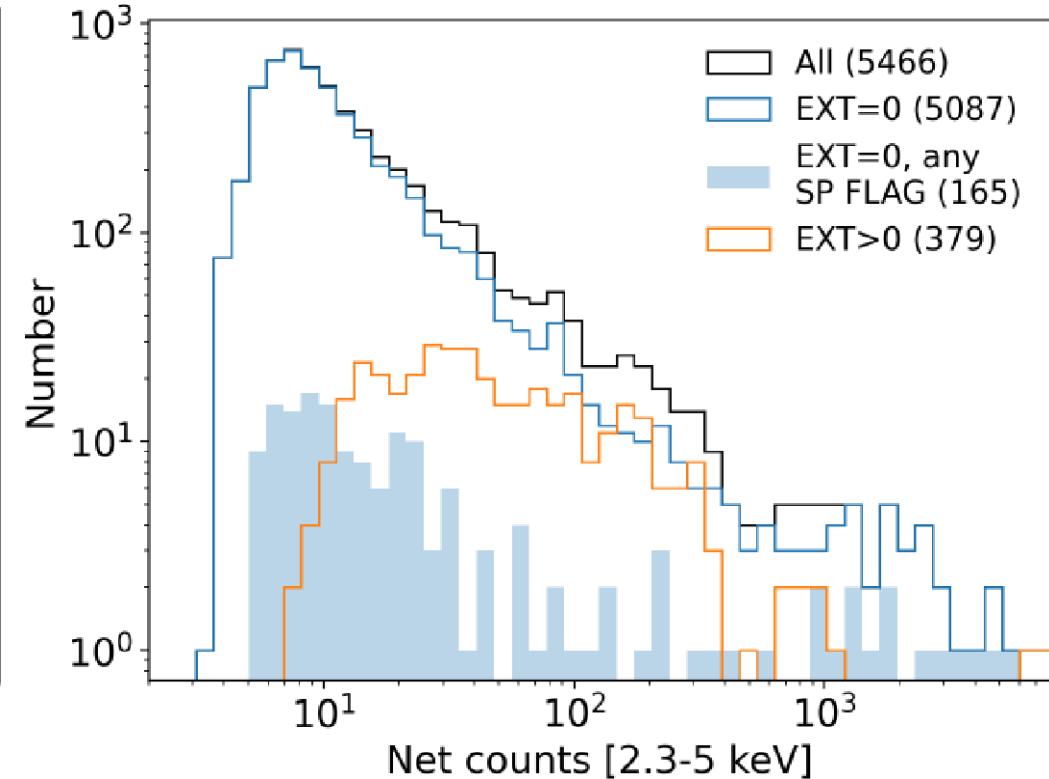
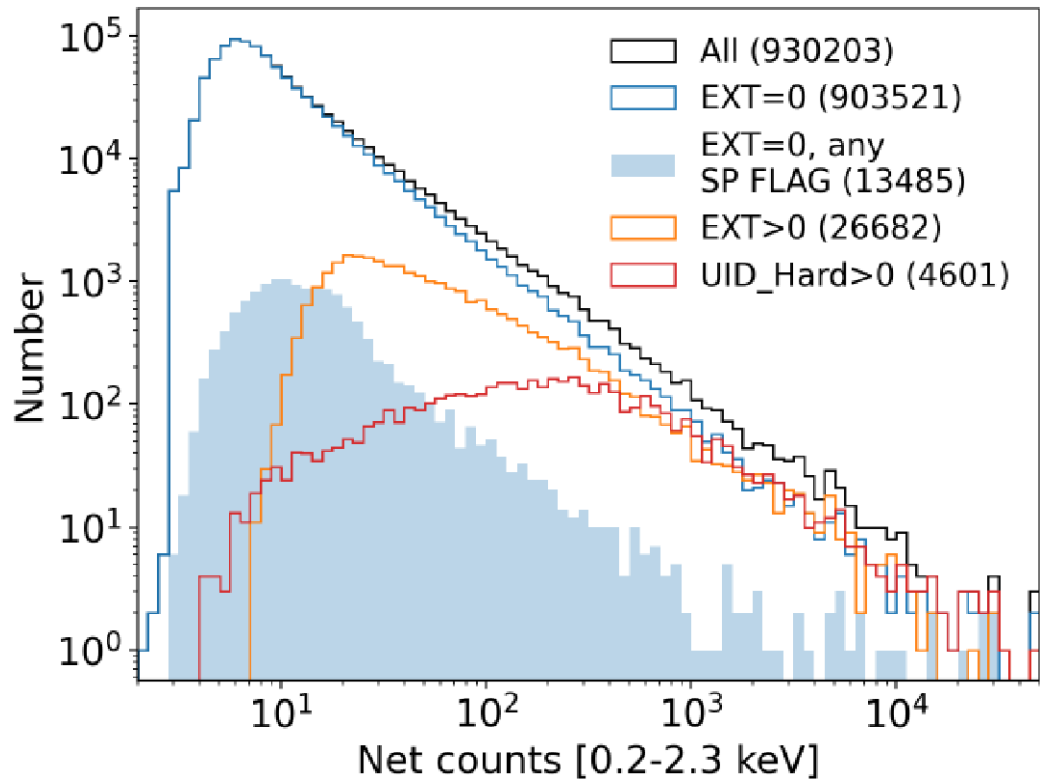
eRASS1 Catalogues

Soft band 0.2-2.3 keV, Point sources: 903k

Soft band 0.2-2.3 keV, extended: 26.6k (of which 12k optically confirmed clusters)

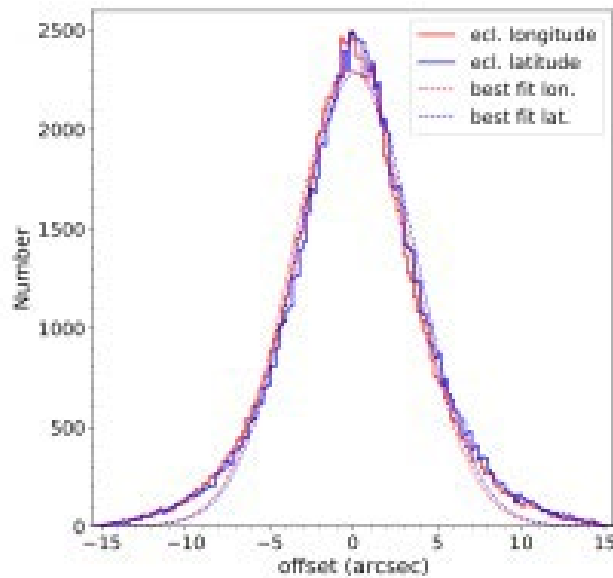
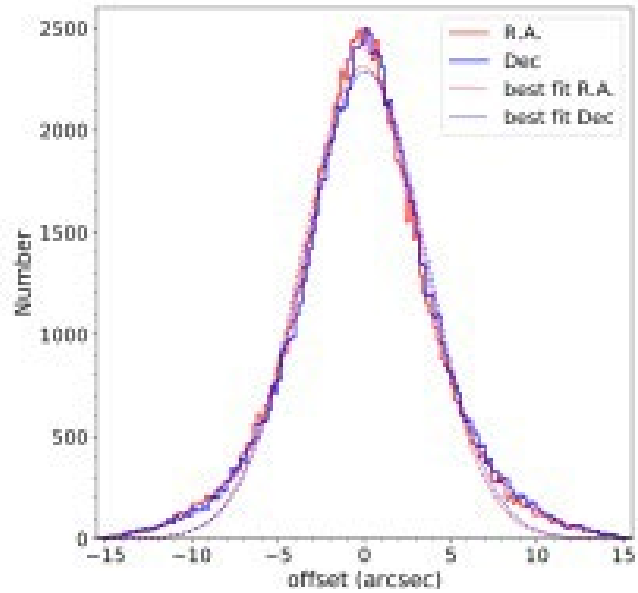
Hard band 2.3-5 keV, Point Sources: 5k

Hard band 2.3-5 keV, Extended: 380

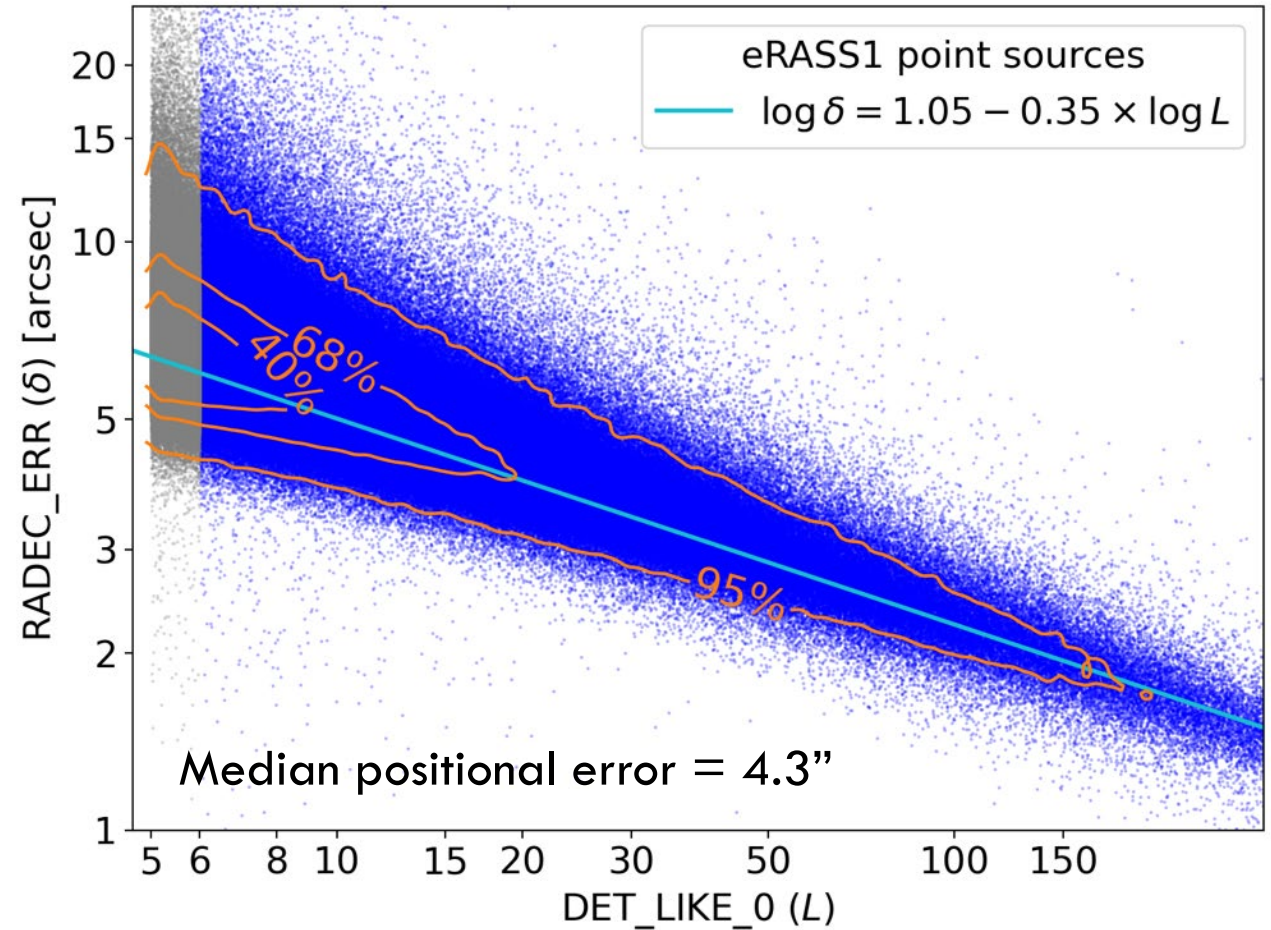


Merloni et al. (2024)

eRASS1 'Main' Catalogue: Astrometry



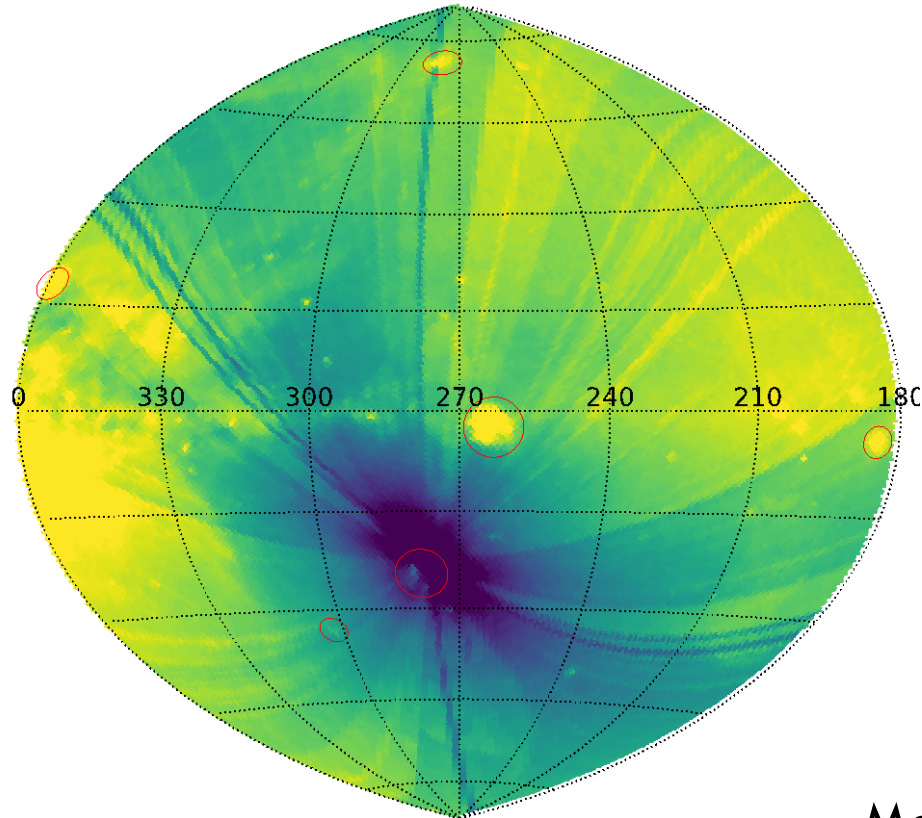
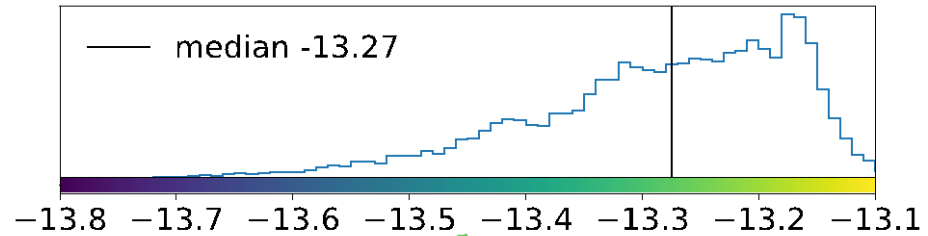
Point sources astrometric accuracy



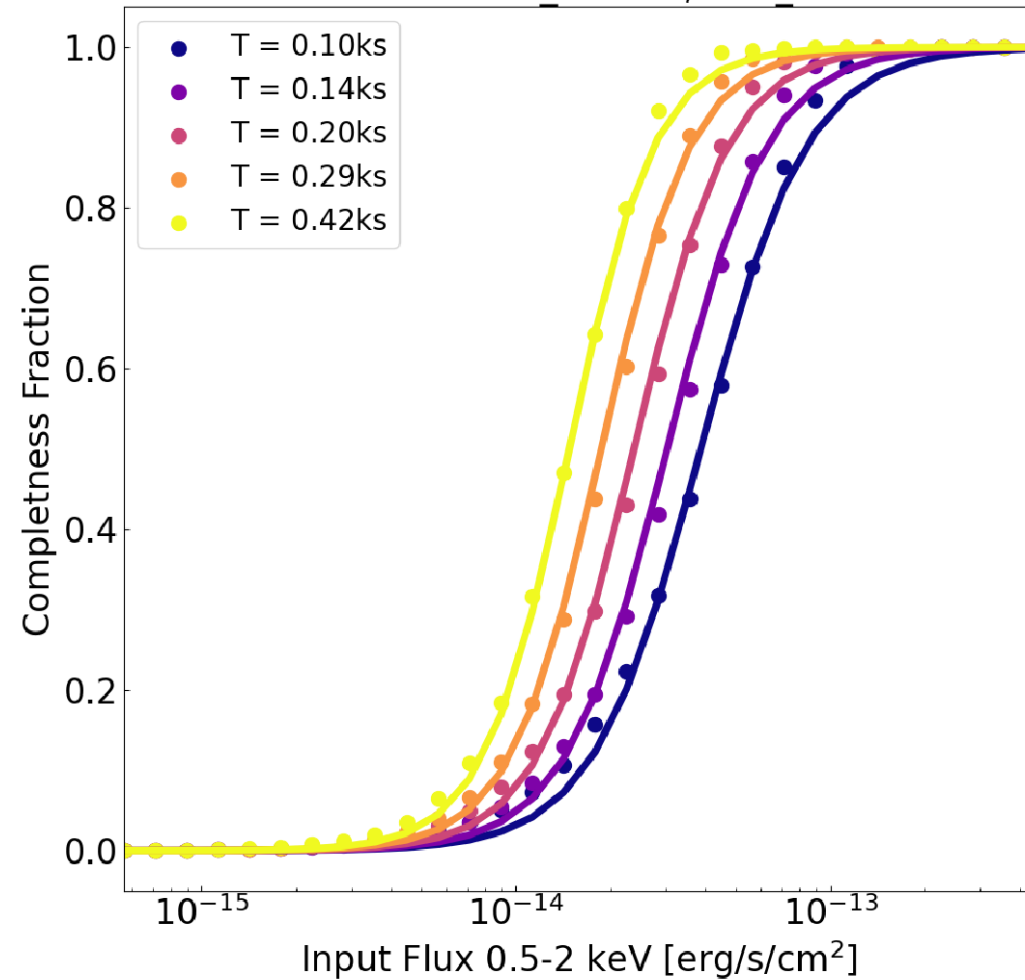
Merloni et al., A&A, in press

eRASS1 Main Catalogue: flux limit

Log of 0.5-2 keV flux limit

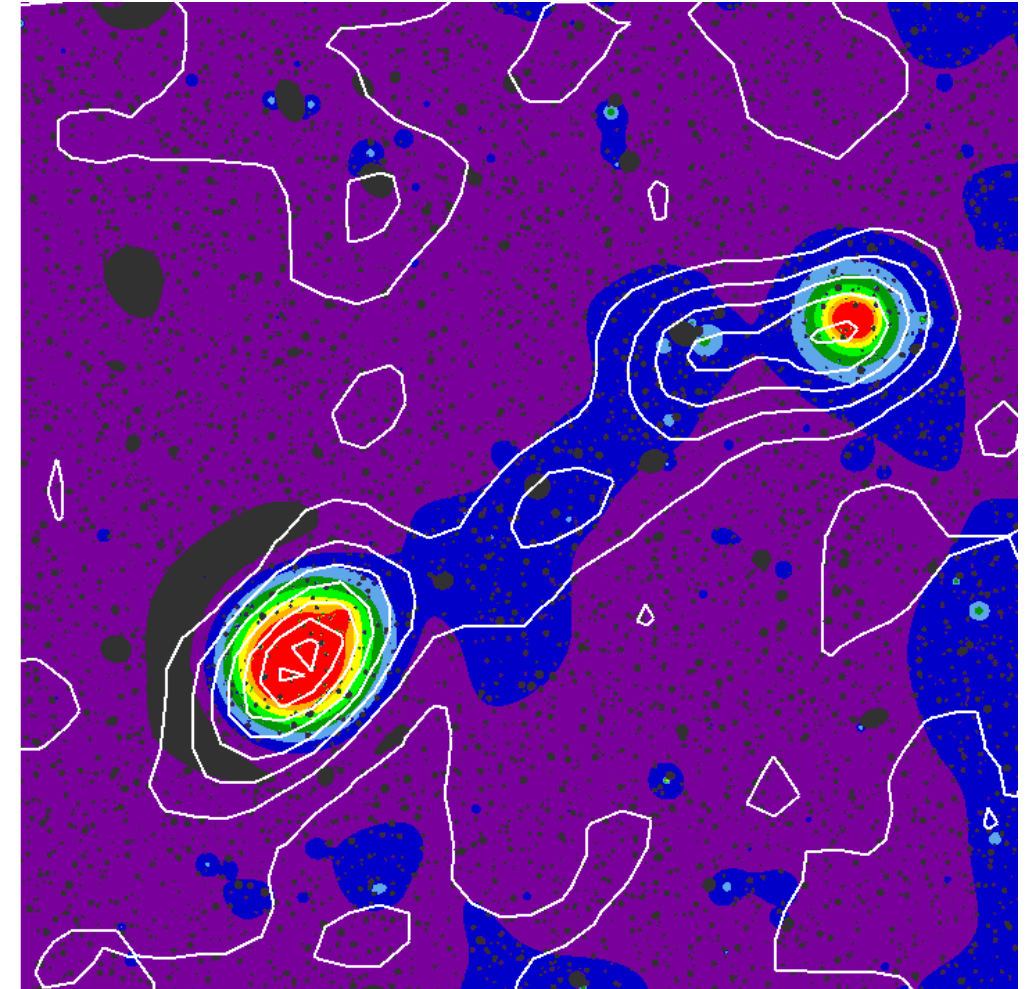
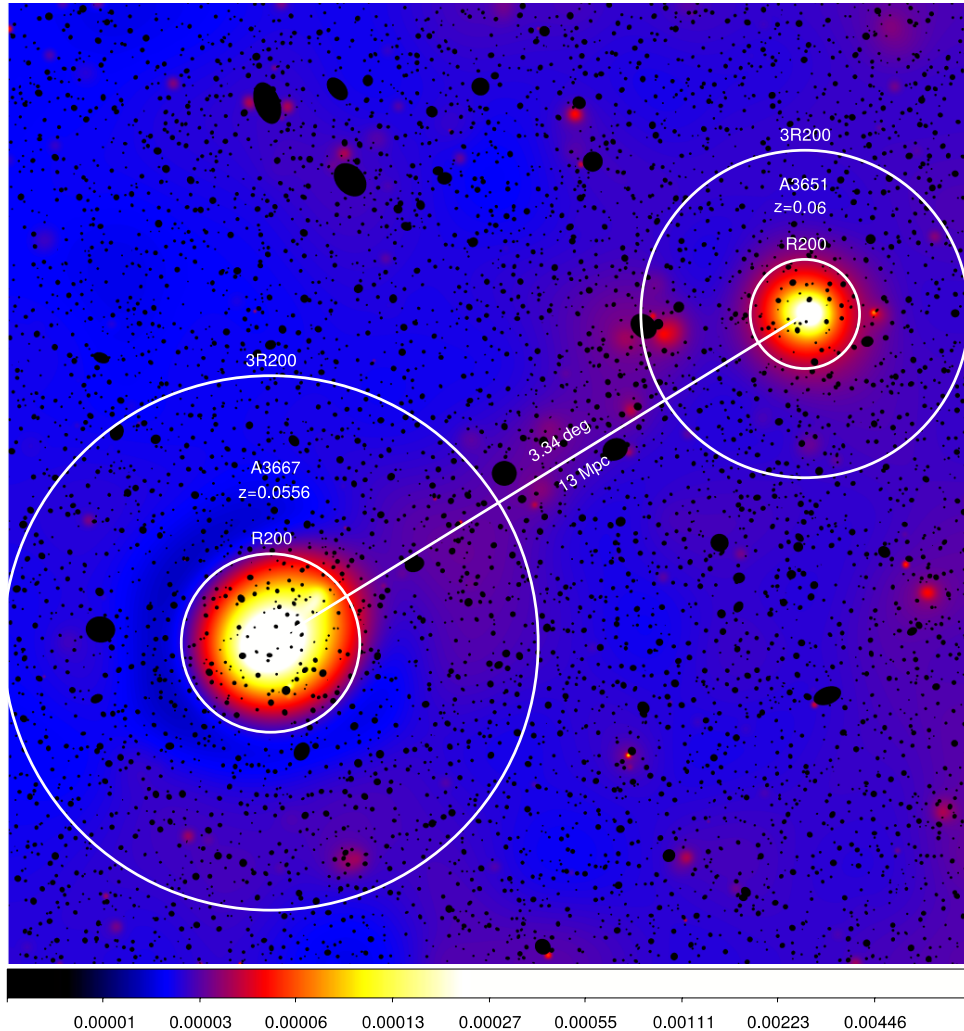


AGN eRASS1 EXT_LIKE=0, DET_LIKE>6



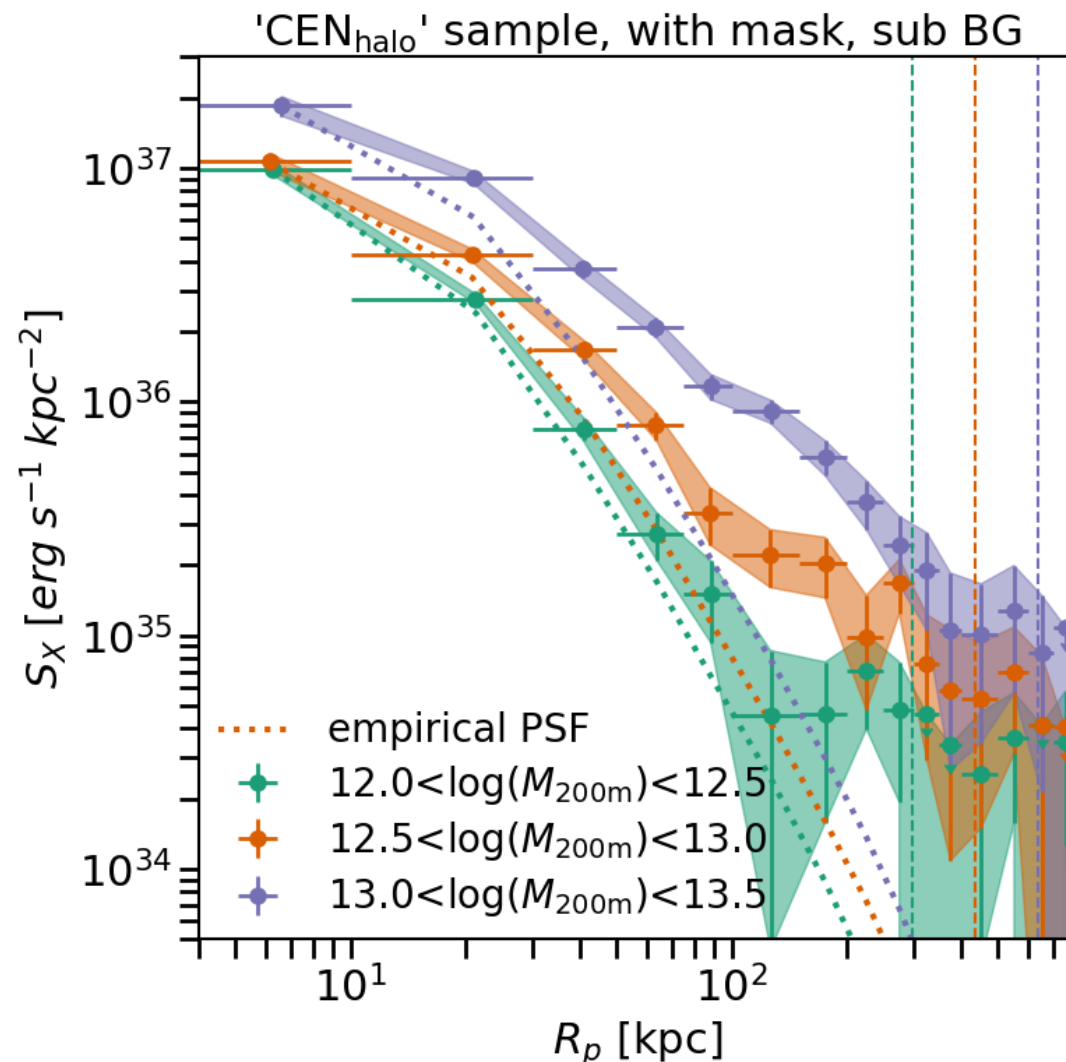
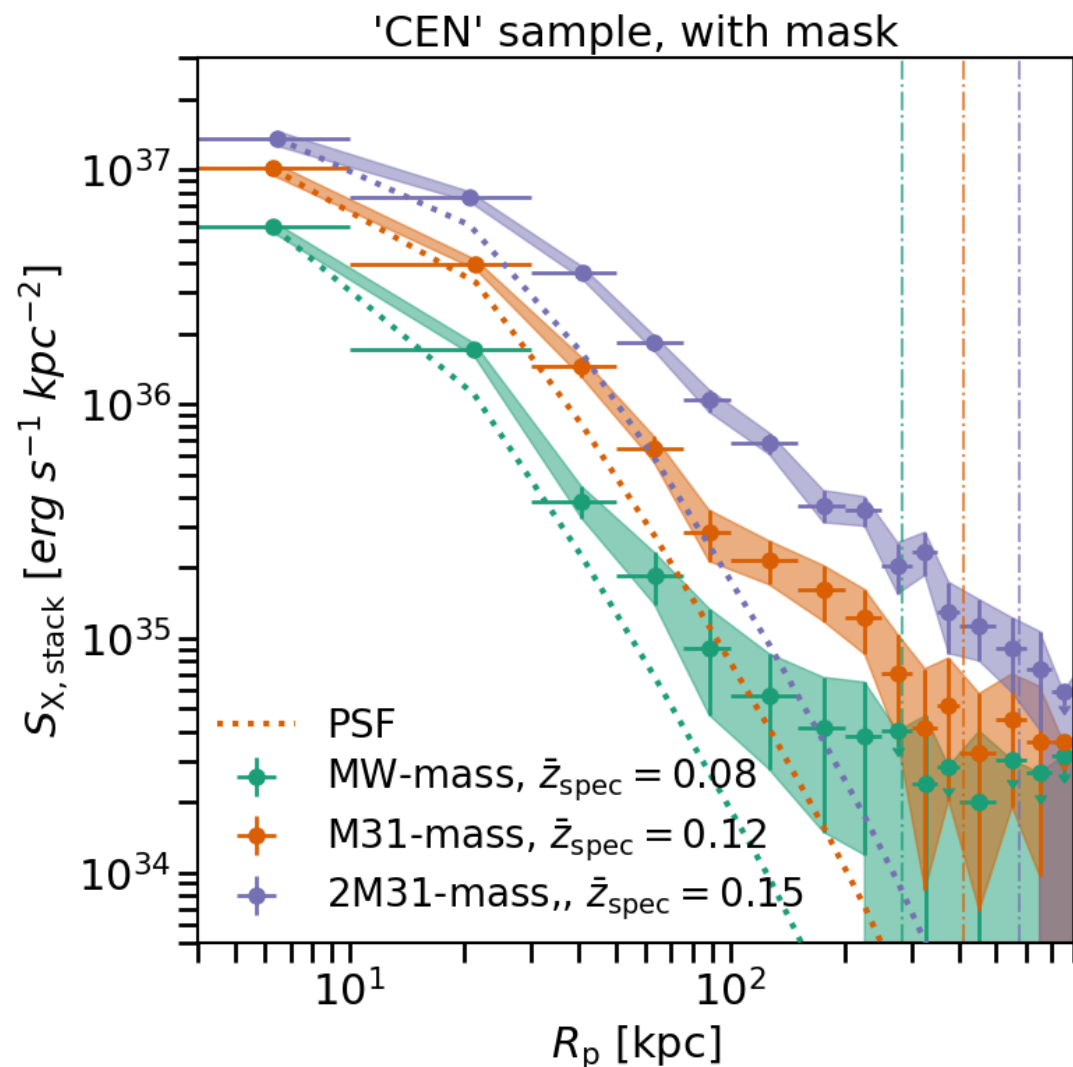
Merloni et al., A&A, in press

Discovery of a >13 Mpc long X-ray filament between two galaxy clusters beyond three times their virial radii (Dietl et al.)

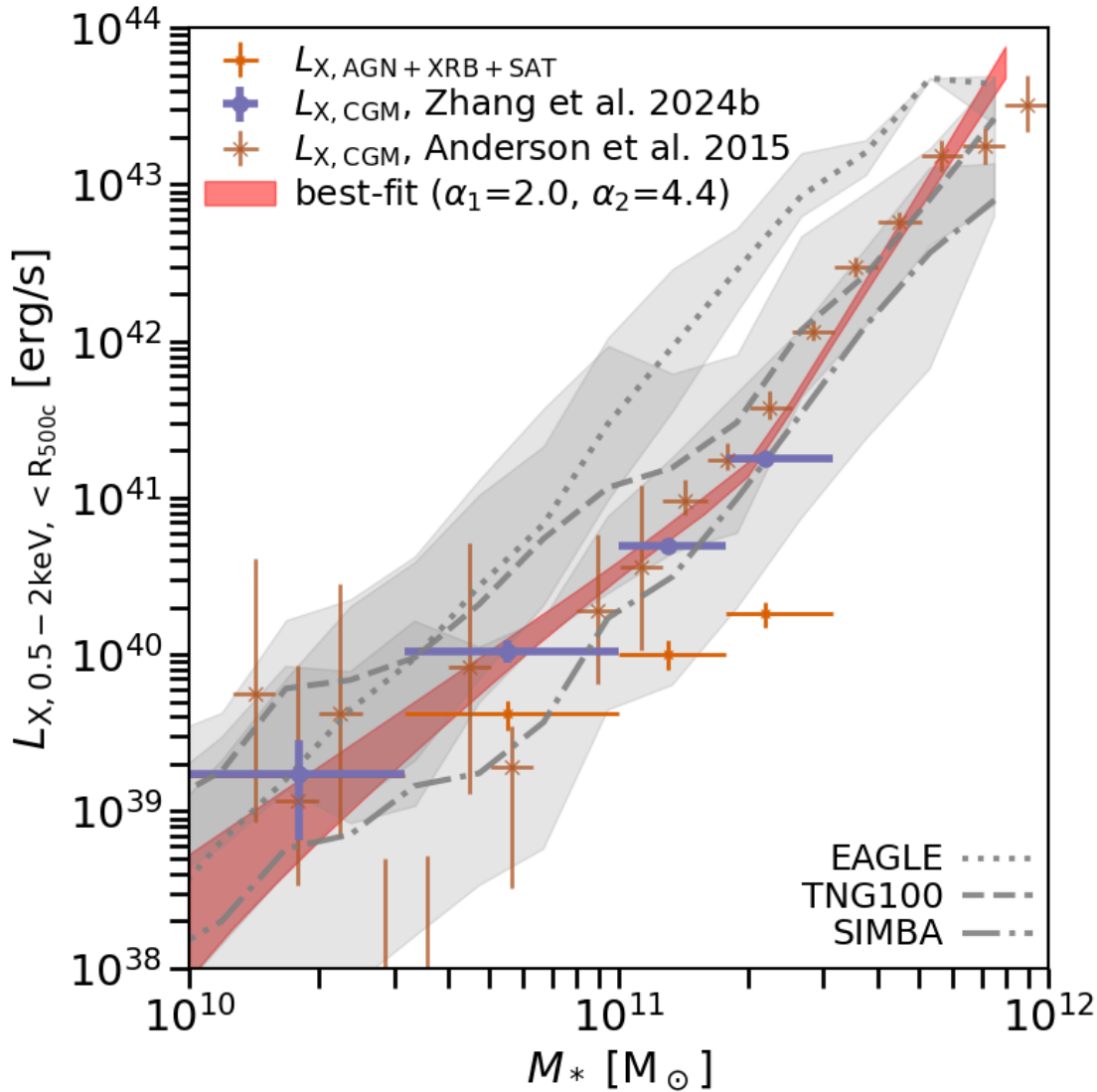


X-ray intensity (wavelt filtered, color) with galaxy overdensity contours (white)

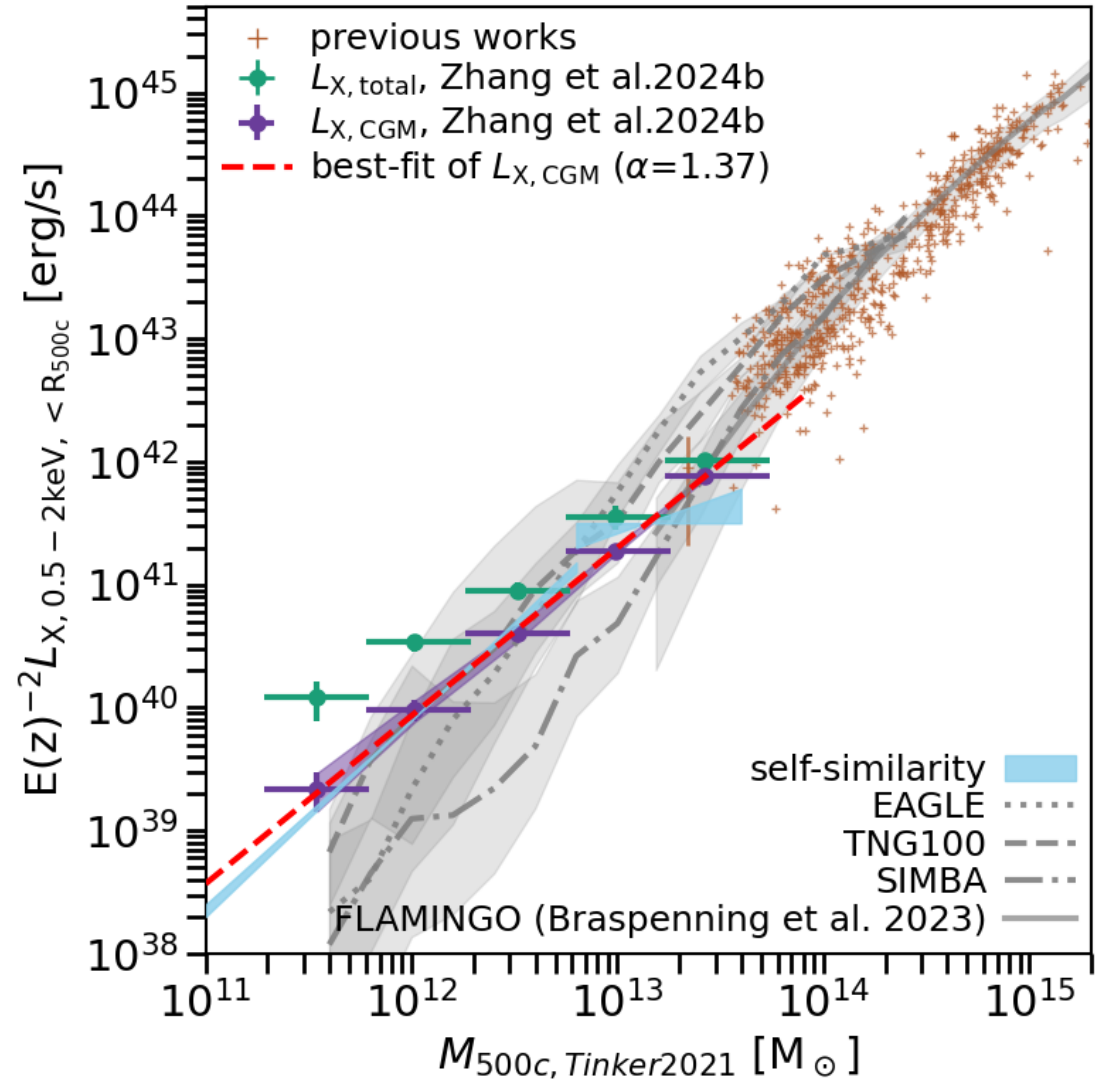
The hot CGM in eRASS1: I. X-ray brightness profiles (Yi et al.)



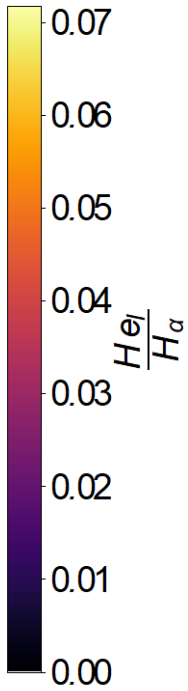
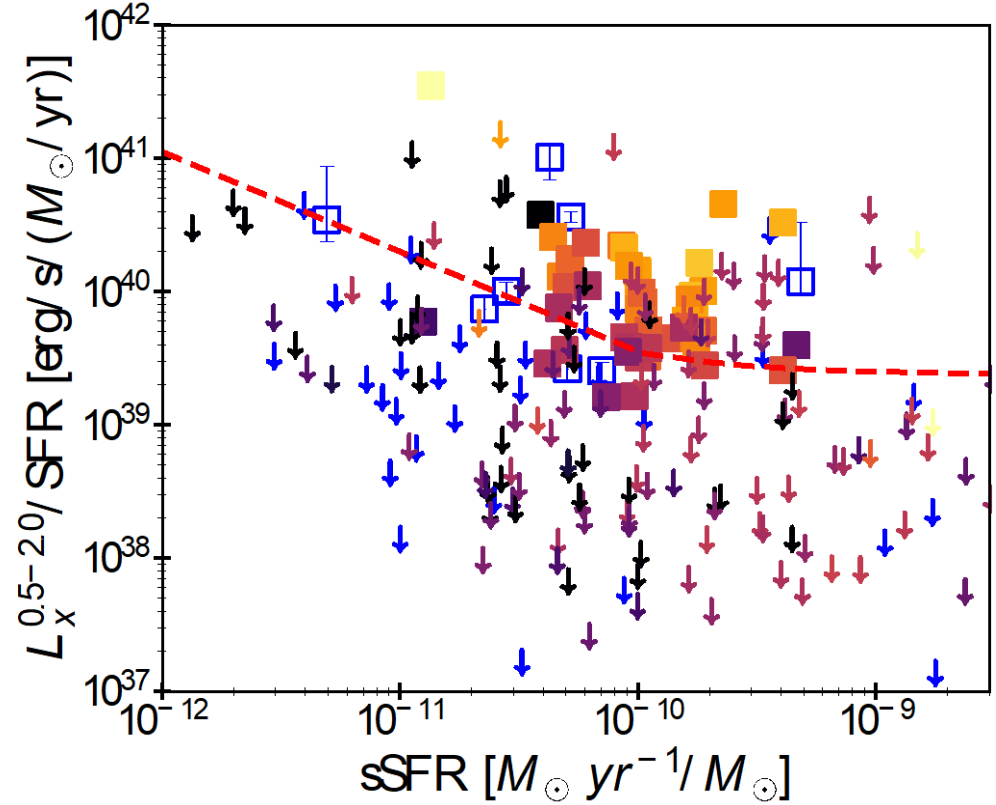
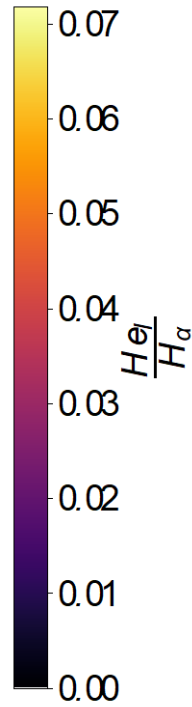
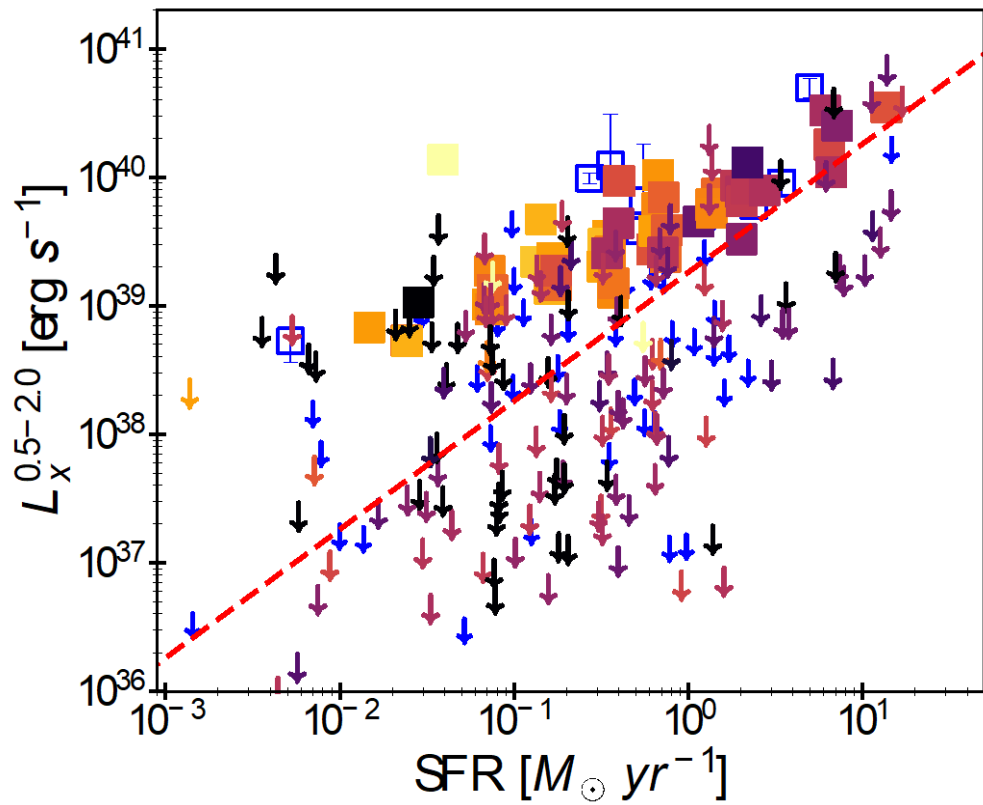
The hot CGM in eRASS1: II. Scaling Relations (Yi et al.)



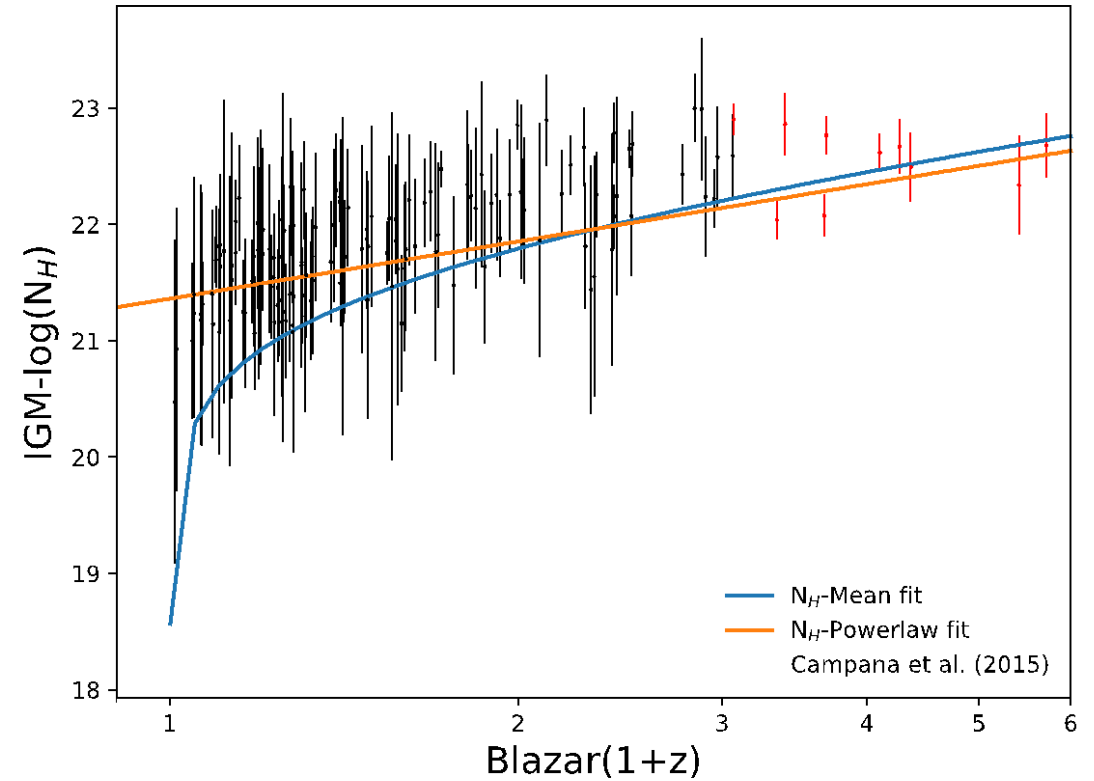
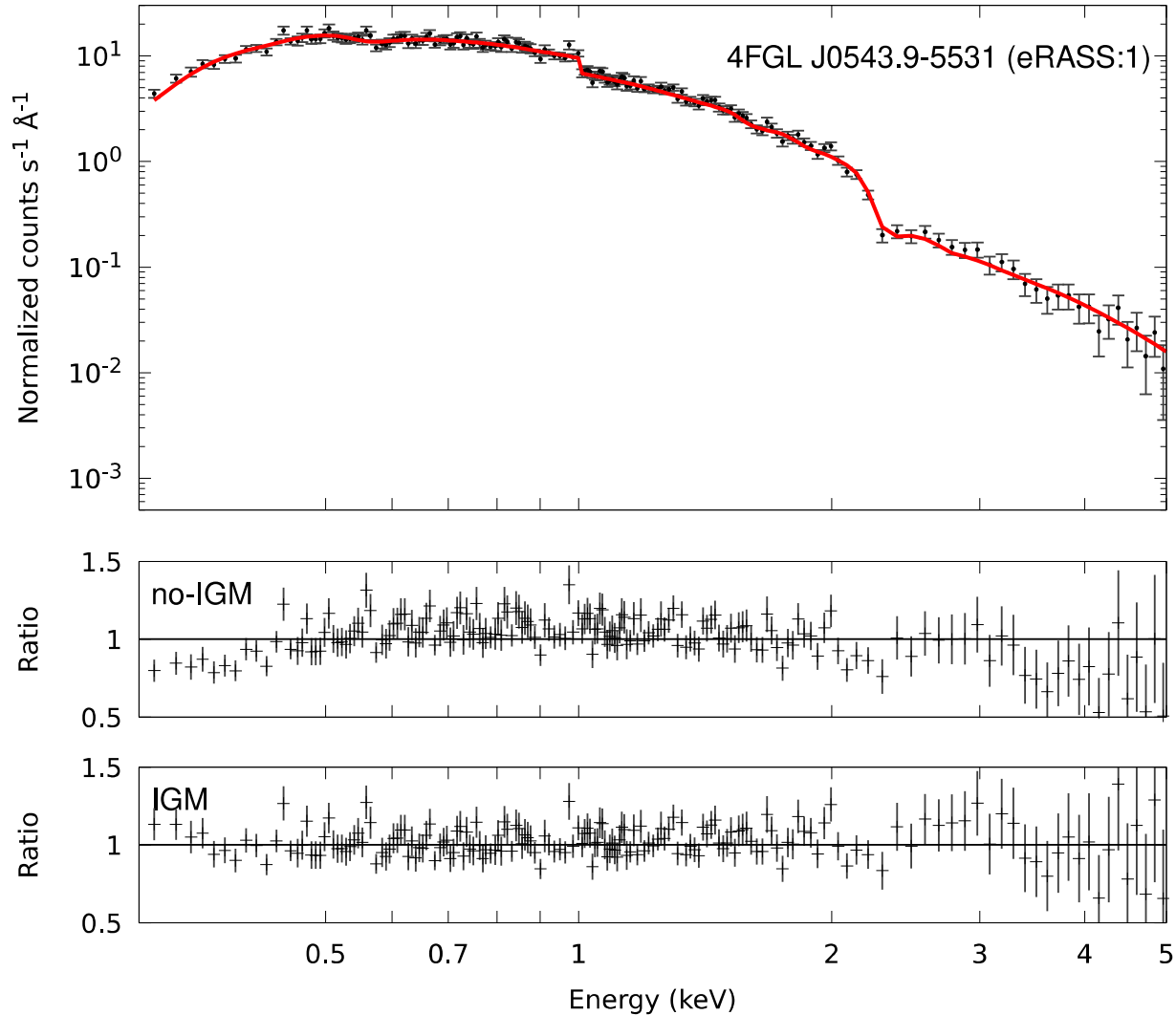
AC



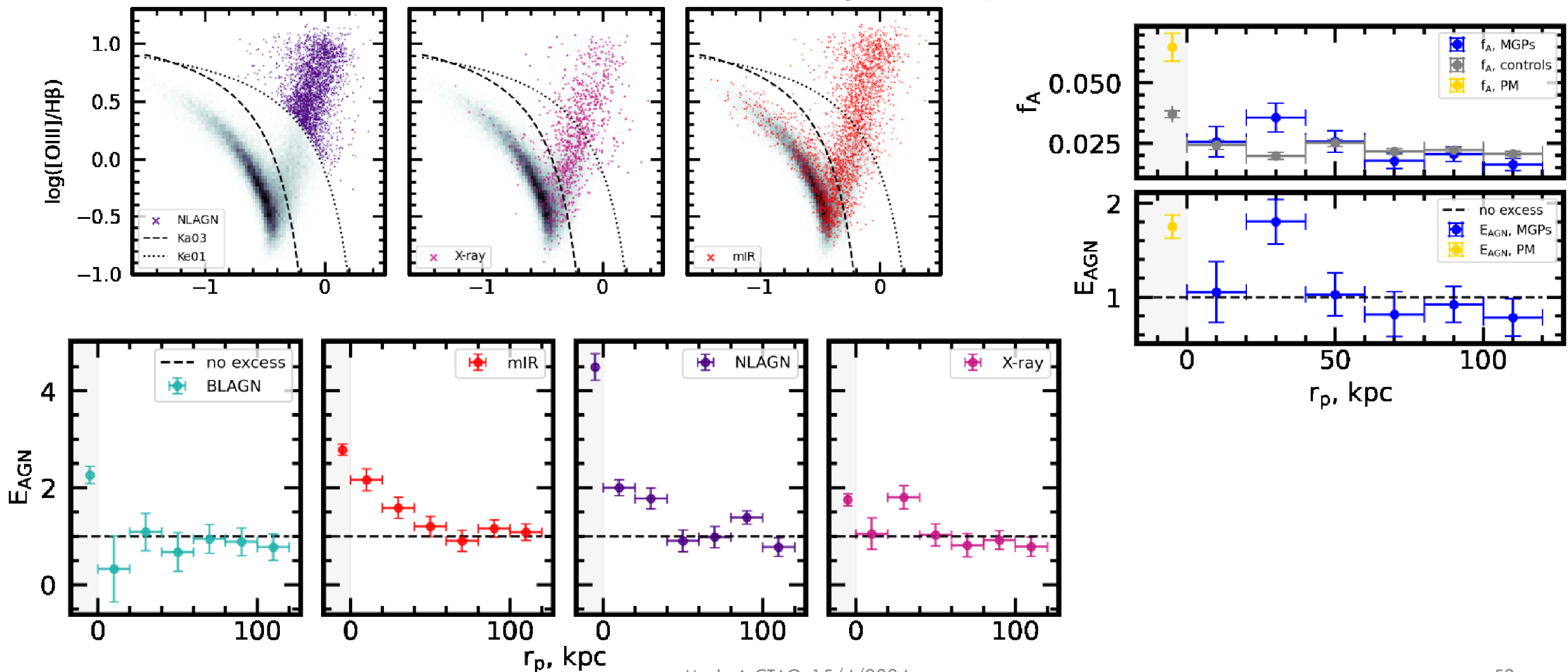
The first all-sky survey of star-forming galaxies with SRG/eROSITA: Scaling relations and populations of X-ray luminous starbursts (Kyritsis et al.)



Probing the physical properties of the IGM using SRG/eROSITA spectra from blazars (Gatuzz et al.)



X-ray AGNs with SRG/eROSITA: Multi-wavelength observations reveal merger triggering and post-coalescence circumnuclear blowout (Bickley et al.)



First Study of the SNR Population in the LMC with eROSITA (Zangrandi et al.)

